TAMPEREEN TEKNILLINEN YLIOPISTO
TAMPERE UNIVERSITY OF TECHNOLOGY

JANI HONKANEN

HARMONIC PERFORMANCE IMPROVEMENT OF STATCOM

Master of Science Thesis

Examiners: Assist. Prof. Tuomas Messo and Ph.D. Jenni Rekola
Examiners and topic approved on 28th February 2018

ABSTRACT

JANI HONKANEN: Harmonic Performance Improvement of STATCOM
Tampere University of Technology
Master of Science Thesis, 82 pages, 3 Appendix pages
April 2018
Master's Degree Programme in Electrical Engineering
Major: Power Electronics
Examiners: Assistant Professor Tuomas Messo and Ph.D. Jenni Rekola

Keywords: STATCOM, harmonic currents, harmonic voltages, reactive power compensation

In this thesis, harmonic performance of STATCOM (Static Synchronous Compensator) was studied. Harmonic performance means the amount of harmonic current emissions and their effect on harmonic voltages at the connection point of the compensator. It has been observed that harmonic current emissions are small when grid voltage is sinusoidal but they increase when harmonics are added to grid voltage. This is a problem as the currents cause harmonic voltages in grid impedances which are added to the existing grid harmonic voltages at the connection point. Standards and transmission operators' specifications set limits for harmonic voltages at the connection point which are exceeded in some cases with the present current emissions.

The objective of the thesis was to study reasons for the problem and decrease harmonic current emissions. The problem was studied by simulations in PSCAD. Harmonic current and voltage spectrums at the connection point of STATCOM were simulated with same grid harmonic voltages in several cases where some STATCOM attributes were modified. Especially, the effect of different control functions on harmonic performance was studied.

Two voltage feedforward options were compared. It was observed that harmonic currents of orders from 20 to 40 were smaller with fundamental component feedforward. Instantaneous value of voltage as feedforward is intended to remove harmonic currents completely. It was noticed that the delay caused by modulator deteriorates its performance especially at high-order harmonics. Low-order harmonics were still smaller than with fundamental feedforward. However, the performance of a real system will not be so good due to errors in harmonic voltage measurement. Also, performance with low-pass filtered feedforward was investigated. Harmonic currents around 30^{th} were well mitigated. Low-order harmonics were smaller than with fundamental feedforward but not as small as with instantaneous feedforward due to filter's phase delay.

Low-order harmonic currents were reduced to almost zero by actively controlling them. Control was implemented by adding resonant branches for these harmonics in PR-controller (proportional-resonant controller). Second harmonic current could be removed only partly by control. Part of it resulted from the controller which controls the average of DC-voltages in STATCOM branches to nominal value. Still, harmonic current control requires exact harmonic current measurement which may be challenging in a real system.

Second harmonic current was observed to increase in voltage control mode when operating point was shifted from capacitive to inductive. To mitigate it, a band-stop filter was designed for voltage d-component which is produced by synchronization.

TIIVISTELMÄ

JANI HONKANEN: STATCOM:n harmonisen suorituskyvyn parantaminen
Tampereen teknillinen yliopisto
Diplomityö, 82 sivua, 3 liitesivua
Huhtikuu 2018
Sähkötekniikan diplomi-insinöörin tutkinto-ohjelma
Pääaine: Tehoelektroniikka
Tarkastajat: Apulaisprofessori Tuomas Messo ja tutkijatohtori Jenni Rekola

Avainsanat: STATCOM, harmoniset virrat, harmoniset jännitteet, loistehon kompensointi

Tässä diplomityössä tutkittiin STATCOM:n harmonista suorituskykyä. Sillä tarkoitetaan tuotettujen harmonisten virtojen määrää ja niiden vaikutusta laitteen liityntäpisteen harmonisiin jännitteisiin. On havaittu, että harmoniset virrat ovat pieniä verkon jännitteen ollessa sinimuotoista. Ne kuitenkin kasvavat, kun jännitteeseen lisätään harmonisia komponentteja. Kasvu on ongelma, sillä virrat aiheuttavat harmonisia jännitteitä verkkoimpedansseissa, jotka lisätään liityntäpisteessä verkon harmonisiin jännitteisiin. Liityntäpisteen harmonisten jännitteiden määrälle asetetaan rajoituksia standardeissa ja verkkoyhtiöiden spesifikaatioissa, jotka ylittyvät nykyisillä virroilla joissain tapauksissa.

Työn tavoitteena oli tutkia ongelman syitä ja pienentää tuotettuja harmonisia virtoja. Ongelmaa tutkittiin tekemällä simulaatioita PSCAD:lla. Niissä tutkittiin harmonisten virtojen ja jännitteiden määrää STATCOM:n liityntäpisteessä, kun verkon harmoniset jännitteet pidettiin samana ja joitain STATCOM:n ominaisuuksia muutettiin. Erityisesti tutkittiin säätöominaisuuksien vaikutusta harmoniseen suorituskykyyn.

Simuloinneissa vertailtiin kahta eri jännitettä myötäkytkentänä. Havaittiin, että perustaajuista jännitettä käytettäessä harmoniset virrat järjestykseltään 20:stä 40:een olivat pienempiä. Hetkellisen jännitteen käyttämisen tarkoitus on poistaa harmoniset virrat täysin, mutta sen suorituskyvyn havaittiin huononevan modulaattorin aiheuttaman viiveen vuoksi etenkin suurilla taajuuksilla. Pienitaajuiset harmoniset virrat olivat kuitenkin pienempiä kuin perustaajuisella myötäkytkennällä. Todellisen järjestelmän suorituskyky ei kuitenkaan ole yhtä hyvä johtuen virheistä harmonisten jännitteiden mittauksessa. Myös alipäästösuodatetun myötäkytkennän suorituskykyä tutkittiin. Virrat 30:n harmonisen ympäristössä olivat hyvin vaimentuneita. Matalataajuiset harmoniset olivat pienempiä kuin perustaajuista jännitettä käytettäessä, mutta ei yhtä pieniä kuin hetkellistä jännitettä käytettäessä suodattimen aiheuttaman viiveen takia.

Matalataajuiset harmoniset virrat saatiin vähennettyä melkein nollaan niitä säätämällä. Säätö toteutettiin lisäämällä PR-säätimeen resonanssihaaroja näille harmonisille komponenteille. Toinen harmoninen pystyttiin poistamaan säädön avulla vain osittain. Osan siitä havaittiin johtuvan säätimestä, joka säätää STATCOM:n haarojen DC-jännitteiden keskiarvon nimelliseen arvoonsa. Säätö vaatii kuitenkin toimiakseen tarkan harmonisten virtojen mittauksen, mikä voi olla todellisessa järjestelmässä haastavaa.

Toisen harmonisen virran havaittiin kasvavan jännitesäätömoodissa, kun toimintapiste siirtyi kapasitiivisesta induktiivista kohti. Virran vaimentamiseksi suunniteltiin kaistanestosuodin synkronisaation tuottamalle jännitteen d-komponentille.

PREFACE

This Master of Science Thesis was written for GE Grid Solutions Oy between September 2017 and April 2018. Thesis project has been an interesting experience from which I have learned a lot.

I have many people to thank for their contribution to the thesis. My instructor Ph.D. Anssi Mäkinen within the company offered me very good guidance and comments which improved the quality of the work considerably. MSc. Sami Kuusinen assisted me especially in PSCAD simulations and commented the work at its early stage. Joni Toppari was writing his thesis simultaneously within the company of a subject related closely to my thesis. Sharing thoughts with him gave me many ideas to improve the work.

I would like to thank Assistant Professor Tuomas Messo and Ph.D. Jenni Rekola for examining my thesis. I also would like to thank my supervisor MSc. Vesa Oinonen for offering me this position and organizing the thesis process. In addition, I would like to thank my colleagues for sharing their knowledge with me. Finally, I am especially grateful to my family and girlfriend for their support during my studies and thesis project.

Tampere, 11.4.2018

Jani Honkanen

CONTENTS

LIST OF SYMBOLS AND ABBREVIATIONS

AC	Alternating Current
DC	Direct Current
GTO	Gate-Turn-Off
IGBT	Insulated Gate Bipolar Transistor
IGCT	Integrated Gate Commutated Thyristor
LPF	Low-Pass Filter
MMC	Modular Multilevel Converter
PCC	Point of Common Coupling
PI	Proportional-integral
PR	Proportional-resonant
p.u	Per unit
PWM	Pulse Width Modulation
RMS	Root-Mean-Square
STATCOM	Static Synchronous Compensator
SVC	Static Var Compensator
TCR	Thyristor Controlled Reactor
TDD	Total Demand Distortion
THD	Total Harmonic Distortion
THD_I	Total Harmonic Distortion for Current
THD_V	Total Harmonic Distortion for Voltage
TSC	Thyristor Switched Capacitor

C	Capacitance
E	Voltage magnitude produced by STATCOM
f_1	Fundamental frequency
f_{res}	Resonance frequency
G_h	Transfer function of a harmonic resonant branch
$G_{h,ideal}$	Transfer function of the sum of ideal harmonic resonant branches
$G_{h,non\text{-}ideal}$	Transfer function of the sum of non-ideal harmonic resonant branches
$G_{PR,ideal}$	Transfer function of ideal PR-controller
$G_{PR,non\text{-}ideal}$	Transfer function of non-ideal PR-controller
h	Harmonic component order
h_{max}	Maximum harmonic order used in TDD and THD calculations
i	Instantaneous value of current
$\boldsymbol{i}$	Current vector
I	RMS value of current
I_1	RMS value of fundamental current
i_{cap}	Instantaneous value of capacitor current
I_C	RMS value of capacitor current
i_d	Current d-component
$i_{d,ab,ref}$	Current d-component reference in stationary frame
$i_{d,ref}$	Current d-component reference
I_{DC}	Current DC-component
I_h	RMS current of harmonic component h
$I_{h,PCC}$	RMS current of harmonic component h at PCC
$\bar{I}_{h,STATCOM}$	Harmonic current produced by STATCOM
i_L	Instantaneous value of inductor current

I_{L}	Total demand current
I_{P}	Current active component
i_{q}	Current q-component
$i_{\mathrm{q,ab,ref}}$	Current q-component reference in stationary frame
$i_{\mathrm{q,ref}}$	Current q-component reference
I_{Q}	Current reactive component
I_{resC}	Capacitor current at the resonance frequency
I_{resL}	Inductor or grid current at the resonance frequency
I_{SC}	Short-circuit current
j	Imaginary operator
k	Discrete time instant
K_{I}	Integral gain
K_{Ih}	Integral gain at harmonic order h
K_{P}	Proportional gain
L	Inductance
n	Number of series-connected submodules in one phase
p	Instantaneous active power
P	Active power
q	Instantaneous reactive power
Q	Reactive power
Q_{C}	Capacitive reactive power
Q_{f}	Quality factor of the resonance circuit
R	Resistance
s	Laplace transform variable
S	Apparent power
t	Time
T_{s}	Sampling period
u_{h}	Resonant controller input for one harmonic
v	Instantaneous value of voltage
$\boldsymbol{v}$	Voltage vector
V	RMS value of voltage
v_0	Zero sequence voltage
V_1	RMS value of fundamental voltage
v_{a}	Instantaneous value of a-phase voltage
v_{b}	Instantaneous value of b-phase voltage
v_{c}	Instantaneous value of c-phase voltage
v_{cap}	Instantaneous value of capacitor voltage
V_{cs}	Resonance frequency voltage at the harmonic source terminals
v_{d}	Voltage d-component
V_{DC}	DC-voltage in a submodule capacitor
$\boldsymbol{v}_{\mathbf{dq}}$	Voltage vector in synchronous frame
V_{h}	RMS voltage of harmonic component h
V_{hi}	Harmonic voltage component h caused by source i
$\overline{V}_{\mathrm{h,grid}}$	Harmonic voltage in grid
$\overline{V}_{\mathrm{h,PCC}}$	Harmonic voltage at PCC
$V_{\mathrm{h,PCC}}$	RMS voltage of harmonic component h at PCC
$V_{\mathrm{h,total}}$	Statistical total harmonic voltage from several sources
v_{L}	Instantaneous value of inductor voltage
V_{n1}	Voltage magnitude at node 1
V_{n2}	Voltage magnitude at node 2

V_{p}	Connection point voltage at the parallel resonance frequency
V_{pcc}	PCC voltage
v_{q}	Voltage q-component
V_{s}	Connection point voltage at the series resonance frequency
v_{α}	Voltage α-component
$\boldsymbol{v_{\alpha\beta}}$	Voltage vector in αβ-frame
v_{β}	Voltage β-component
X	Reactance
X_{C}	Capacitive reactance
$X_{\mathrm{h,grid}}$	Grid reactance at harmonic order h
X_{L}	Inductive reactance
X_{source}	Transmission line reactance
X_{T}	Transformer reactance
y_{h}	Resonant controller output for one harmonic
z	Z-transform variable
$\bar{Z}$	Complex impedance
Z_{grid}	Grid impedance magnitude
$\overline{Z}_{\mathrm{h,grid}}$	Grid impedance at harmonic order h
$Z_{\mathrm{h,STATCOM}}$	STATCOM impedance magnitude at harmonic order h
Z_{p}	Parallel impedance at the resonance frequency
α	α-axis
β	β-axis
γ	Exponent used in summing harmonic voltages from different sources
δ	Angle difference between voltages
δu	Imaginary part of voltage drop
Δu	Real part of voltage drop
θ	Transformation angle in *αβ- to dq* -transformation
$\bar{\imath}$	Current phasor
$\bar{v}_1$	Phasor of voltage at node 1
$\bar{v}_2$	Phasor of voltage at node 2
φ	Angle difference between voltage and load current
φ_{h}	Angle of the harmonic component h
φ_{I}	Current angle
$\varphi_{\mathrm{I,h,PCC}}$	Current angle at harmonic order h at PCC
φ_{V}	Voltage angle
$\varphi_{\mathrm{V,h,PCC}}$	Voltage angle at harmonic order h at PCC
$\varphi_{\mathrm{Z,h,STATCOM}}$	STATCOM impedance angle at harmonic order h
ω	Angular frequency
ω_1	Fundamental angular frequency
ω_{c}	Cut-off angular frequency
ω_{pw}	Pre-warp angular frequency
ω_{res}	Resonance angular frequency

1. INTRODUCTION

The increasing use of power electronic converters has caused the amount of harmonic currents and voltages to increase in power systems [1]. Harmonics cause harmful effects on power system components and some devices connected in the grid such as power losses and heating. Thus, their amount is limited by standards and transmission system operators' specifications. Usually, harmonic voltages at the connection point of a customer or a device are limited.

At the same time, the demand for electricity is growing in many areas. Many loads like electric motors need inductive reactive power which reserves transmission capacity from the active power. To maximize the active power transmission capacity of the grid and support grid voltage, reactive power is compensated. One modern solution for reactive power compensation is STATCOM (Static Synchronous Compensator) which consists of a step-down transformer, a reactor and a voltage-source converter [2].

Harmonic performance of a STATCOM system is studied in this thesis. Harmonic current emissions of studied STATCOM are small if grid voltage is sinusoidal but the problem is that they increase as harmonic voltages in grid increase. The purpose of this thesis is to study reasons for the problem and the effect of increased harmonic currents on harmonic voltages at the connection point. Another objective is to find solutions to decrease harmonic current emissions so that standard and specification requirements would be met. Harmonic performance is studied by simulations using a PSCAD-model which is introduced later in the thesis.

In chapter 2, harmonics, their effects and standards that limit them are introduced. In chapter 3, common reactive power compensation systems are described. Especially, the structure of studied STATCOM and its control system are explained. In chapter 4, the phenomenon of increasing STATCOM's harmonic current emissions due to increasing grid harmonic voltages is shown. Harmonic emissions are compared with two considered voltage feedforward options. Moreover, effect of harmonic currents on harmonic voltages at the connection point of STATCOM and the reduction of harmonic currents by increasing the impedance of passive components are studied.

In chapter 5, the impacts of modulator and different control functions on harmonic current emissions are investigated. Solutions to improve these functions in the viewpoint of harmonics are developed or suggested. In chapter 6, future work to improve harmonic performance further is suggested. Finally, conclusions are given in chapter 7.

2. HARMONICS

Harmonic currents and voltages cause adverse effects in power systems. They are produced by nonlinear loads in the network. The growing use of power electronics increases harmonic voltage and current levels in the grid. That is why harmonic emission limits for equipment are set by standards.

In this chapter, harmonics and their harmful effects are described. Also, resonances are described which amplify the existing harmonic levels. Total amount of harmonics can be expressed as indexes which are introduced. Moreover, standards which limit the amount of harmonics are introduced.

2.1 Harmonic currents and voltages

In ideal network currents and voltages are sinusoidal typically at 50 or 60 Hz frequency. In real network, they are usually periodical but distorted which means that they differ from ideal sinusoidal shape. Mathematician Joseph Fourier figured that this kind of signal can be presented as a sum of a constant signal, a sinusoid at fundamental frequency and sinusoids whose frequencies are fundamental frequency multiplied by an integer. These integer multiplied frequencies are called harmonic frequencies. So, current signal *i(t)* can be presented as Fourier series:

$$i(t) = I_{\mathrm{DC}} + \sum_{\mathrm{h}=1}^{\infty} \sqrt{2} I_{\mathrm{h}} \sin(2\pi h f_1 t + \varphi_{\mathrm{h}}), \quad (1.1)$$

where I_{DC} is current DC-component, I_{h} is the RMS (Root-Mean-Square) value of the harmonic component h current, f_1 is fundamental frequency (typically 50 or 60 Hz), t is time and φ_{h} is the angle of harmonic component h [3].

Figure 1 presents a distorted current signal which consists of fundamental frequency as well as 3rd, 5th and 7th harmonic components. It is typical that even harmonics are small in electric networks because most devices behave equally positive and negative polarity. Signal does not contain even harmonics when it is symmetrical with respect to time axis. One exception is half-wave rectifier which draws current only one polarity. [4]

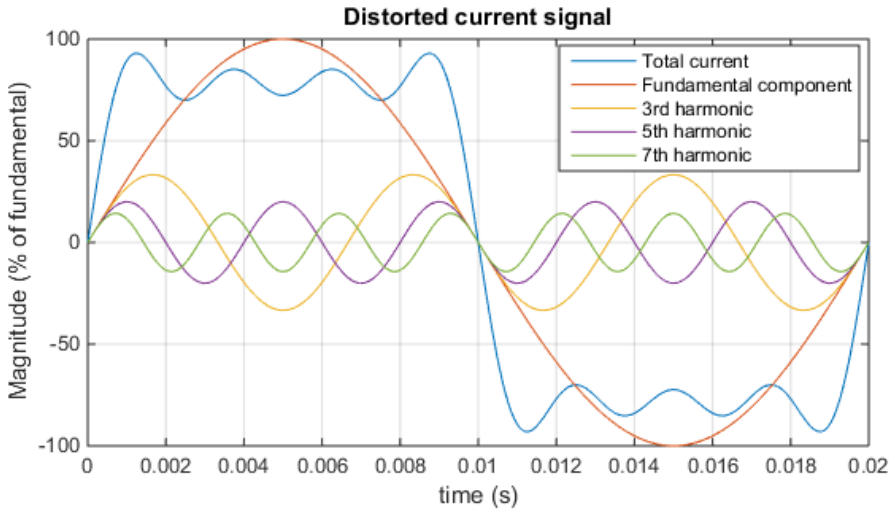

Figure 1. *Total current signal divided to its harmonic components.*

Load is linear when voltage over it and current which flows through it have identical shape. Resistors, capacitors and inductors are linear loads. Voltage and current are not identical shape for nonlinear loads. [4] A simple example is nonlinear resistor shown in Figure 2 whose resistance changes as a function of voltage. The current of resistor is not sinusoidal even though voltage at its terminals is perfectly sinusoidal. It means that the resistor produces harmonic currents.

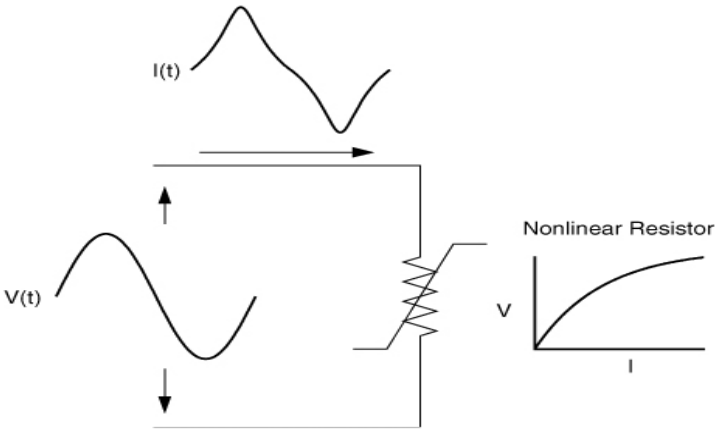

Figure 2. *Nonlinear resistor which produces harmonic currents [4].*

The sources of harmonic currents are typically DC (direct current) drives, AC (alternating current) drives, three-phase power converters, arc furnaces, arc welders, loads, which are fed by DC-DC converters, like home electronics and discharge type lighting such as fluorescent lighting. In addition, if transformer's core saturates, its voltage-current characteristics become nonlinear and it produces harmonic currents. [4]

Harmonic voltages are usually caused by harmonic currents. Figure 3 presents network where produced voltage by generator pure sinusoid. Nonlinear load is connected to the network which draws harmonic currents. The harmonic current components flow through

the network impedances causing voltage drop at each harmonic component. The voltage at the connection point of the load is the original sinusoidal voltage minus the voltage drop. Thus, also the voltage at the connection point contains harmonic components.

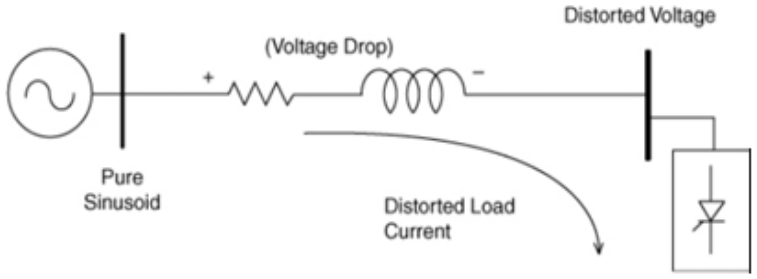

Figure 3. *The principle of harmonic voltage generation [4].*

2.2 Effects of harmonics

Harmonic currents and voltages cause many unfavorable effects. Because harmonic currents are additional currents flowing through grid conductors and transformers they cause power losses. Moreover, harmonic voltages cause additional losses due to eddy currents and hysteresis in transformer core [5]. Also, conductor resistance increases as a function of frequency because of skin and proximity effects [6]. Increased resistance means even more losses.

The additional losses in the network components cause them to heat. The increase of temperature can shorten cable and transformer lifetimes [7, 8]. Also, if voltage peak value increases because of the harmonic voltages, more dielectric stress is caused to the cable and transformer insulators. Increased dielectric stress shortens insulator lifetime [9]. If the system is desired to have a certain lifetime, voltage ratings of the components must be chosen larger than without harmonics.

Harmonic voltages at the connection point of electric motor cause harmonic magnetizing currents in stator and thus harmonic magnetic fluxes in the iron core and rotor [4]. These harmonic fluxes induce eddy currents to the core and harmonic currents to the rotor. Thus, power losses of the motor increase. Some harmonic components are positive sequence which means 120-degree phase shift between phases in normal A-B-C rotation order [4]. Some of them are negative sequence which means same phase shift between phases but in order A-C-B [4]. Positive sequence currents cause torques to same direction and negative sequence currents to another direction than the positive sequence fundamental component [9]. The torque components introduced by harmonics make the total torque pulsating. Pulsating torque causes mechanical stress to the motor and increased vibration [10]. Increased vibration causes higher audible noise in motors [11]. Harmonic currents also increase vibrations and noise in transformers [12].

Especially harmonics whose orders are odd multiples of the third harmonic (3, 9, 15, 21, …) are harmful if they are not considered in the planning of the system. If current is balanced in three phases, these triplen harmonic currents are in the same phase in all phase conductors and they add in the wye point to the neutral conductor. In balanced condition, three times higher current at the triplen harmonic frequency flows in neutral conductor compared to the phase conductors. That may cause neutral conductor overloading and telephone interference. These harmonics in different phase conductors which have equal magnitude and are in phase with each other are called zero sequence harmonics. [4]

The flow of the balanced triplen harmonics, or more generally zero sequence currents, from transformer primary to secondary or vice versa can be blocked by appropriate transformer connections. In Figure 4 is presented the flow of the balanced triplen harmonic currents in wye-delta connection.

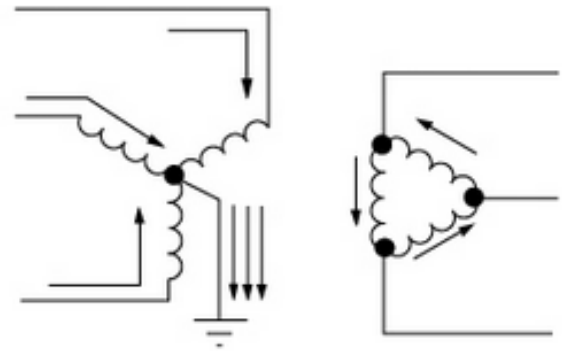

Figure 4. *The flow of balanced triplen harmonic currents in wye-delta transformer [4].*

The triplen harmonics are induced in the secondary but as they are in phase and equal magnitude they flow only in the delta and do not appear in secondary line currents. However, this applies only if currents are balanced in three phases. If triplen harmonic currents are unbalanced, only part of them are zero sequence. Rest of them are positive and/or negative sequence which can flow to the secondary phase conductors also. [4]

Moreover, harmonic currents can cause errors in older electric energy meters [4] or in operation of older electronic relays whose protection limits are based on current peak value [13]. They can also cause interference to electronic appliances and communication networks [1].

2.3 Resonances

Shunt capacitor banks are used to compensate reactive power in the network which is explained in detail later. However, they may cause parallel or series resonances which amplify existing harmonic currents and voltages. Figure 5 presents the principle of how parallel resonance is composed. There is a current source which emits harmonic currents. From its viewpoint inductive grid impedance and capacitor bank's capacitive impedance

are parallel. In the figure, grid impedance consists of transmission line reactance X_{source} and transformer reactance X_{T}.

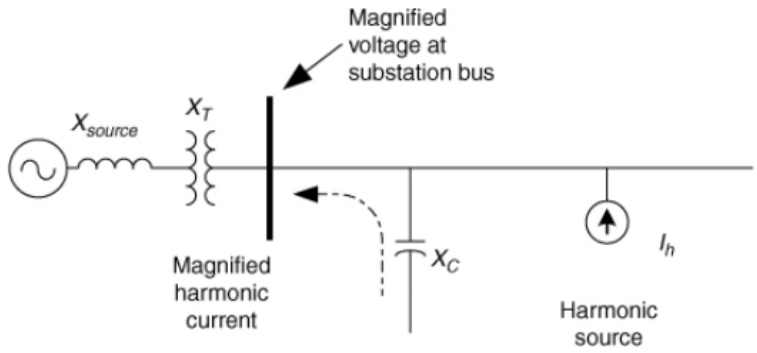

Figure 5. *The principle of parallel resonance [4].*

Parallel resonance occurs at the resonance frequency

$$f_{\text{res}} = \frac{1}{2\pi}\sqrt{\frac{1}{LC} - \frac{R^2}{4L^2}} \approx \frac{1}{2\pi}\sqrt{\frac{1}{LC}}, \tag{1.2}$$

where L is the sum of network and transformer inductances, R the sum of their resistances and C is the capacitor bank's capacitance. Resistance is small compared to the inductance so resonance occurs approximately at the frequency where inductive and capacitive reactances are equal. [4]

At the resonance frequency, the impedance magnitude seen by the current source is

$$Z_{\text{p}} = \frac{X_{\text{C}}(X_{\text{L}}+R)}{X_{\text{C}}+X_{\text{L}}+R} = \frac{X_{\text{C}}(X_{\text{L}}+R)}{R} \approx \frac{{X_{\text{L}}}^2}{R} = \frac{{X_{\text{C}}}^2}{R} = Q_{\text{f}}X_{\text{L}} = Q_{\text{f}}X_{\text{C}}, \tag{1.3}$$

where capacitive reactance X_{C} and inductive reactance X_{L} are equal magnitude but different sign and thus their sum is zero. Q_{f} is called the quality factor of a resonant circuit. [4] Because reactance is usually larger than resistance, the quality factor and parallel impedance are quite high. Harmonic current at the resonance frequency causes voltage V_{p} to capacitor connection point [4]:

$$V_{\text{p}} = Z_{\text{p}}I_{\text{h}} = Q_{\text{f}}X_{\text{L}}I_{\text{h}}. \tag{1.4}$$

Thus, high voltage harmonic component at the resonance frequency occurs at the capacitor connection point. Also, currents through capacitor and network increase considerably at the resonance frequency according to the equations below [4]:

$$I_{\text{resC}} = \frac{V_{\text{p}}}{X_{\text{C}}} = \frac{Q_{\text{f}}X_{\text{C}}I_{\text{h}}}{X_{\text{C}}} = Q_{\text{f}}I_{\text{h}}, \tag{1.5}$$

$$I_{\text{resL}} = \frac{V_{\text{p}}}{X_{\text{L}}} = \frac{Q_{\text{f}}X_{\text{L}}I_{\text{h}}}{X_{\text{L}}} = Q_{\text{f}}I_{\text{h}}. \tag{1.6}$$

Series resonance is another type of resonance whose principle is presented in Figure 6. From the viewpoint of harmonic current source, network inductive lines and transformer and capacitive capacitor bank are in series. At the resonance frequency, the inductive reactance and capacitive reactance have equal magnitude but different sign. Thus, only resistances of the components limit the current that flows from the harmonic current source to the capacitor bank.

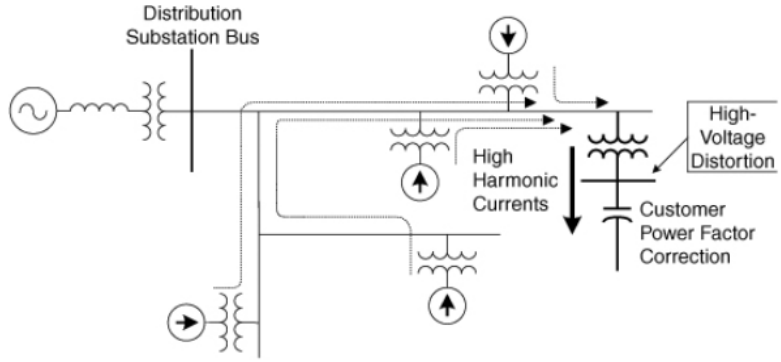

Figure 6. *The principle of series resonance [4].*

Voltage V_s at the resonance frequency at the connection point of capacitor is

$$V_s = \frac{X_C}{X_C+X_L+R} V_{cs} \approx \frac{X_C}{R} V_{cs}, \tag{1.7}$$

where X_C is the capacitive reactance of the bank, X_L is the inductive reactance of the transmission line and possible transformer, R the sum of the all component resistances and V_{cs} the resonance frequency voltage component at the connection point of the harmonic current source [4]. As reactance is larger than resistance, voltage at the resonance frequency increases compared to the original harmonic voltage magnitude.

Increased current at the resonance frequency causes additional losses in capacitors and thus their heating. Increased voltage at the resonance frequency may increase the voltage peak value and thus cause more dielectric stress to the capacitors' insulators. These impacts may shorten capacitors' lifetimes or cause instant damage to them [9].

2.4 Harmonic indexes

The amount of harmonic currents and voltages are often expressed as a ratio of harmonic component RMS value to fundamental component RMS value. Combined effect of harmonics is typically expressed as an index THD (Total Harmonic Distortion) which is defined for voltage as follows:

$$\mathrm{THD_V} = \frac{\sqrt{\sum_{h=2}^{hmax} {V_h}^2}}{V_1}, \tag{1.8}$$

where V_h is the RMS voltage of harmonic component h, V_1 is the RMS value of fundamental voltage and h_{max} is typically 50 [14]. Current THD can be defined similarly:

$$\mathrm{THD_I} = \frac{\sqrt{\sum_{h=2}^{hmax} {I_h}^2}}{I_1}, \tag{1.9}$$

where I_h is the RMS current of harmonic component h and I_1 is the RMS value of fundamental current [14].

THD is a good indicator of the amount of harmonic voltages because the fundamental voltage component varies only a few percent depending on the loading situation. On the other hand, fundamental current component varies significantly as a function of loading. When loading is light, current THD can be high even though harmonic currents are not a problem to the network. Therefore, another index called TDD (Total Demand Distortion) is introduced for current. [4] It is defined by equation:

$$\mathrm{TDD} = \frac{\sqrt{\sum_{h=2}^{hmax} {I_h}^2}}{I_L}, \tag{1.10}$$

where I_h is the RMS current of harmonic component h, h_{max} typically 50 and I_L total demand current. I_L is defined by measuring fundamental frequency current RMS value, choosing the maximum value of the month and calculating average of the maximum values from the previous 12 months. This index describes usually the amount of harmonic currents in the network better than THD. [4]

2.5 Harmonic emission standards

The most widespread standards to limit harmonic currents and voltages are IEEE standard 519 and IEC 61000-series standards [10]. They define recommendations for harmonic current and voltage limits. Table 1 presents IEEE 519 recommendations for harmonic voltages as percent of fundamental component and THD at different grid voltage levels.

The concept PCC in the table is Point of Common Coupling which is electrically the closest point to the customer in the grid where other loads are, or could be, connected. Measurements are performed at PCC since typically loads cancel part of the harmonic currents the other loads produce. Thus, if measurements are performed closer to the customer, they will not provide realistic currents flowing to the grid. [14]

Table 1. *IEEE 519 harmonic voltage limits [14].*

Bus voltage *V* at PCC	Individual harmonic (%)	THD (%)
$V \leq 1.0$ kV	5.0	8.0
1 kV < $V \leq$ 69 kV	3.0	5.0
69 kV < $V \leq$ 161 kV	1.5	2.5
$V >$ 161 kV	1.0	1.5

The short time values (average of 10 minutes) should be less than the values in Table 1 95 percent of the time weekly. Very short time values (average of 3 seconds) should be less than 1.5 times the values in the table for 99 percent of the time daily. [14]

In IEEE 519 current distortion limit recommendations are given for different system voltage levels. Because high voltage systems are studied in this thesis, only their limits are shown here. Table 2 presents recommended current distortion limits for systems rated from 69 kV to 161 kV. Individual harmonic currents are expressed in percent of the total demand current I_L. The limits in the table are for odd harmonics only. Even harmonic components are limited to 25 percent of the odd harmonic limits. Recommendations vary also as a function of I_{SC}/I_L. I_{SC} means the short-circuit current at PCC. For all power generation equipment, the current limits are the first-row limits regardless of the actual I_{SC}/I_L-ratio. [14]

Table 2. *IEEE 519 harmonic current limits for systems rated from 69 kV to 161 kV [14].*

Individual harmonic component *h* in percent of I_L						
I_{SC}/I_L	**$3 \le h < 11$**	**$11 \le h < 17$**	**$17 \le h < 23$**	**$23 \le h < 35$**	**$35 \le h \le 50$**	**TDD**
<20	2.0	1.0	0.75	0.3	0.15	2.5
20 - 50	3.5	1.75	1.25	0.5	0.25	4.0
50 - 100	5.0	2.25	2.0	0.75	0.35	6.0
100 - 1000	6.0	2.75	2.5	1.0	0.5	7.5
>1000	7.5	3.5	3.0	1.25	0.7	10.0

Weekly 95 percent of the short time (10 minutes) harmonic currents should be less than the values given in Table 2. Weekly 99 percent of the short time (10 minutes) harmonic currents should be less than 1.5 times the values in the table and daily 99 percent of the very short values (3 seconds) should be less than 2.0 times the values in the table. [14]

Table 3 presents recommended current distortion limits for systems rated above 161 kV. The clarifications made for lower voltage level systems apply for them also.

Table 3. *IEEE 519 harmonic current limits for systems rated above 161 kV [14].*

Individual harmonic component *h* in percent of I_L						
I_{SC}/I_L	**$3 \le h < 11$**	**$11 \le h < 17$**	**$17 \le h < 23$**	**$23 \le h < 35$**	**$35 \le h \le 50$**	**TDD**
<20	1.0	0.5	0.38	0.15	0.1	1.5
20 - 50	2.0	1.0	0.75	0.3	0.15	2.5
≥50	3.0	1.5	1.15	0.45	0.22	3.75

IEC 61000-series includes a few standards which define limits for harmonics. IEC 61000-2-2 defines compatibility levels for harmonic voltages in low voltage networks [15] and IEC 61000-2-4 defines compatibility levels for harmonic voltages in industrial plants at

nominal voltages up to 35 kV [16]. IEC 61000-2-12 defines compatibility levels for harmonic voltages in medium voltage power systems from 1 kV to 35 kV [17].

IEC 61000-3-2 sets limits for harmonic current emissions for equipment which input current is equal or below 16 amperes [18] and IEC 61000-3-12 for equipment which input current is between 16 and 75 amperes [19]. Both standards are for low voltage networks.

IEC/TR 61000-3-6 technical report gives indicative planning levels for harmonic voltages in medium, high and extra high voltage power systems [20]. Table 4 presents the planning levels for high voltage (from 35 kV to 230 kV) and extra high voltage (higher than 230 kV) systems in percent of the fundamental voltage.

Table 4. *IEC/TR 61000-3-6 planning levels for harmonic voltages in systems which nominal voltage is higher than 35 kV [20].*

Odd harmonics non-multiple of 3		**Odd harmonic multiple of 3**		**Even harmonics**	
Harmonic order *h*	**Harmonic voltage (%)**	**Harmonic order *h***	**Harmonic voltage (%)**	**Harmonic order *h***	**Harmonic voltage (%)**
5	2	3	2	2	1.4
7	2	9	1	4	0.8
11	1.5	15	0.3	6	0.4
13	1.5	21	0.2	8	0.4
$17 \leq h \leq 49$	$1.2*17/h$	$21 < h \leq 45$	0.2	$10 \leq h \leq 50$	$0.19*10/h + 0.16$

In IEC/TR 61000-3-6, total harmonic distortion planning level for high and extra high voltage systems is 3 % [20]. It is not so strict as IEEE 519 limit for high voltage systems.

For reactive power compensation systems, explained more specifically in the next chapter, transmission system operators usually specify the limits for harmonic voltages at PCC of the shunt compensator. The limits may be based on the standards explained above. If the existing harmonic voltages in grid are large, the harmonic limits for the compensator may be strict.

3. REACTIVE POWER COMPENSATION

Like harmonics, reactive power flow is an undesired phenomenon in power systems. However, reactive power is needed to build magnetic fields for example in transformers, generators and motors. This reactive power type is called inductive. Reactive power is also needed to build electric fields for example in capacitors. This type of reactive power is called capacitive. Reactive power is not converted into heat, light or torque like active power but fluctuates between capacitive and inductive loads. Still it increases the current flowing in the network. [21] Due to growth of current, transmission system losses increase [22]. Reactive power should be compensated for various reasons such as to increase active power transmission capacity in the grid, to keep the grid node voltages in the desired limits, to improve stability of the network and to mitigate power oscillations [23].

In this chapter, the definition of reactive power, principles of its compensation and different compensation solutions are introduced. Basic compensation solutions are passive shunt and series compensators. Modern compensators are based on power electronics. The most common power electronic compensators are SVC (Static Var Compensator) and STATCOM (Static Synchronous Compensator) which are introduced. Studied STATCOM topology in this thesis is MMC (Modular Multilevel Converter) whose operation is described. The basics of STATCOM's control system and modulator are also explained. Compensators have different harmonic current emissions and effect on resonances which are described for each compensator.

3.1 Reactive power

Reactive power definition can be derived from instantaneous power p which is

$$p(t) = vi, \tag{3.1}$$

where v is instantaneous value of voltage and i instantaneous value of current. The average value of power is called active power P and assuming sinusoidal voltage and current it is

$$P = VI\cos(\varphi_{\mathrm{V}} - \varphi_{\mathrm{I}}), \tag{3.2}$$

where V is the RMS value of voltage, I the RMS value of current, φ_{V} voltage angle and φ_{I} current angle.

The instantaneous power includes a term oscillating at twice the frequency of current and voltage and whose average is zero. The peak value of this oscillating power is called reactive power Q: [21]

$$Q = VI\sin(\varphi_{\mathrm{V}} - \varphi_{\mathrm{I}}). \tag{3.3}$$

Reactive power is positive and called inductive if voltage leads current and negative and called capacitive if current leads voltage. There is also a third power term called apparent power S which is the product of voltage and current RMS values:

$$S = VI. \tag{3.4}$$

The following relation applies for powers:

$$S = \sqrt{P^2 + Q^2}. \tag{3.5}$$

Increased reactive power means thus increased apparent power and current. When voltage and current contain harmonics, also instantaneous power includes harmonics. In a common definition, reactive power still refers to reactive power caused by fundamental frequency variables and harmonics are considered in additional power term called distortion power [21].

3.2 Passive shunt compensators

Many loads draw inductive reactive power from the network. A simple way to compensate it is to connect a capacitor as shunt to the transmission line. Shunt compensation principle is shown in Figure 7.

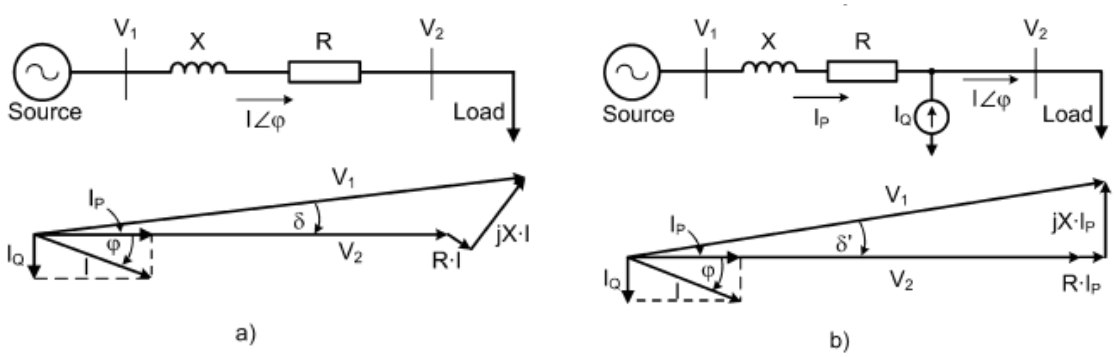

Figure 7. *Principle of shunt compensation, a) situation without compensation, b) with compensation [23].*

In Figure 7. a) load is inductive-resistive which means that current I lags voltage V_2. Current has an active current component I_{P} and a reactive component I_{Q} which of whom the latter should be compensated. In Figure 7. b) current source is added parallel to the load having the same reactive component magnitude I_{Q} as the load but a 180-degree phase shift. This capacitive current component cancels the inductive current drawn by the load. The resulting current drawn from the grid has only an active component which means that only active power is transferred. Because total current is smaller, power losses decrease. Therefore, more active power can be transmitted with same losses.

As capacitive current is needed for compensation, a capacitor can be used instead of current source. However, capacitor current I_C and thus supplied reactive power Q_C depend on grid voltage V at its connection point according to the equations below.

$$I_C = \frac{V}{X_C}, \tag{3.6}$$

$$Q_C = VI_C = \frac{V^2}{X_C}, \tag{3.7}$$

where X_C is the capacitive reactance of the capacitor. If voltage varies, also supplied reactive power varies. Thus, the reactive power consumed by the load will not be compensated fully if it does not change likewise.

Shunt capacitors can be fixed or mechanically switched. In a fixed capacitor bank the capacitance is not controllable. A switched capacitor bank consists of multiple capacitor units which can be switched on and off individually. Therefore, amount of capacitive reactance and supplied reactive power can be controlled. However, mechanical switches (circuit breakers) are quite slow and can not be switched on and off many times a day, so capacitors having mechanical switches can not be used for dynamic compensation of rapidly changing loads. [22]

In transmission networks the objective is not to compensate reactive power of single loads. Purpose is to impose an optimal voltage profile in grid nodes so that grid transfer capability would be maximized, losses minimized and high voltage stability achieved [22]. Reactive power affects grid voltages which can be shown by considering a simple grid consisting of two nodes. Grid and phasor diagram of its voltages and currents are presented in Figure 8.

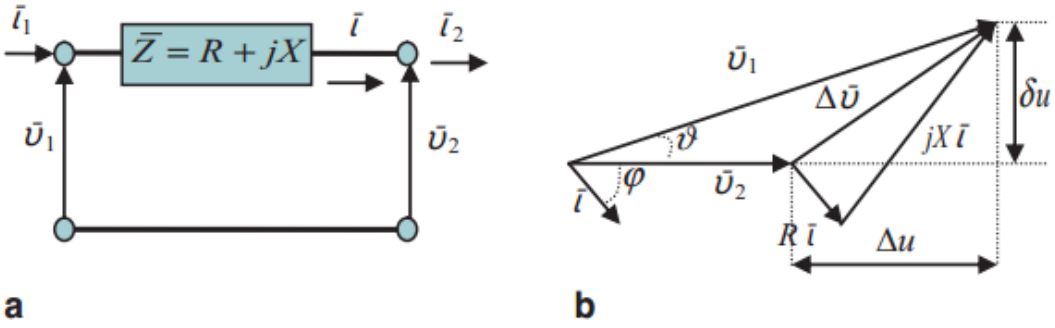

Figure 8. *a) Simple grid and b) phasor diagram of its variables to illustrate reactive power effect on voltage [22].*

In the diagram load is inductive-resistive so the angle difference φ between $\bar{U}_2$ and $\bar{I}$ is positive. The current components are $I_P = I\cos\varphi$ and $I_Q = I\sin\varphi$ and for inductive loads $\bar{I} = I_P - jI_Q$, where j is the imaginary operator. The complex voltage drop in grid impedance has real and imaginary components:

$$\Delta u = RI_{\mathrm{P}} + XI_{\mathrm{Q}}, \tag{3.8}$$

$$\delta u = XI_{\mathrm{P}} - RI_{\mathrm{Q}}, \tag{3.9}$$

which are shown in the phasor diagram [22]. Complex power in one phase is

$$S = V_{\mathrm{n2}}\left(I_{\mathrm{P}} + jI_{\mathrm{Q}}\right) = P + jQ, \tag{3.10}$$

where V_{n2} is voltage at node 2. Equations 3.8 and 3.9 can be written as a function of powers as follows:

$$\Delta u = \frac{RP+XQ}{V_2}, \tag{3.11}$$

$$\delta u = \frac{XP-RQ}{V_2}. \tag{3.12}$$

Because transmission grid's resistance is usually much smaller than reactance, the voltage drop components become [22]

$$\Delta u \approx \frac{XQ}{V_2}, \tag{3.13}$$

$$\delta u \approx \frac{XP}{V_2}. \tag{3.14}$$

Voltage drop magnitude, which is close to Δu, is mainly affected by reactive power injected from node 1 to node 2 and phase difference between node voltages is mainly affected by active power flow between nodes [22]. Grid impedance is usually inductive-resistive at fundamental frequency, which means that X is positive. When load is capacitive instead of inductive the reactive power changes polarity from positive to negative. Voltage drop is then negative and voltage at node 2 is higher than at node 1. This means that capacitors can be used to increase voltage at the nodes they are placed. When the capacitive reactive power propagates further, it increases also the voltages at the nodes near the node where capacitor is placed according to the same equations.

Shunt capacitors can be used to support voltage but they have some disadvantages. As mentioned they are either fixed or mechanically switched and thus can not be used for dynamic voltage compensation. Another problem of shunt capacitor is that it is used to support voltage but as voltage decreases, its reactive power output decreases proportional to voltage squared according to equation 3.7 [22]. Also, as the load is light and voltage high, capacitor's reactive power output increases which increases the voltage even more [22].

Capacitor itself is not a suitable compensator because of the resonance phenomenon described in chapter 2.3. To avoid resonances with the inductive network a reactor must be connected in series with the capacitor. The reactor and capacitor form a series resonance

circuit which is tuned typically to 189 Hz in 50 Hz grid. The series connection absorbs a small portion of the fifth and seventh harmonic currents. The tuning frequency of 189 Hz is normally the most economical choice considering the needed amount of reactor material. [21]

Moreover, when capacitor bank is energized or grid voltage changes fast in transient situations, capacitor current changes stepwise to a large value according to basic relation of capacitor voltage and current:

$$i_{\mathrm{cap}}(t) = C\,\frac{dv_{\mathrm{cap}}(t)}{dt}, \tag{3.15}$$

where i_{cap} is the capacitor current, C capacitance, v_{cap} capacitor voltage and t time. This high current flowing through the grid causes oscillations in grid voltage. Adding the series reactor reduces this inrush current and voltage oscillations. [24]

Shunt compensators can be designed to supply reactive power and act also as harmonic filters to improve power quality. In this case, their impedances are capacitive at frequencies below the tuning frequency and inductive above the tuning frequency. The idea is to compensate reactive power at fundamental frequency and offer a low impedance path for some harmonic currents so that they would flow to the filter instead of grid. [21]

There are many different filter configurations. Some of the basic configurations are presented in Figure 9.

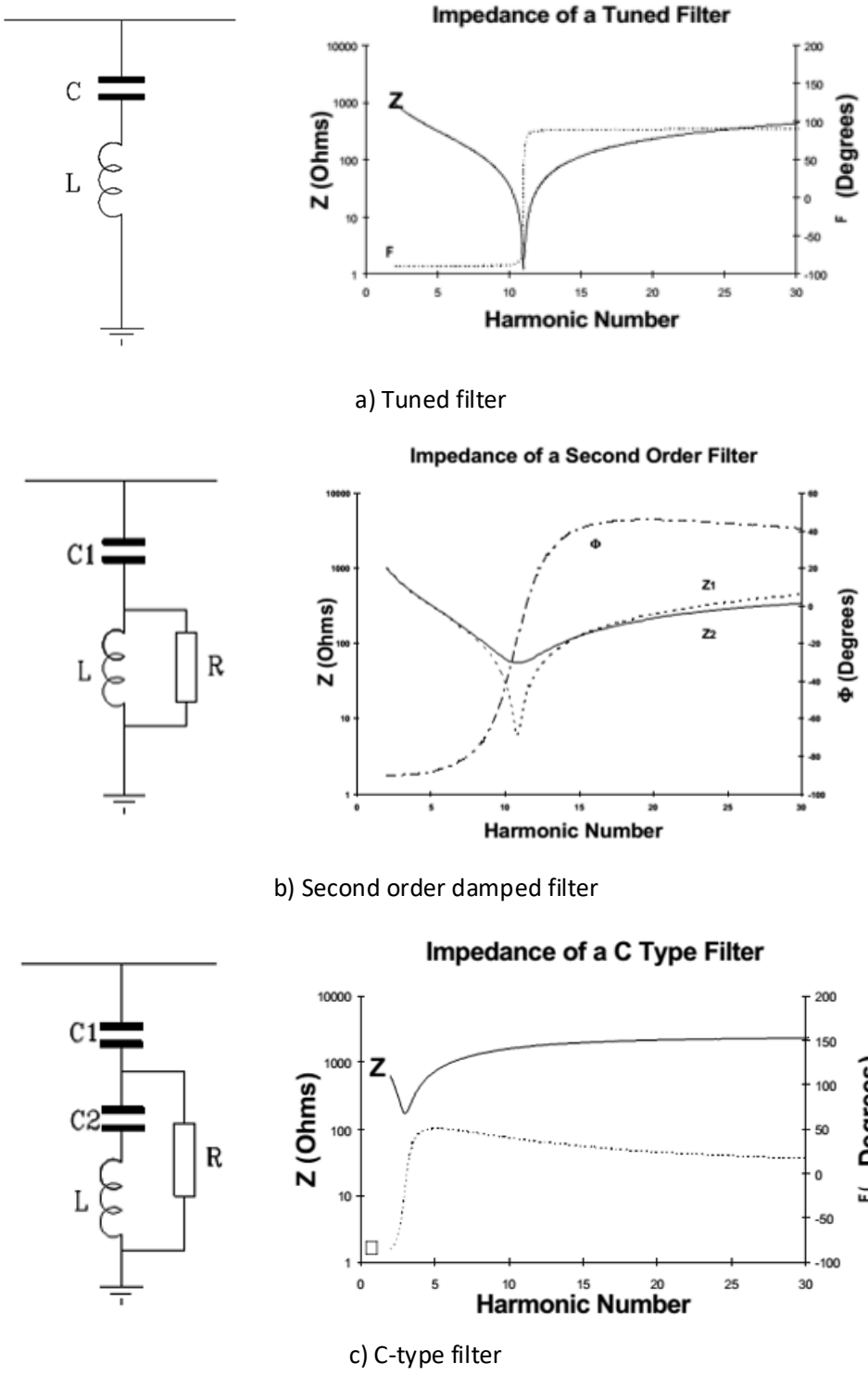

Figure 9. *Typical harmonic filters and their impedances: a) tuned filter, b) second order damped filter and c) C-type filter [25].*

The simplest of the filters is a tuned filter which consists of a series connection of capacitor and reactor. At the tuning frequency of series connection, the impedance of the filter is only the resistance of the reactor [25]. The tuning frequency is chosen to be almost the frequency of desired harmonic to be filtered but not precisely to avoid extremely high

currents flowing to the filter [21]. The advantages of a tuned filter are that it is simple, it offers optimum attenuation for one harmonic current and its losses are low. Its disadvantages are that multiple filters are needed if many harmonics need attenuation and its tuning frequency is susceptible to de-tuning factors such as component manufacturing tolerances, temperature changes and grid frequency variations. The de-tuning can be avoided by making the inductance adjustable using inductor taps but that increases costs. [25]

A second order damped filter is similar to tuned filter but a resistor is connected in parallel with the reactor. This addition reduces the impedance magnitude dip at the tuning frequency but broadens the dip around it. The advantages of a damped filter are that it can attenuate multiple harmonics at the same time and the broadened impedance dip means that the attenuation at desired frequency is not so sensitive to de-tuning factors. Disadvantages are the reduced attenuation at the tuning frequency and higher losses at both fundamental and harmonic frequencies because of the added resistor. [25]

In a C-type filter second capacitor is added in series with the reactor. Second capacitor and inductor form a series resonance at the fundamental frequency and thus all fundamental current flows through the series connection instead of resistor. Advantage is that losses at the fundamental frequency are minimized. Disadvantage is that the LC-circuit resonance frequency may change because of the previously mentioned de-tuning factors and then the current flows also through the resistor. Thus, resistor needs to be rated for part of the fundamental current also or the inductor needs to be adjustable. Also, the harmonic attenuation is slightly worse than with second order damped filter. [25]

Adding a filter to the network may cause parallel resonances between the filter and network. The impedance of the filter is capacitive below the tuning frequency and the grid impedance is usually inductive. This means that parallel resonance might occur at some frequency below the tuning frequency. [21] The possible resonances should be considered in filter design. Usually the customer specifies the network harmonic impedances which will change over time because of different system configurations and connection and disconnection of loads and generators. Often the network impedances are presented as impedance envelopes such as sector or circle diagrams that include all the possible impedance values. [25] Using this data possible resonances can be identified.

3.3 Passive series compensators

Reactive power can be compensated also by adding a capacitor in series with the transmission line. The idea is to decrease the inductive reactance of the power line at the fundamental frequency and consequently decrease the absorbed inductive reactive power in the line [23]. Series capacitor with its protection system is shown in Figure 10. Typically, a metal oxide varistor, a spark gap and a fast bypass switch are used as overvoltage protection for the compensator [23].

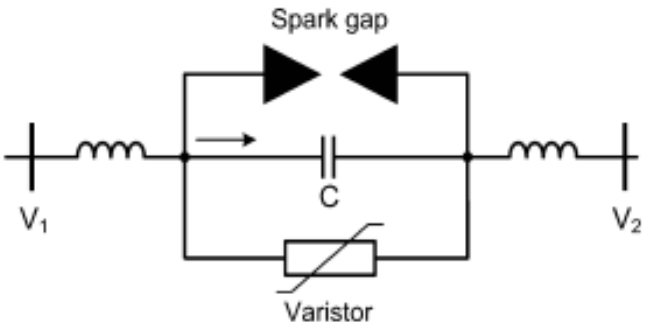

Figure 10. *Series capacitor compensator and its protection system [23].*

Active power transmitted through the transmission line is without compensation

$$P = \frac{V_{n1} V_{n2} \sin \delta}{X_L}, \tag{3.16}$$

where V_{n1} is voltage magnitude at node 1, V_{n2} voltage magnitude at node 2, δ voltage angle difference between nodes 1 and 2 and X_L is inductive reactance of the line [26]. When capacitor is added, the transmitted power is

$$P = \frac{V_{n1} V_{n2} \sin \delta}{X_L - X_C}, \tag{3.17}$$

where X_C is the capacitive reactance of the capacitor bank. Adding the capacitor bank thus increases the active power transmission capacity. [26] If the inductive reactance is fully compensated, meaning X_C=X_L, a series resonance occurs at fundamental frequency [27]. To avoid very large fundamental current, it is not recommended to compensate more than 80 % of the reactance [27].

3.4 SVC

Static Var Compensator (SVC) is a controllable shunt compensator based on power electronic switches. Typically, it consists of a step-down transformer, thyristor-controlled reactors (TCRs), thyristor-switched capacitors (TSCs) and harmonic filters [28]. A typical SVC configuration is presented in Figure 11. Because of controllable thyristor switches, shunt reactance and reactive power output of SVC can be controlled [29]. That makes it possible to control also the PCC voltage as equation 3.13 states.

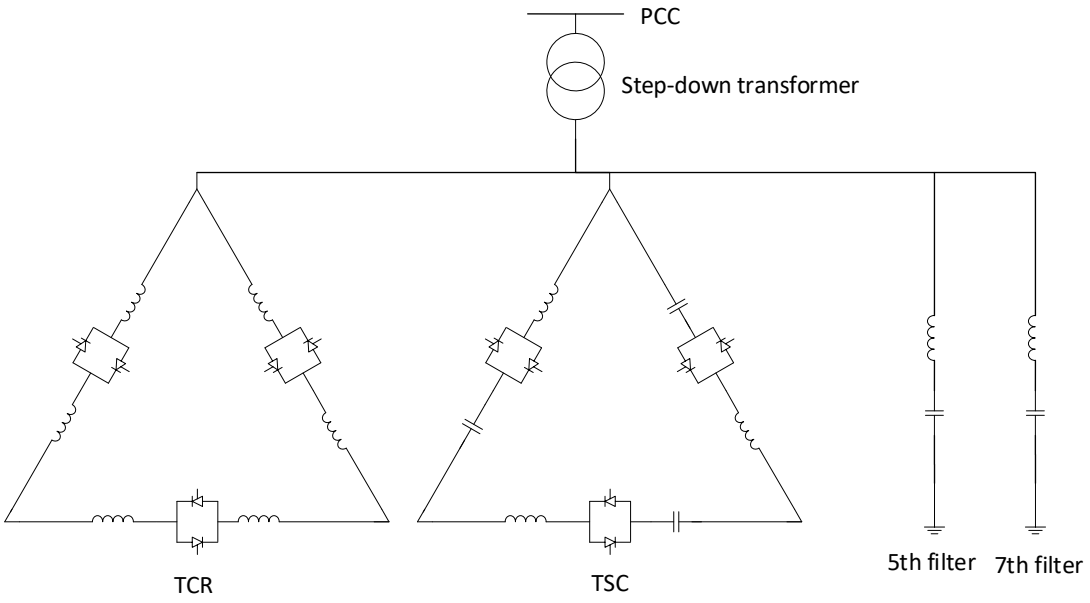

Figure 11. *Typical SVC configuration.*

TCR consists of anti-parallel connected pair of thyristor valves in series with a reactor. One of the thyristor valves conducts positive half-waves of current and the other negative half-waves. The starting of current flow is determined by the thyristor firing angle which is measured from the moment of voltage zero crossing. In TCR, thyristor firing angles are controlled from 90 to 180 degrees. 90° angle means that the reactor current is continuous and 180° that the thyristors do not conduct at all. The current flow of thyristor ceases naturally as it reaches zero. The firing angle determines the impedance of TCR seen from the connection point. Consequently, fundamental inductive current component changes as the applied voltage magnitude is constant. However, when firing angle is between 90 and 180 degrees, the reactor current is non-sinusoidal and harmonics are generated. [28] The harmonics in phase current produced by symmetrically controlled three-phase delta-connected TCR are presented as a function of firing angle in Figure 12. Harmonics are expressed in percent of produced fundamental frequency phase current.

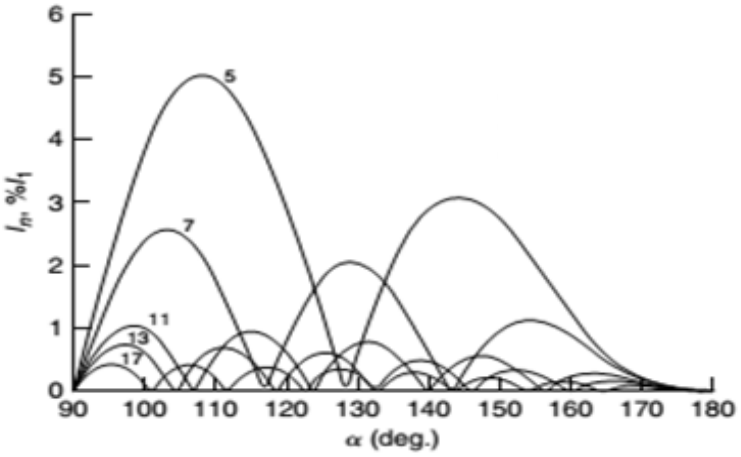

Figure 12. *Harmonic current emissions of symmetrically controlled delta-connected three-phase TCR as a function of thyristor firing angle [28].*

As can be seen, different harmonics do not peak at the same firing angle. When both anti-parallel thyristor valves are fired with same firing angle, the even harmonic currents do not exist. When three TCRs are connected in delta and are controlled symmetrically, the produced triplen harmonics (3, 9, 15, …) are equal in each branch and thus circulate in the delta and do not flow into the network. Because the TCR produces quite large harmonics at especially 5^{th} and 7^{th} harmonics, harmonic filters are usually needed. The filters also provide capacitive reactive power at fundamental frequency. [28]

TSC consists of anti-parallel connected pair of thyristor valves in series with a capacitor and current limiting reactor. As described earlier for passive shunt compensators, capacitor needs the small reactor to limit the current in overvoltage and switching situations. The reactor is usually chosen so that the series resonance frequency of the circuit is between the 4^{th} and 5^{th} harmonic. This ensures that TSC does not create a resonance circuit with the network at some harmonic frequency. The thyristors are only switched on or off so there is not firing angle control as in TCR. This also means that the current of TSC is sinusoidal in steady-state. [28]

3.5 STATCOM

Static Synchronous Compensator (STATCOM) is also a shunt compensator based on power electronic switches but its operating principle differs from SVC's. STATCOM is a controllable voltage source behind a reactor [2]. It can produce its rated inductive and capacitive reactive current independent of grid voltage whereas SVC's maximum reactive current depends linearly on grid voltage [2]. Other STATCOM advantages over SVC are smaller size, faster response, and possibility to have short-term transient overload capability [2]. Also, harmonic current emissions are lower especially with STATCOM based on multilevel converter [23]. STATCOM is however more expensive [30].

3.5.1 Operating principle

STATCOM consists of a coupling or step-down transformer, a coupling reactor and a voltage source converter. The voltage source converter is comprised of a capacitor energy storage and a DC-AC converter. [2] Basic configuration of STATCOM is presented in Figure 13 with phasor diagrams of its electrical variables in capacitive and inductive operating points.

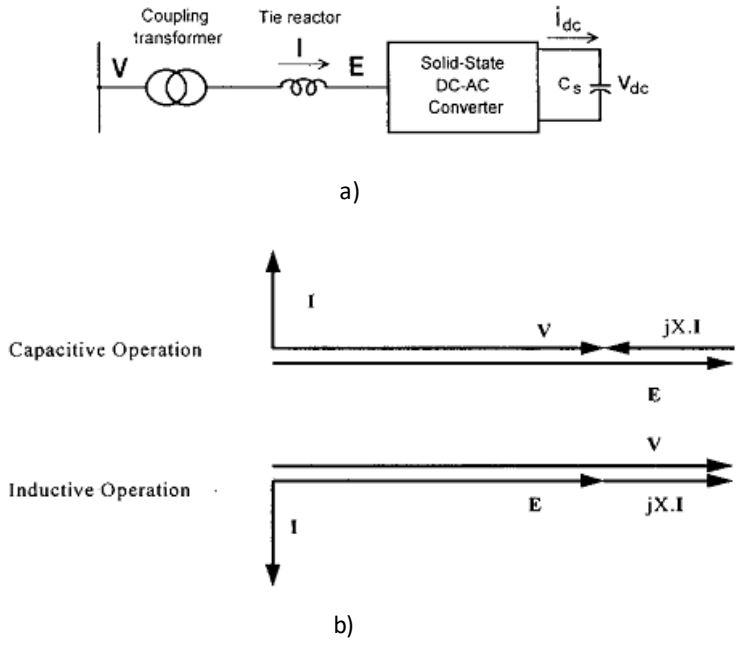

Figure 13. *STATCOM, a) basic configuration, b) phasor diagrams in capacitive and inductive operating points [2].*

STATCOM's reactive power generation is based on the voltage magnitude difference between grid connection point voltage V and converter produced voltage E. If losses are neglected, converter produces three-phase voltages in phase with the grid three-phase voltages. Then, the drawn reactive current in one phase is

$$I_{\mathrm{Q}} = \frac{V-E}{X}, \tag{3.18}$$

where X is the sum of transformer and coupling reactor reactances [2]. The reactive power drawn from the grid is therefore [2]

$$Q = VI_{\mathrm{Q}} = \frac{1-\frac{E}{V}}{X}V^2. \tag{3.19}$$

By controlling the magnitude of produced voltage E, the reactive power output can be controlled. When the produced voltage magnitude is larger than grid voltage magnitude, resulting current is leading grid voltage and the converter generates capacitive reactive power. If the produced voltage magnitude is smaller than grid voltage, lagging current is

produced and inductive reactive power is absorbed. [2] Resulting currents in both situations are illustrated in phasor diagrams in Figure 13.

In a real STATCOM, there are losses in converter switches which causes the capacitor energy to discharge. The energy to cover these losses can be supplied from the grid by making the converter produced voltage lag the grid voltage by a small angle as equation 3.16 indicates. The capacitor voltage can be thus kept in desired limits. [2]

There are different topologies, switching devices and switching strategies used in the voltage-source converter of STATCOM. Basic topologies are two-level, three-level and multilevel converters, where the level corresponds to the number of possible voltage output levels in one phase of the converter. Common switching devices are GTO (Gate-Turn-Off) thyristor, IGBT (Insulated Gate Bipolar Transistor) and IGCT (Integrated Gate Commutated Thyristor). GTO thyristor is rated for higher currents but IGBT and IGCT have faster response times and lower switching losses. [31]

In low-level converters, switching of a single switch on and off can be done once or many times in a fundamental cycle. If it is done many times, switching pattern is achieved by comparing a sinusoidal reference signal and a high-frequency triangle carrier. This switching method is called PWM (Pulse Width Modulation). If switching is done only once in a fundamental cycle, harmonics in produced voltage will be large. This can be overcome by having multiple converters connected parallel, triggering the switches of parallel converters with appropriate displacement angles with respect to each other and summing the produced voltages together using appropriate transformer connections. The result is a multilevel voltage waveform at transformer primary which approximates a sinusoid. When PWM is used in low-level converters, the voltage waveform will be closer to sinusoid which decreases the harmonic voltages. However, the switching losses in high-power low-level converters are large and thus PWM is not generally used in them. In multilevel converters, the desired voltage is produced from several capacitor DC-voltage sources. Thus, low harmonic distortion in voltage can be achieved with fundamental frequency switching of individual converter if the level number is high enough. [31]

Common for all the voltage-source converters is that the produced voltage only approximates a sinusoid. Thus, there are harmonics in output voltage. The harmonic voltages cause harmonic currents to be drawn from the grid [2]. Harmonic currents decrease as a function of frequency because of the increasing reactances in transformer and coupling reactor [2].

3.5.2 Modular Multilevel Converter

Modular Multilevel Converter (MMC) is a common multilevel converter type which can act as a voltage source in STATCOM. It consists of a series connection of submodules in each of the three phases. One submodule, called full-bridge, is comprised of four switches

and one capacitor. A switch is typically an IGBT and a diode connected anti-parallel which enables current flow to both directions. One full-bridge submodule can produce three output voltage levels $+V_{DC}$, 0 or $-V_{DC}$, where V_{DC} is the voltage in the submodule capacitor. The total voltage of the series connection is the sum of individual submodule voltages. Therefore, it is possible to produce $2n+1$ voltage levels in one phase, where n is the number of series-connected submodules. Submodules are switched so that a staircase voltage waveform is produced which approximates a sinusoid. The single-phase series-connected structures can be connected in star- or delta-configuration to form a three-phase converter. [32] MMC configurations are shown in Figure 14. In this thesis, STATCOM based on MMC with full-bridge submodules connected in delta-configuration is studied.

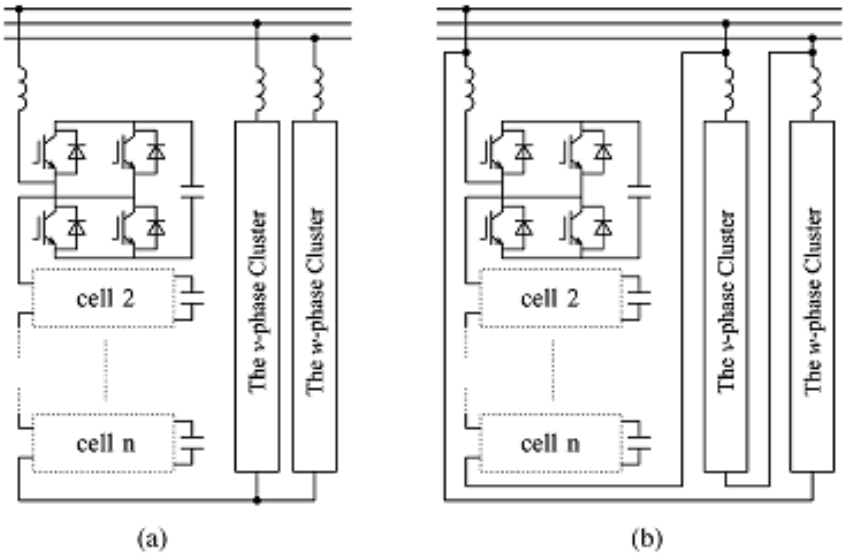

Figure 14. *MMC, a) star-configuration, b) delta-configuration [33].*

In medium and high voltage applications, MMC has several advantages compared to conventional two-level converters that use high switching frequency pulse width modulation. The switches can be rated based on the submodule capacitor voltages which are substantially smaller than full DC-link voltage in a two-level converter. In MMC, output voltage with low harmonic distortion can be produced without high switching frequencies. Because switching causes losses, MMC's losses are smaller than those of two-level converters. In high voltage levels, high voltage blocking capability is needed in two-level converter switches which increases the losses in one switching action. Switching frequency of those converters must be limited to about 1 kHz due to high losses which means increased harmonic voltages. [34] In MMC submodules are identical and can be connected in series to form modules with desired total voltage levels. This modularity enables cheaper and faster manufacturing. [32] Fault tolerance can be enhanced by adding redundant submodules in series so that faulty submodules can be bypassed [34].

Disadvantage of MMC is that a great number of semiconductor switches with gate drive circuits are needed. That makes the system more complex and expensive. [32] In a two-

level converter, all phases are connected to a common DC-link so there is no need for power balancing between phases. In MMC, all submodules have a capacitor energy storage and their energies must be actively balanced. [34]

3.5.3 Control system

Despite the simple principle of reactive power compensation in STATCOM and simple modular structure of MMC, quite complex control system is needed to achieve good and stable performance. In this subchapter, the overall control block diagram of studied STATCOM is presented and the purpose of each block is shortly described. In this thesis, a balanced three-phase system is assumed which means that the magnitudes of three-phase voltages are equal and their phase shifts are exactly 120 degrees. Therefore, control system characteristics related to unbalanced grid conditions are not introduced here.

The control is partly done in synchronous reference frame and partly in three-phase frame (abc-frame). Three-phase voltage and current can be transformed to αβ-frame and then to synchronous reference frame (dq-frame). For voltage, the transformation from abc- to αβ-frame is [34]

$$\begin{bmatrix} v_\alpha \\ v_\beta \\ v_0 \end{bmatrix} = \begin{bmatrix} \frac{2}{3} & -\frac{1}{3} & -\frac{1}{3} \\ 0 & \frac{1}{\sqrt{3}} & -\frac{1}{\sqrt{3}} \\ \frac{1}{3} & \frac{1}{3} & \frac{1}{3} \end{bmatrix} \begin{bmatrix} v_\mathrm{a} \\ v_\mathrm{b} \\ v_\mathrm{c} \end{bmatrix}, \tag{3.20}$$

where v_α is voltage α-component, v_β voltage β-component, v_0 zero sequence voltage, v_a instantaneous value of phase a voltage, v_b instantaneous value of phase b voltage and v_c instantaneous value of phase c voltage. Zero sequence voltage can be neglected in balanced three-phase system. The axes α and β are 90 degrees shifted from each other and thus form a complex plane. The three-phase voltage can be presented as a space vector which rotates counterclockwise with the fundamental angular frequency ω_1 in the plane: [34]

$$\boldsymbol{v_{\alpha\beta}} = v_\alpha + jv_\beta. \tag{3.21}$$

The magnitude of the vector is same as the peak value of phase voltage. Synchronous reference frame is also a complex plane which rotates to same direction as space vector with the fundamental angular frequency. Thus, in synchronous frame, space vector is standing still. [34] For voltage, the transformation from αβ- to dq-frame is

$$\begin{bmatrix} v_\mathrm{d} \\ v_\mathrm{q} \end{bmatrix} = \begin{bmatrix} \cos\theta & \sin\theta \\ -\sin\theta & \cos\theta \end{bmatrix} \begin{bmatrix} v_\alpha \\ v_\beta \end{bmatrix}, \tag{3.22}$$

where v_d is voltage d-component, v_q voltage q-component and θ the transformation angle which is chosen so that frame's d-axis is aligned with the voltage vector [34]. The voltage vector in dq-frame is

$$\boldsymbol{v_{dq}} = v_d + jv_q. \tag{3.23}$$

Transformation matrices are the same for current. Inverse transformation from dq- to abc-frame can be derived from equations 3.20 and 3.22. In Figure 15 voltage and current vectors in stationary and synchronous frames are illustrated. In stationary frame, the vectors rotate and in synchronous frame the dq-frame rotates with angular speed ω_1.

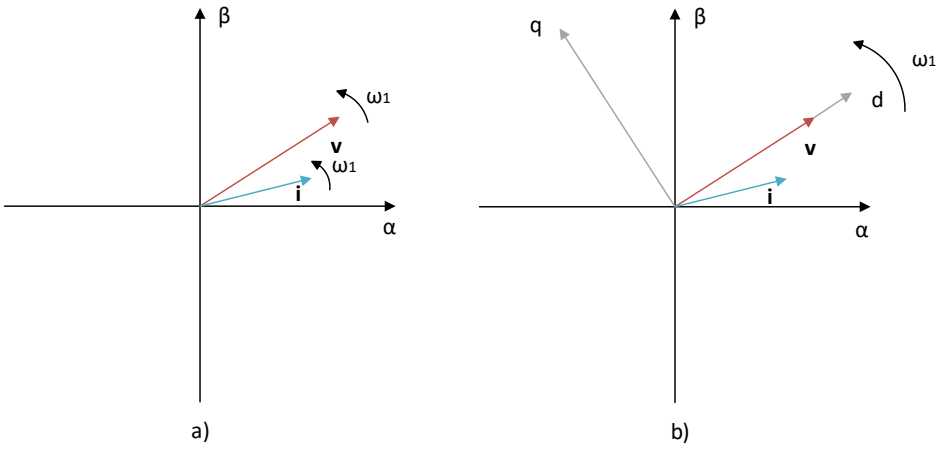

Figure 15. *Voltage and current vectors in a) stationary frame, b) synchronous frame.*

When dq-frame is aligned with the voltage vector, voltage d-component is equal to voltage magnitude and q-component is zero. Then, instantaneous active power p is [34]

$$p = \frac{3}{2} v_d i_d \tag{3.24}$$

and instantaneous reactive power q is [34]

$$q = -\frac{3}{2} v_d i_q. \tag{3.25}$$

According to the equations, active power depends on current d-component and reactive power depends on current q-component. Thus, it is possible to control powers independently. [34]

STATCOM's control block diagram is shown in Figure 16 and in larger size in Appendix A, Figure 1. Also, the explanations for diagram abbreviations are given in the appendix. The control cycle shown in the diagram is executed at 10 kHz frequency.

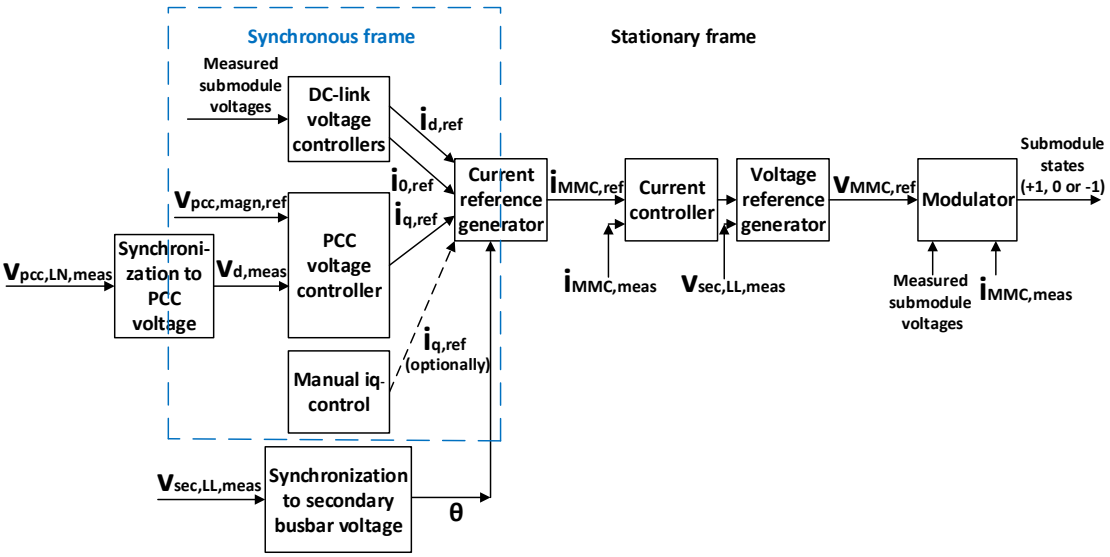

Figure 16. *Control block diagram of STATCOM.*

One synchronization block tracks PCC line-to-neutral voltage fundamental frequency d-component by controlling voltage q-component to zero. The block calculates voltage d-component magnitude from the measured voltage which is equal to fundamental voltage magnitude. Another synchronization block tracks the line-to-line voltage of secondary busbar. It produces the transformation angle θ which is used in the dq-to-abc transformation.

Voltage controller produces current q-component reference by controlling the difference between PCC voltage magnitude reference and measured PCC voltage fundamental component magnitude to zero. Current q-component can be used for reactive power control according to equation 3.25 and PCC voltage can be controlled by produced or absorbed reactive power as equation 3.13 states. As the reference is a DC-value, PI-controller (proportional-integral controller) can be used to track it [34]. Another option is to use manual control where current q-component reference is set manually.

The total DC-voltage in each delta branch should be kept close to nominal value so that desired output voltages can be produced. The losses in switches cause the capacitors' voltages to decrease so active power is needed from grid to compensate the losses as described earlier. There are two controllers to perform this task. First PI-controller controls the average DC-voltage of three branches to the nominal value by producing the current d-component reference. Still, there might be unbalance between DC-link branch voltages if grid voltage is unbalanced. Branch voltages can be balanced by forcing an appropriate zero sequence current to circulate in delta connection [34]. Second controller produces the current zero sequence component reference.

Current reference generator forms the reference current for MMC in abc-frame from the current reference d-, q- and zero-sequence components. The transformation angle produced by synchronization block is used in the transformation. MMC is connected in delta-configuration, so the references are calculated for each delta branch.

There are three current controllers, one for each delta branch which control the difference between current references and measured MMC branch currents to zero. PI-controllers can not track sinusoidal reference signals, so PR-controllers (proportional-resonant controllers) are used which can perform the task [35]. PR-control theory is more discussed in chapter 5.2.

Voltage reference generator generates the three-phase voltage reference for MMC. The reference for each delta-branch is calculated by subtracting the current controller output from the measured secondary busbar voltage. This voltage feedforward can be either instantaneous three-phase voltage with all the harmonics or only the fundamental component. These two feedforward options are compared later in this thesis from the viewpoint of produced harmonic currents.

Finally, modulator is needed to transform the voltage references to information which submodules in each branch should be connected and which bypassed. Modulator's outputs are the states of each submodule: +1, 0 or -1. State +1 means that the submodule should produce $+V_{DC}$ voltage at its terminals, state -1 means that it should produce $-V_{DC}$ voltage at its terminals and state 0 that the module must be bypassed.

In addition to reference voltage production, modulator must balance individual submodule DC-voltages in each branch. The voltage of a submodule stays unchanged when it is bypassed but increases or decreases when it is connected to AC-terminals depending on the power flow direction [34]. Without balancing that would lead to large voltages in some submodules and small voltages in some submodules. Large voltages could break the capacitors. A logic for choosing the submodule to be connected or bypassed is based on the power flow direction and the measured submodule voltages.

4. HARMONIC CURRENTS AND VOLTAGES OF STATCOM

STATCOM model implemented in PSCAD simulation program was used to simulate the harmonic current emissions of STATCOM. In the simulation model, modular multilevel converter is modelled as voltage source whose three-phase voltage is produced by control system and modulator described in chapter 3.5.3. Changes of submodule DC-voltages are calculated every simulation step according to equation 3.15. STATCOM model includes also the coupling reactor and its parasitic resistance, transformer model, measurements and some additional protection functions not meaningful in steady-state operation. Grid is modelled as series connection of voltage source and impedance. Harmonic currents and voltages were extracted from measured waveforms using Fast Fourier Transform block provided by PSCAD and exported to Excel for calculations and graph drawing.

First, STATCOM's current was simulated when grid voltage was sinusoidal at fundamental frequency 50 Hz. Then, harmonics were added to grid voltage and simulation was repeated to illustrate the increasing harmonic currents of STATCOM. Goal was to find out how harmonic current emissions affect harmonic voltages at PCC which are limited by standards and transmission system operators' specifications. The harmonic current mitigation performance of increased reactances in coupling reactor and transformer were also illustrated. In all simulations, manual current q-component control was used. As described in chapter 3.5.3, this current component affects the reactive power output of STATCOM and thus PCC voltage. To see if operating point has any effect on harmonic currents, capacitive, inductive and zero current reference situations were simulated.

4.1 Harmonic current emissions with sinusoidal grid voltage

In the first simulations grid voltage was sinusoidal at 50 Hz. Grid positive sequence voltage was 138 kV and there was no negative sequence voltage. Transformer's connection was YNd11 and its secondary nominal voltage was set to 34.5 kV. Used grid resistance and reactance at fundamental frequency were 0.9292 Ω and 9.477 Ω, respectively. Grid impedance corresponds to 2000 MVA short-circuit level at PCC. Used transformer reactance was 0.115 p.u (per unit). STATCOM's rated power was 100 MVAr and it consisted of 40 submodules per branch. All grid and STATCOM parameters used in the simulations are shown in Appendix B, Table 1. The configuration used in the simulations is illustrated as single line diagram in Figure 17.

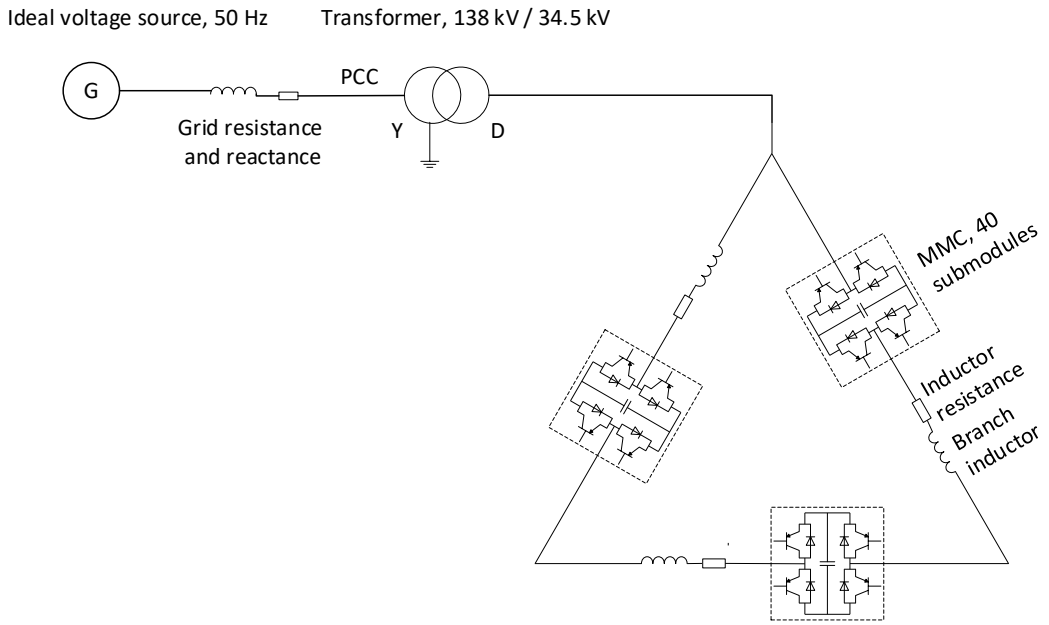

Figure 17. *Single line diagram of the circuit used in the first simulations.*

As explained in chapter 3.5.3, STATCOM's voltage reference is calculated by subtracting the current controller's output from the feedforward of secondary busbar voltage. The two feedforward options considered are fundamental voltage and instantaneous voltage feedforward. Fundamental voltage feedforward means that only fundamental component of the secondary busbar voltage is used. Instantaneous voltage feedforward means that the measured secondary busbar voltage, including all the harmonics, is used. In the simulations with sinusoidal grid voltage, fundamental feedforward was used. However, feedforward method has not a great significance on harmonic performance when grid voltage is sinusoidal. Only harmonic currents produced by STATCOM cause harmonic voltages to the secondary busbar.

First, simulation was done in capacitive operating point. The current q-component reference was set to 1.0 p.u which means 1000 A fundamental frequency capacitive current in STATCOM's delta branch. A-phase current at PCC was simulated for 1 second. Harmonic current spectrum changes a bit as function of time so average of the harmonic currents was taken from interval 0.9 s to 1.0 s. This averaging was used in all following simulations. Figure 18 presents the harmonic spectrum of PCC current in a-phase. To compare different operating points, the harmonic currents were calculated as percent of the used fundamental frequency current maximum. Used fundamental component maximum was $\sqrt{3}$*1000 A in one phase in secondary which is converted to primary using ratio of secondary nominal voltage 34.5 kV to primary nominal voltage 138 kV.

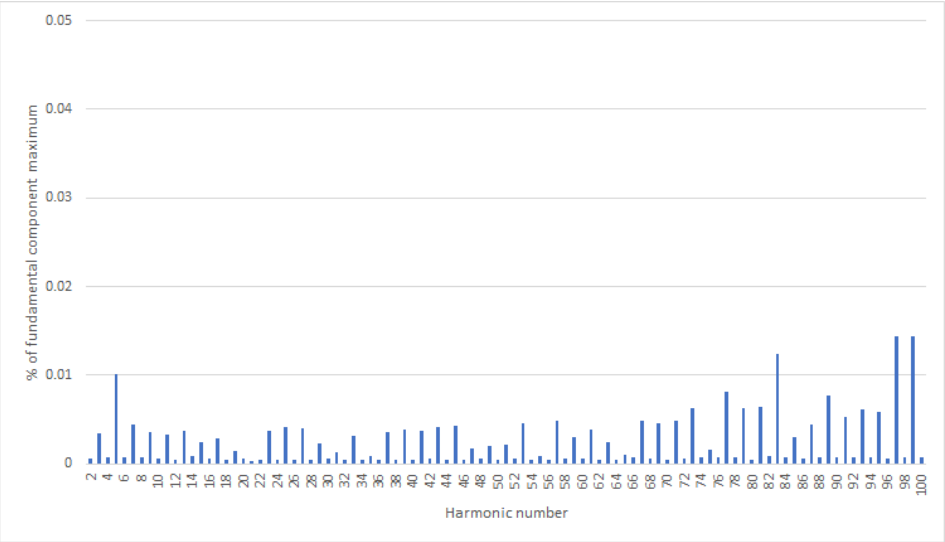

Figure 18. *Harmonic spectrum of PCC current in capacitive operating point in sinusoidal grid.*

Calculated current TDD was 0.038 % when all 100 harmonic components were considered. The current distortion is very low and does not usually cause any problems.

Next, simulation was done in inductive operating point. The current q-component reference was set to -1.0 p.u which means 1000 A fundamental frequency inductive current in STATCOM's delta branch. Same parameters were used as for capacitive operating point. A-phase harmonic currents at PCC are presented in Figure 19.

Simulation was also done in zero current operating point. The current q-component reference was set to 0 p.u which means 0 A fundamental frequency current in STATCOM's delta branch. Figure 20 shows the harmonic spectrum of PCC current in a-phase.

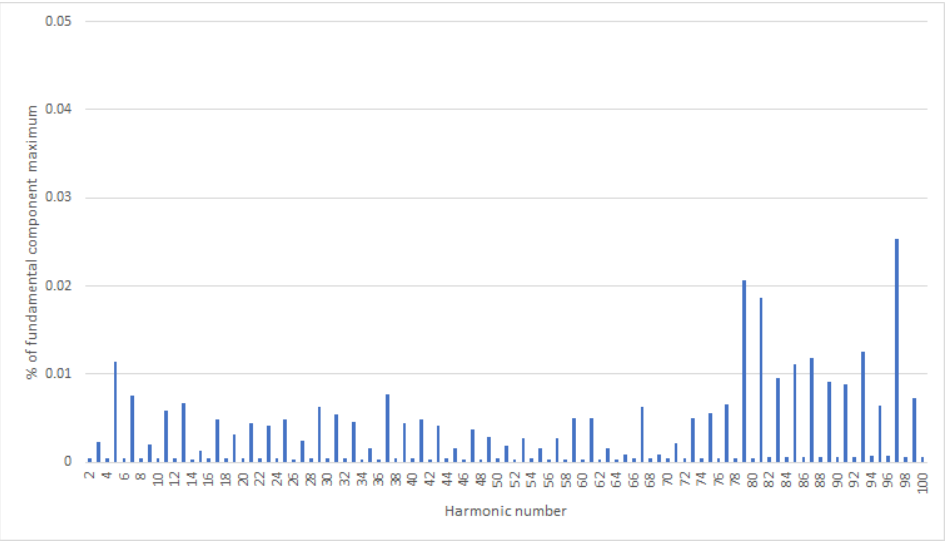

Figure 19. *Harmonic spectrum of PCC current in inductive operating point in sinusoidal grid.*

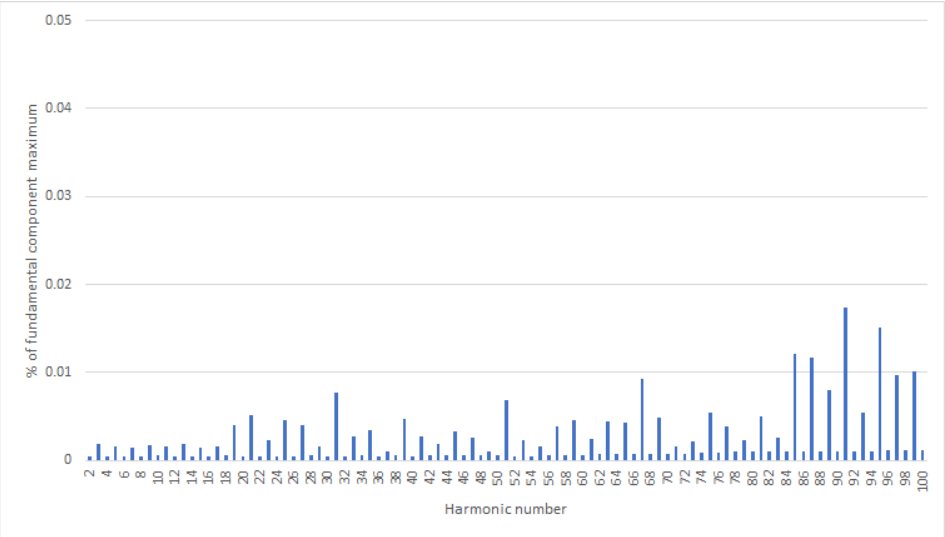

Figure 20. *Harmonic spectrum of PCC current in zero current operating point in sinusoidal grid.*

Calculated current TDDs were 0.055 % and 0.041 %, respectively. It seems that there are no major differences in harmonic current spectrums between capacitive, inductive and zero current operating points.

4.2 Harmonic current emissions with distorted grid voltage

Harmonic voltage source was added to the grid in series with the fundamental frequency voltage source. The used voltage spectrum was adopted from IEC/TR 61000-3-6 planning levels for high voltage networks (Table 4). The voltage THD calculated from the individual harmonic limits is 5.33 %. However, the same standard sets 3 % limit for THD. Therefore, Table 4 values were scaled by a factor of 0.55. The standard does not set limits for harmonics above order 50. Their effect is also wanted to be studied and thus voltage magnitude of 0.1 % from the fundamental was added for harmonic orders from 51 to 100. The resulting voltage THD is 3.015 %. The used voltage spectrum is presented in Figure 21. All harmonics were chosen to be positive sequence and the angles of harmonics to be 0 degrees with respect to fundamental frequency voltage angle. Nothing else was changed from the previous simulations.

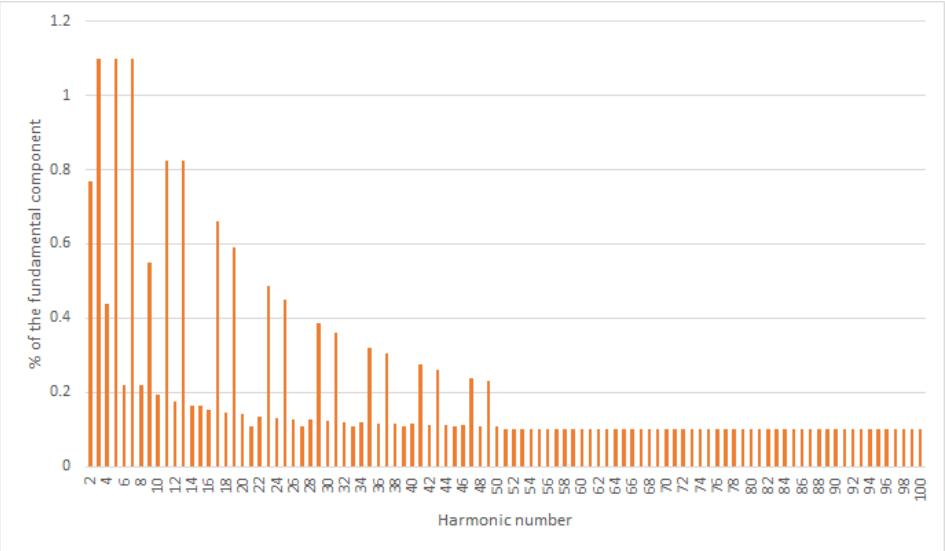

Figure 21. *Grid's harmonic voltage spectrum used in the simulations.*

Simulations were done with the harmonic voltage source. They were done with both secondary busbar voltage feedforward options and in the same three operating points as with sinusoidal grid voltage. First, fundamental voltage feedforward was used. Simulated harmonic spectrum of PCC current in capacitive operating point is shown in Figure 22.

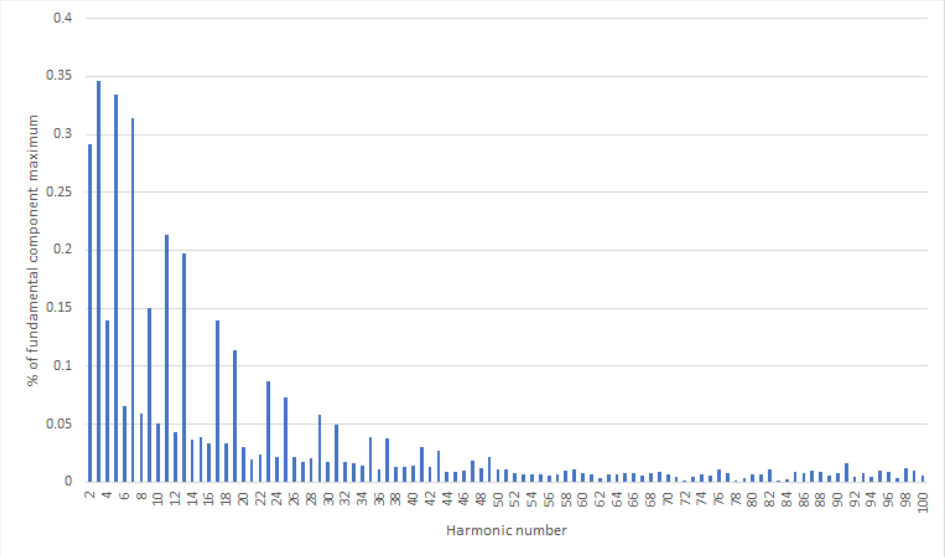

Figure 22. *Harmonic spectrum of PCC current in capacitive operating point in distorted grid with fundamental voltage feedforward.*

Calculated current TDD was 0.790 % when all 100 harmonic components were considered. It is almost 21 times the simulated current TDD with sinusoidal grid voltage. Clear correlation between voltage and current harmonic spectrums can be seen. In other words, at those harmonics where largest voltages were introduced, current increased the most. Comparable PCC harmonic current spectrums in inductive and zero current operating points are shown in Figure 23 and Figure 24.

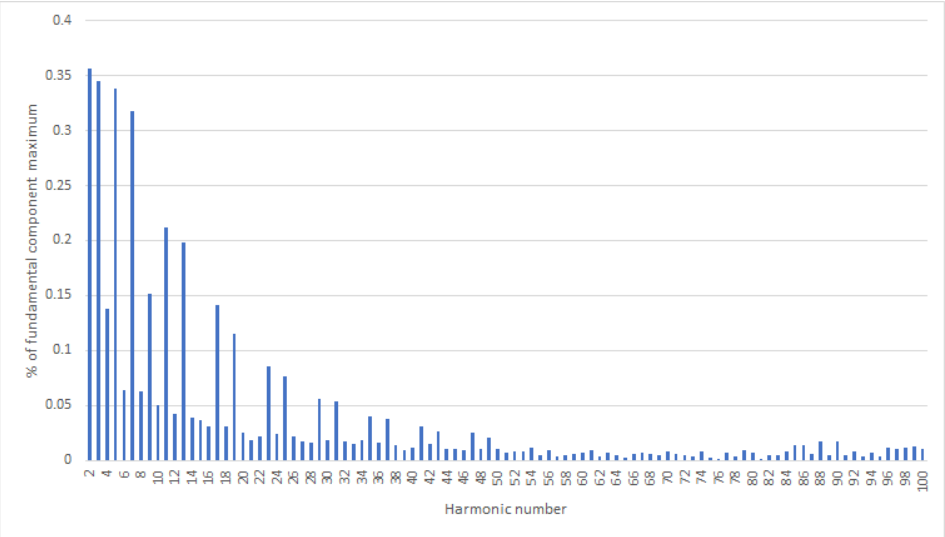

Figure 23. *Harmonic spectrum of PCC current in inductive operating point in distorted grid with fundamental voltage feedforward.*

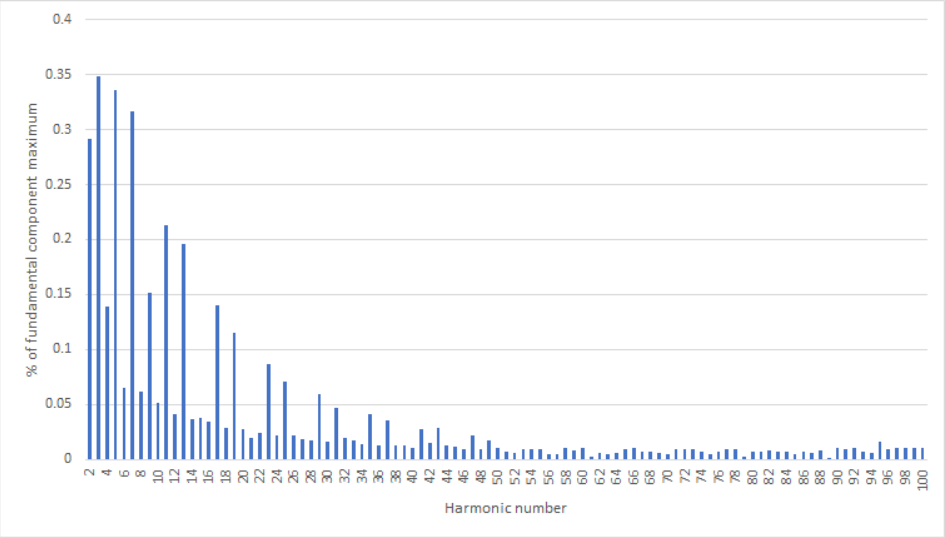

Figure 24. *Harmonic spectrum of PCC current in zero current operating point in distorted grid with fundamental voltage feedforward.*

Calculated current TDDs were 0.820 % and 0.792 %, respectively. The current spectrums of simulated cases are very similar and they all show that if magnitude of harmonic voltage order *h* is increased also the magnitude of same order harmonic current increases.

Simulated harmonic spectrums with instantaneous voltage feedforward differ from the fundamental voltage feedforward results. Spectrums in capacitive, inductive and zero current operating points are presented in Figure 25, Figure 26 and Figure 27.

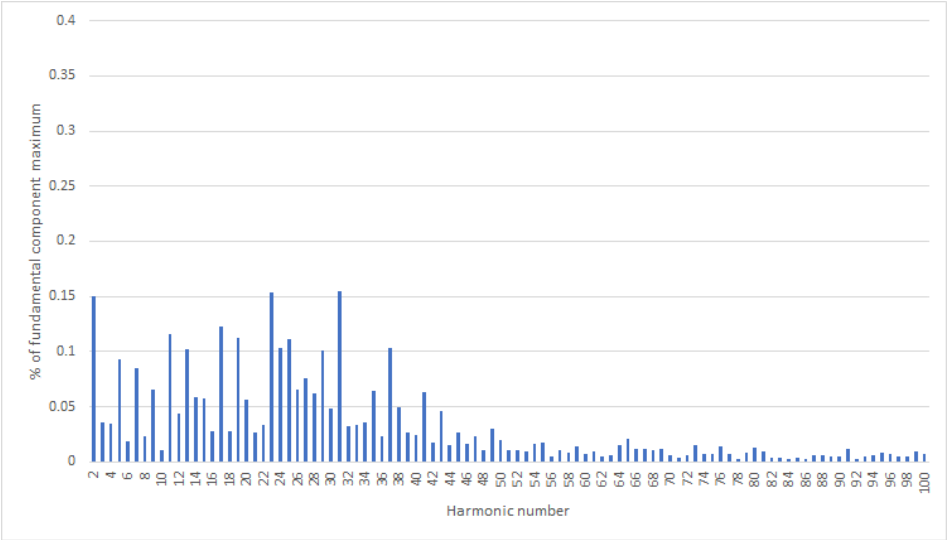

Figure 25. *Harmonic spectrum of PCC current in capacitive operating point in distorted grid with instantaneous voltage feedforward.*

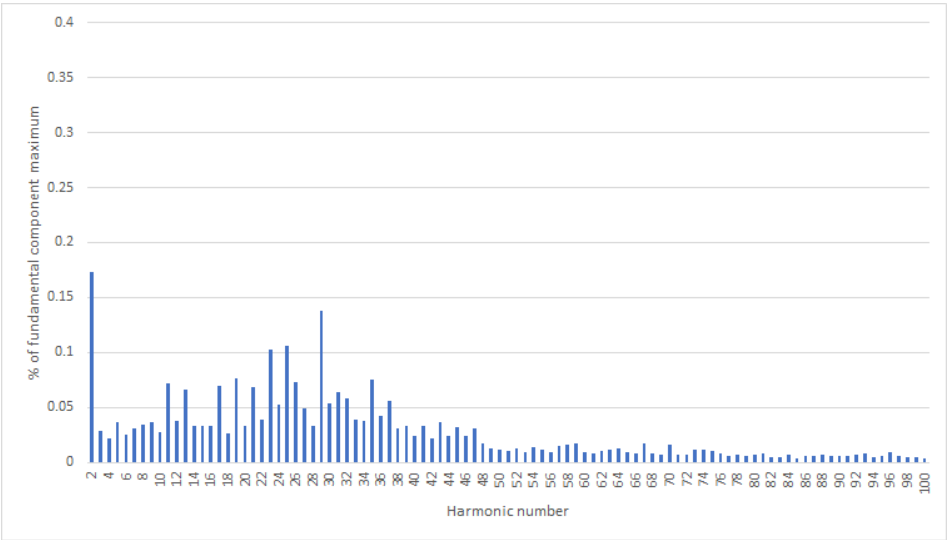

Figure 26. *Harmonic spectrum of PCC current in inductive operating point in distorted grid with instantaneous voltage feedforward.*

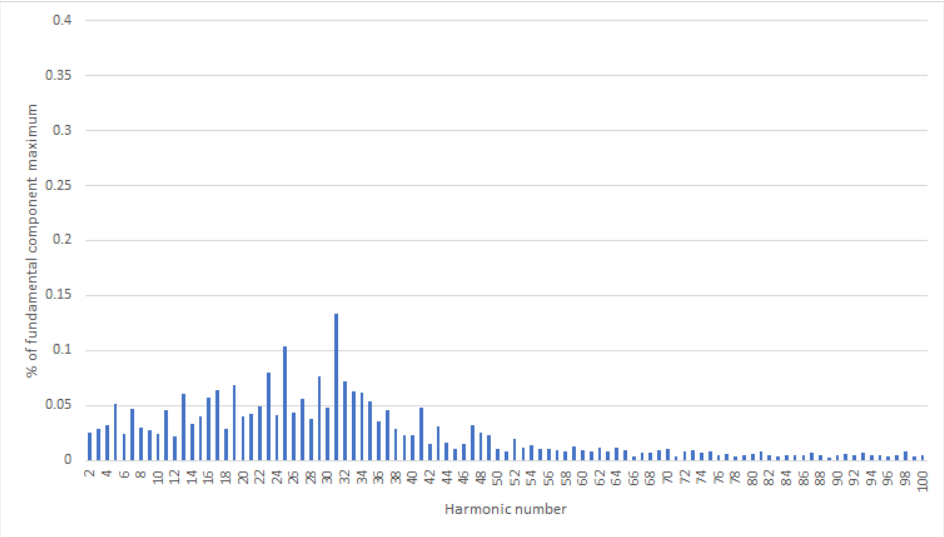

Figure 27. *Harmonic spectrum of PCC current in zero current operating point in distorted grid with instantaneous voltage feedforward.*

Calculated current TDDs were 0.496 %, 0.401 % and 0.346 %. They are 7 - 13 times the respective current TDDs with sinusoidal voltage. TDDs and low-order harmonics are yet lower than with fundamental voltage feedforward. Harmonic currents of orders from 20 to 40 are however larger. With fundamental voltage feedforward current spectrum resembled the grid voltage spectrum. Now current spectrums are not so predictable any more.

4.3 Effect of harmonic currents on PCC voltage in inductive grid

The harmonic spectrum of PCC current in capacitive operating point with fundamental voltage feedforward was shown in Figure 22. Compared to IEEE 519 harmonic current distortion limits (Table 2), the produced harmonic currents are still small and not a problem with respect to that. However, harmonic currents flowing through the grid impedances affect harmonic voltages at PCC as explained in chapter 2.1. As voltage THD in grid was already at the limit of IEC/TR 61000-3-6 standard, STATCOM produced harmonic currents should not increase the voltage distortion at PCC. Simulated grid and PCC voltage spectrums in capacitive operating point with fundamental voltage feedforward are presented in Figure 28 and Figure 29. Harmonic voltages are expressed as percent of nominal fundamental frequency line-to-neutral voltage which is $138/\sqrt{3}$ kV.

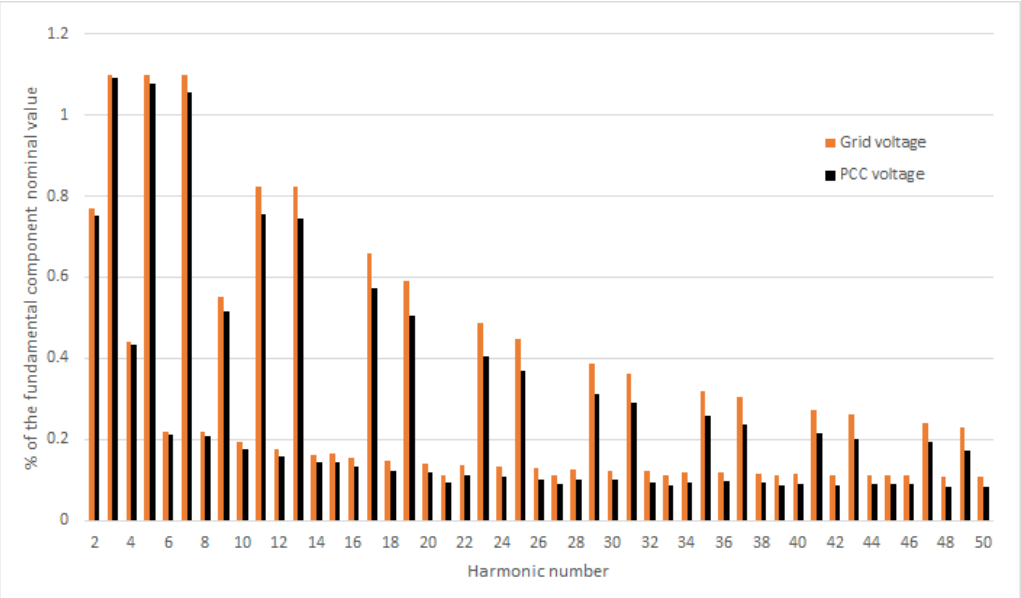

Figure 28. *A-phase harmonic voltages from 2nd to 50th in grid and PCC with fundamental voltage feedforward.*

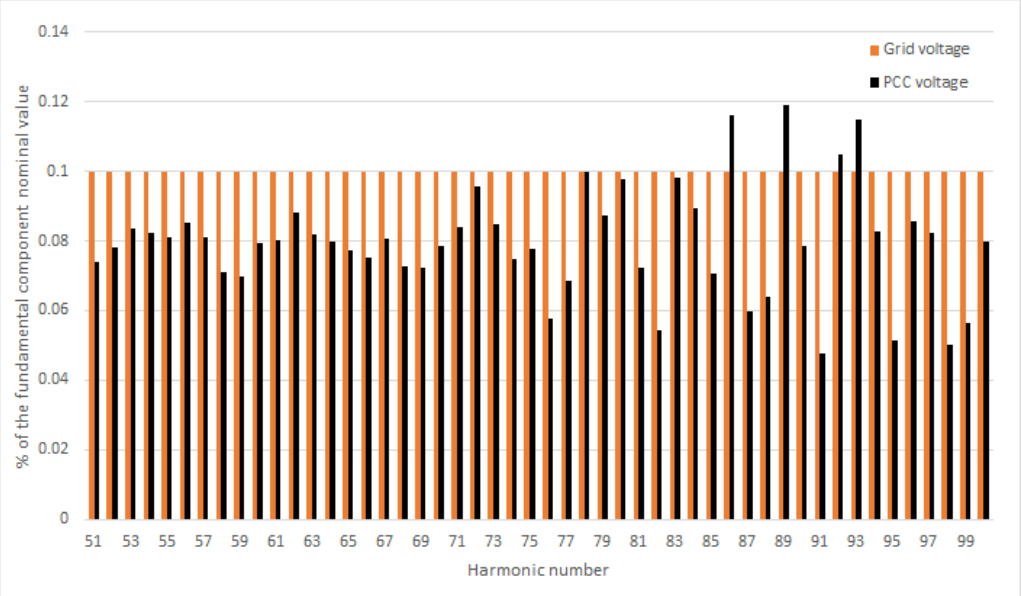

Figure 29. *A-phase harmonic voltages from 51st to 100th in grid and PCC with fundamental voltage feedforward.*

Calculated voltage THD in grid was 3.015 % and at PCC 2.771 %. It seems that STATCOM's harmonic currents cancel part of grid's harmonic voltages. In other words, it acts as a harmonic voltage filter. This was studied more by calculating STATCOM's harmonic impedances. Harmonic impedance is the relationship between harmonic voltage at the connection point and the injected harmonic current of same order from the converter [36]. Harmonic impedance magnitudes $Z_{h,STATCOM}$ and angles $\varphi_{Z,h,STATCOM}$ at PCC can be calculated according to equations below:

$$Z_{\mathrm{h,STATCOM}} = \frac{V_{\mathrm{h,PCC}}}{I_{\mathrm{h,PCC}}}, \tag{4.1}$$

$$\varphi_{\mathrm{Z,h,STATCOM}} = \varphi_{\mathrm{V,h,PCC}} - \varphi_{\mathrm{I,h,PCC}}, \tag{4.2}$$

where $V_{\mathrm{h,PCC}}$ is the measured harmonic voltage magnitude, $I_{\mathrm{h,PCC}}$ is the measured harmonic current magnitude, $\varphi_{\mathrm{V,h,PCC}}$ is the measured harmonic voltage angle and $\varphi_{\mathrm{I,h,PCC}}$ is the measured harmonic current angle at PCC.

Calculated impedance magnitude in capacitive operating point is presented in Figure 30 and angle in Figure 31. As a comparison, the impedance magnitude and angle of STATCOM's passive components seen from PCC are presented in the same figures. The passive components mean the series connection of transformer reactance and STATCOM's coupling reactance and resistance.

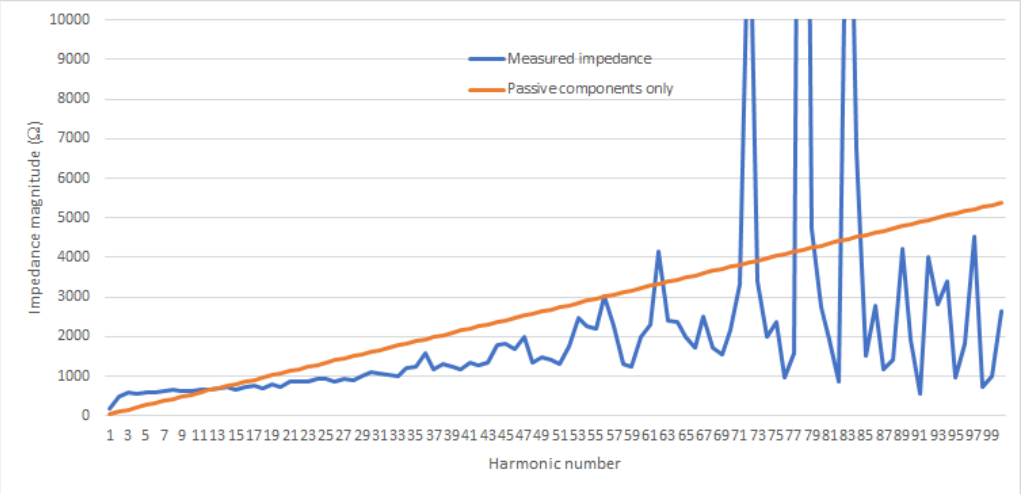

Figure 30. *Measured STATCOM's impedance magnitude with fundamental voltage feedforward versus impedance magnitude of passive components.*

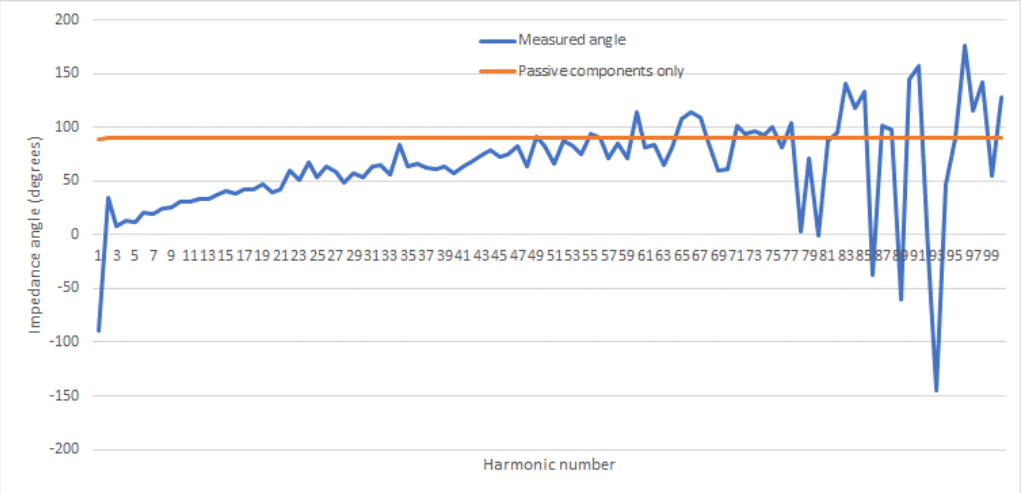

Figure 31. *Measured STATCOM's impedance angle with fundamental voltage feedforward versus impedance angle of passive components.*

At most frequencies STATCOM's impedance is inductive-resistive (angle positive) and at those frequencies harmonic voltages at PCC mitigate. Some harmonic impedances (86^{th}, 89^{th} and 93^{rd}) are capacitive-resistive (angle negative) and at those frequencies harmonic voltages increase at PCC. Fundamental component of impedance is almost capacitive as expected in capacitive operating point.

The reason for previous phenomenon can be found from Kirchoff's voltage law and phasor diagram for the harmonic component. According to the voltage law, voltage of the simulated circuit can be presented as

$$\overline{V}_{\mathrm{h,grid}} = \overline{V}_{\mathrm{h,PCC}} + \overline{Z}_{\mathrm{h,grid}}\overline{I}_{\mathrm{h,STATCOM}}, \tag{4.3}$$

where $\overline{V}_{\mathrm{h,grid}}$ is the harmonic voltage in grid, $\overline{V}_{\mathrm{h,PCC}}$ is the harmonic voltage at PCC, $\overline{Z}_{\mathrm{h,grid}}$ is the grid's harmonic impedance and $\overline{I}_{\mathrm{h,STATCOM}}$ is the produced harmonic current of STATCOM. According to the equation a phasor diagram can be drawn. In Figure 32 phasor diagrams are drawn in two situations. In the first situation, the harmonic current of STATCOM is inductive-resistive (current lags voltage) and in the second it is capacitive-resistive (current leads voltage). Grid impedance is simplified to have only inductive reactance component $jX_{\mathrm{h,grid}}$, because in the simulations reactance was about 10 times larger than resistance at fundamental frequency. As the inductive reactance increases as function of frequency, the ratio between reactance and resistance is even larger at harmonics.

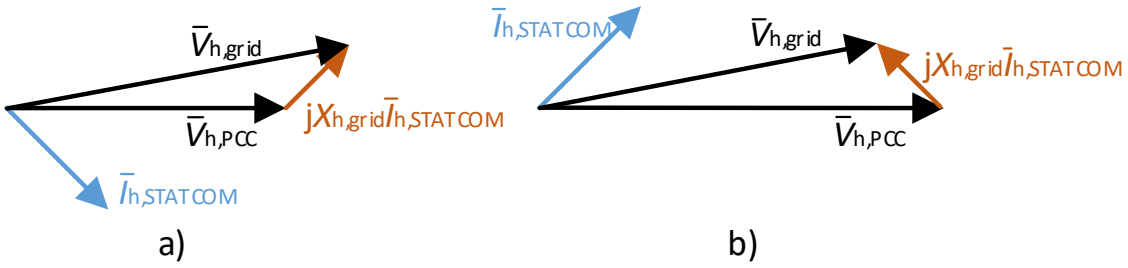

Figure 32. *Phasor diagram of grid's and PCC's harmonic voltages in inductive grid, when STATCOM's harmonic current is a) inductive-resistive, b) capacitive-resistive.*

The voltage drop in grid impedance causes difference between grid's and PCC's harmonic voltage amplitudes. When STATCOM's harmonic current is inductive-resistive, harmonic voltage amplitude at PCC is smaller than the harmonic voltage amplitude in grid. When the current is capacitive-resistive, situation is the opposite.

It seems that if fundamental voltage feedforward is used, harmonic voltage at PCC sees STATCOM as inductive-resistive impedance at harmonics up to 70^{th} order. This causes inductive-resistive current and smaller PCC voltage at those harmonics. The measured impedance resembles the calculated passive component impedance to some extent but there is also deviation between them. At least at lower frequencies, measured resistance

is clearly larger than calculated. This deviation implies that the total impedance is affected also by the produced STATCOM voltage. Thus, changing STATCOM's voltage output by the means of control and modulation can lead to higher impedance and lower harmonic current emissions. Ideally, converter's harmonic impedance would be infinite which would mean zero harmonic currents independent of grid harmonic voltages [36].

The situation changes if instantaneous voltage feedforward is used. The harmonic current spectrum in capacitive operating point was presented in Figure 25. In this operating point, harmonic voltage spectrums in grid and PCC are presented in Figure 33 and Figure 34.

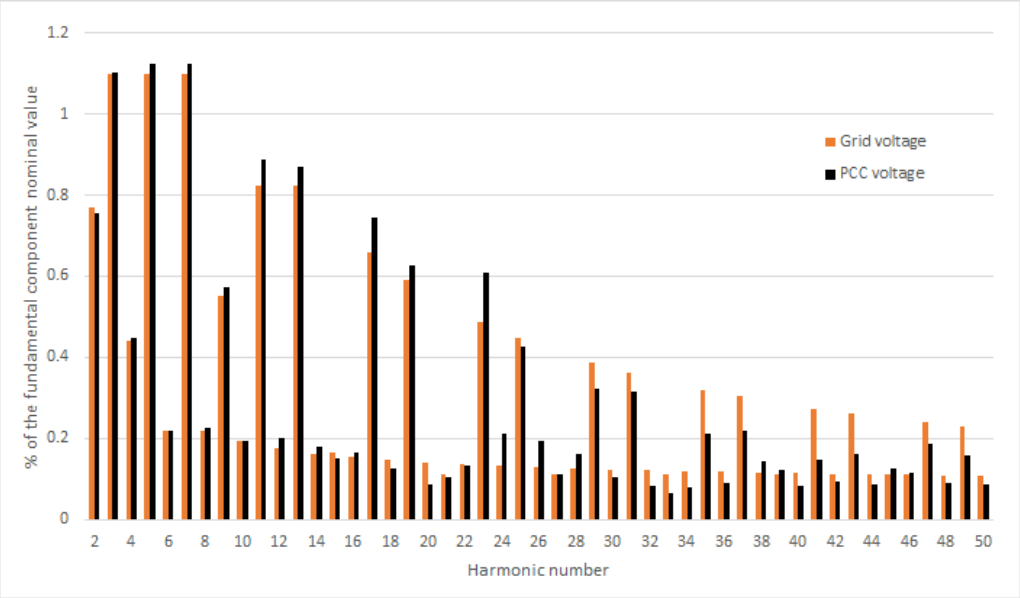

Figure 33. *A-phase harmonic voltages from 2nd to 50th in grid and PCC with instantaneous voltage feedforward.*

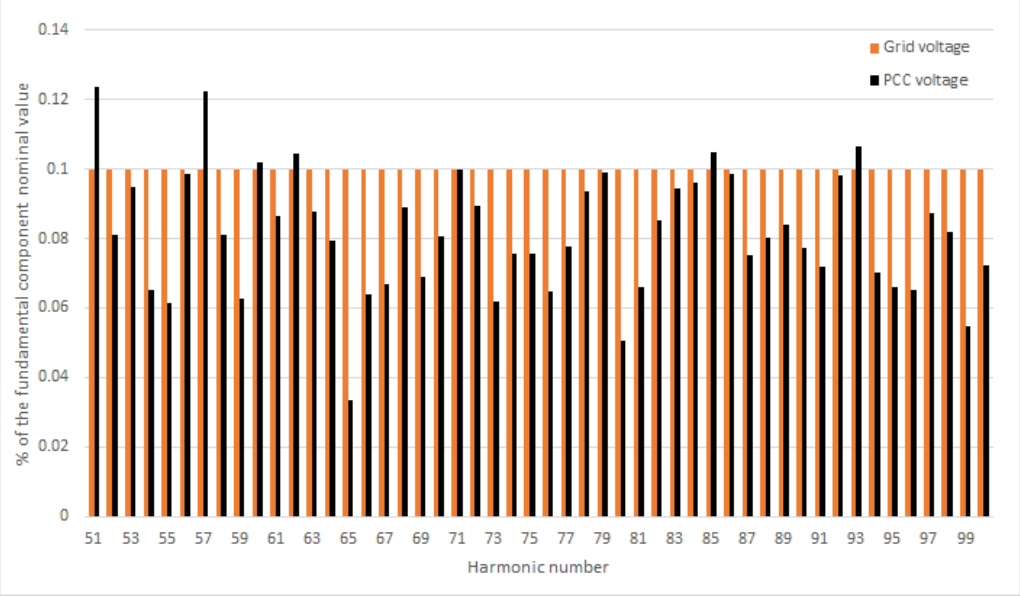

Figure 34. *A-phase harmonic voltages from 51st to 100th in grid and PCC with instantaneous voltage feedforward.*

Voltage THD at PCC was now 3.034 % which is higher than THD of grid voltage. Even though the total amount of harmonic current emissions is smaller than with fundamental voltage feedforward, these harmonic currents produce harmonic voltages at grid impedances so that many of the PCC harmonic voltages increase. Again, STATCOM's harmonic impedances were calculated from measured PCC voltage and current. Impedance magnitude is presented in Figure 35 and angle in Figure 36.

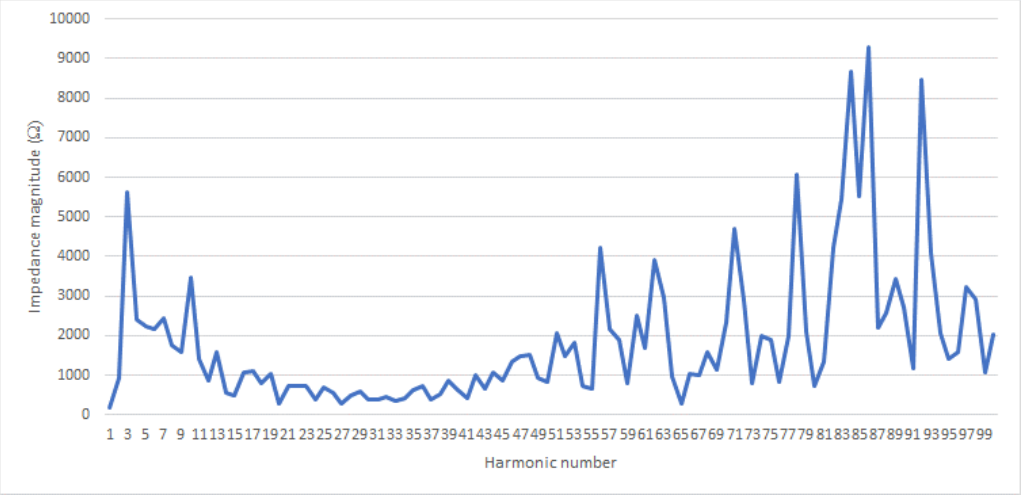

Figure 35. *STATCOM's impedance magnitude measured at PCC with instantaneous voltage feedforward.*

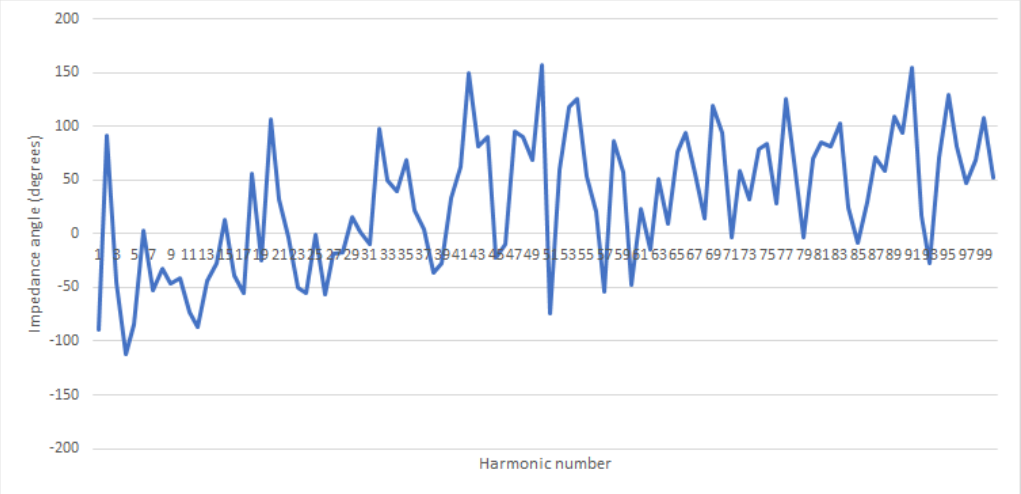

Figure 36. *STATCOM's impedance angle measured at PCC with instantaneous voltage feedforward.*

Now STATCOM's impedance is capacitive-resistive also at many low-order harmonics. This means that STATCOM produces capacitive-resistive current at those frequencies which cause harmonic voltages at PCC to rise compared to the grid harmonic voltages.

The idea of instantaneous voltage feedforward is to remove the effect of grid harmonic voltages on produced harmonic currents by adding an additional voltage term to the current controller output [37]. In case of inverter connected to the grid through an LCL-filter,

this voltage term should have proportional and derivative terms of measured instantaneous grid voltage [37]. Proportional term is the inverse of modulator's gain and derivative terms are related to the LCL-filter [37]. In the studied STATCOM, filter is only a reactor and thus derivative terms are not needed. Additionally, studied STATCOM has a nearest-level modulator which produces voltage close to the reference every modulation cycle. Thus, its gain can be assumed close to 1 and measured voltage can be directly used as feedforward.

If the grid's harmonic voltages were produced in MMC all the time, the harmonic voltages over coupling reactor would be zero and harmonic currents would not be induced. It seems that at small frequencies the harmonic currents decrease and impedances increase in magnitude so the feedforward of harmonics works to some extent. However, at harmonics of orders from 20 to 40, the harmonic current magnitudes increase compared to the currents with fundamental voltage feedforward, so the harmonic voltage feedforward does not work at all. It has been observed that delay in feedforward path causes phase difference between inverter produced and grid harmonic voltages and this difference increases as the harmonic order increases [38]. As there is difference, feedforward will not work as planned and with large differences it can even magnify the produced harmonic currents [38]. Voltage measurement is ideal in the PSCAD model and measured signal is not filtered at all so delay is not caused due to them. However, modulator algorithm is executed once in 100 µs which causes delay that may deteriorate the performance.

4.4 Effect of harmonic currents on PCC voltage in capacitive grid

In the previous simulations grid impedance was inductive-resistive. If it is capacitive-resistive, the effect on harmonic voltages at PCC might be opposite as the voltage drop vector is to opposite direction compared to Figure 32. Therefore, simulations were done also with capacitive-resistive grid impedance. Resistor of 0.1 Ω and capacitor of 15.9155 µF were connected in series. The capacitor corresponds to 200 Ω reactance at fundamental frequency.

Because capacitive reactance decreases as function of frequency, impedance at harmonics is quite low. Thus, voltage drop in grid impedance would be small and the difference between grid and PCC voltages would not be seen. Therefore, grid harmonic voltages were increased at some frequencies to increase STATCOM current distortion and voltage drop in grid impedance. Grid harmonic voltages were increased to 5 % of fundamental component at harmonic orders 3, 9, 11, 13, 17, 19, 23, 29, 31 and 41. As a result, THD of grid voltage increased to 15.96 %.

Fundamental frequency voltage would also change to opposite direction compared to normal situation due to capacitive impedance. In equation 3.7 the reactance sign changes,

which means that now capacitive current would cause PCC voltage to decrease. To prevent the nonconventional behavior, simulation was done with zero reactive current reference. STATCOM produced harmonic current spectrum at PCC with fundamental voltage feedforward is presented in Figure 37.

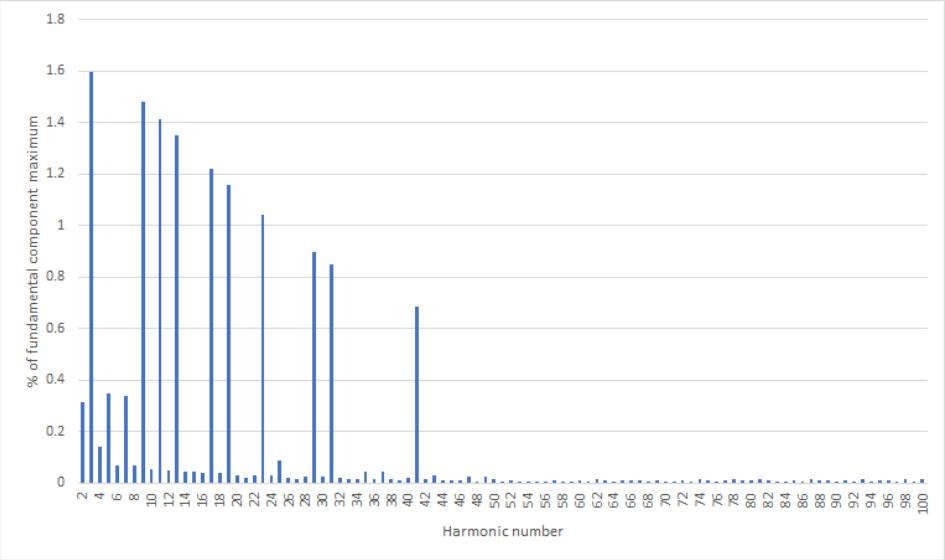

Figure 37. *Harmonic spectrum of PCC current in zero current operating point in capacitive-resistive grid with fundamental voltage feedforward.*

Currents are increased a lot at those harmonics where voltages were increased. The resulting current TDD was 3.86 %. IEEE 519 current distortion limits (Table 2) are exceeded at some of the increased harmonics. Also, current TDD is higher than the limit in the standard. Resulting grid and PCC voltages are presented in Figure 38 and Figure 39.

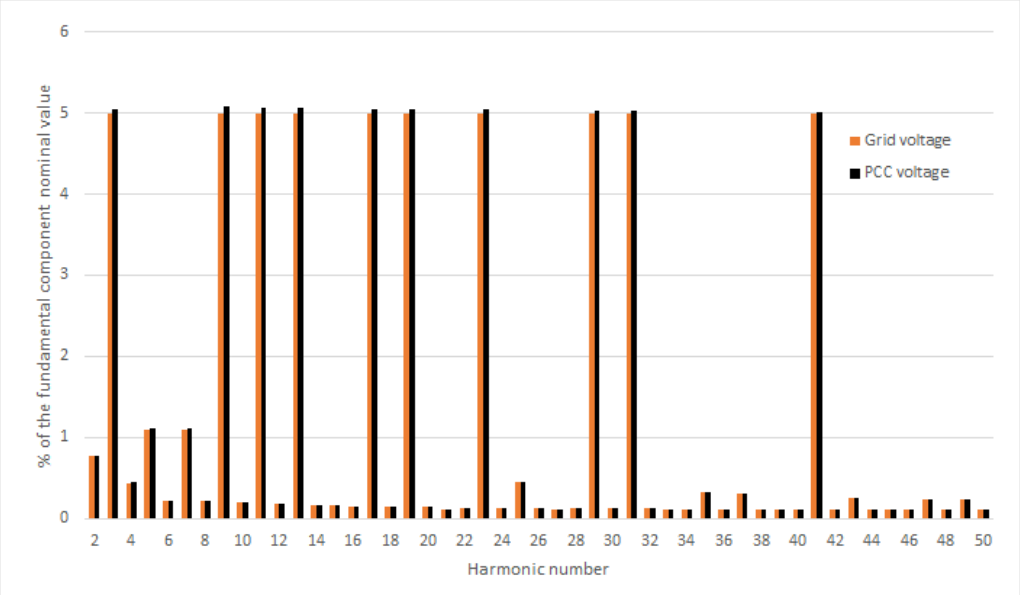

Figure 38. *A-phase harmonic voltages from 2nd to 50th in grid and PCC with fundamental voltage feedforward when grid is capacitive-resistive.*

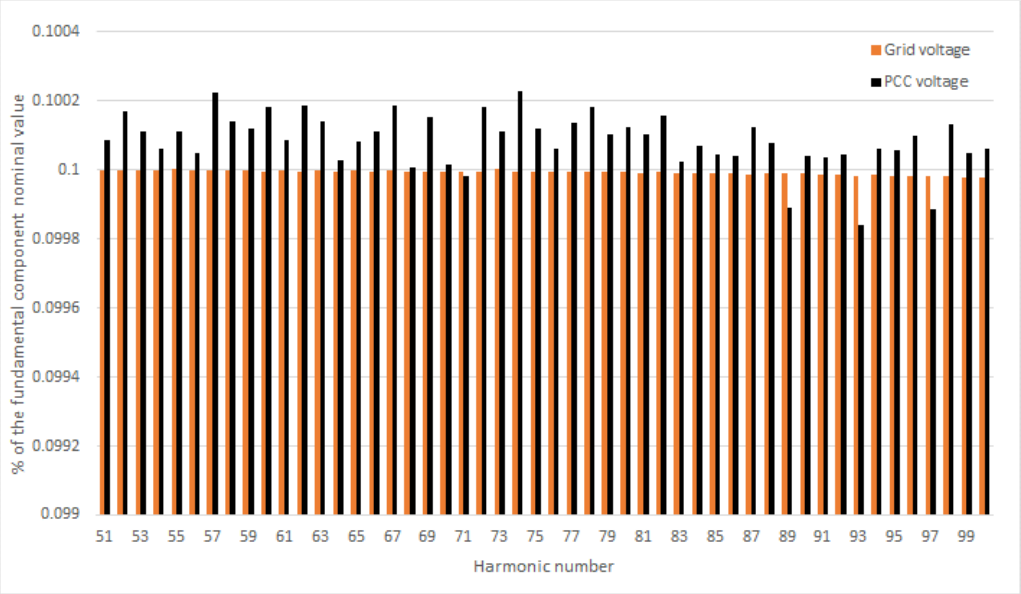

Figure 39. *A-phase harmonic voltages from 51st to 100th in grid and PCC with fundamental voltage feedforward when grid is capacitive-resistive.*

As expected harmonic voltages increase at PCC because of the capacitive grid. Because grid impedance is small, the difference between grid and PCC voltages is small but the trend can be seen. Since impedance decreases as function of frequency the difference between voltages also decreases. The voltage THD at PCC was 16.11 % which is higher than in the supplying grid.

STATCOM's harmonic impedances were calculated from measured PCC voltage and current. The impedance is still inductive-resistive at most frequencies even though operating point was changed. Impedance magnitude is presented in Figure 40 and angle in Figure 41.

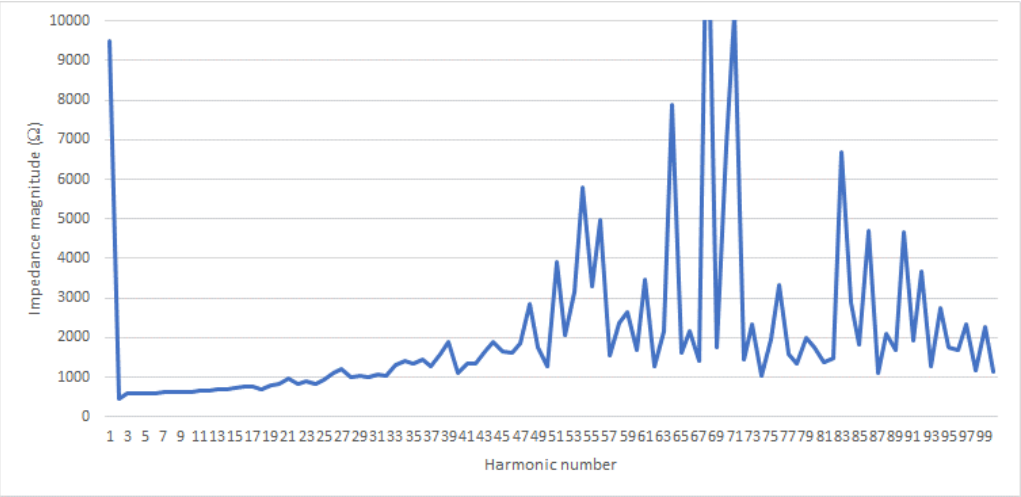

Figure 40. *STATCOM's impedance magnitude measured at PCC in zero current operating point with fundamental voltage feedforward.*

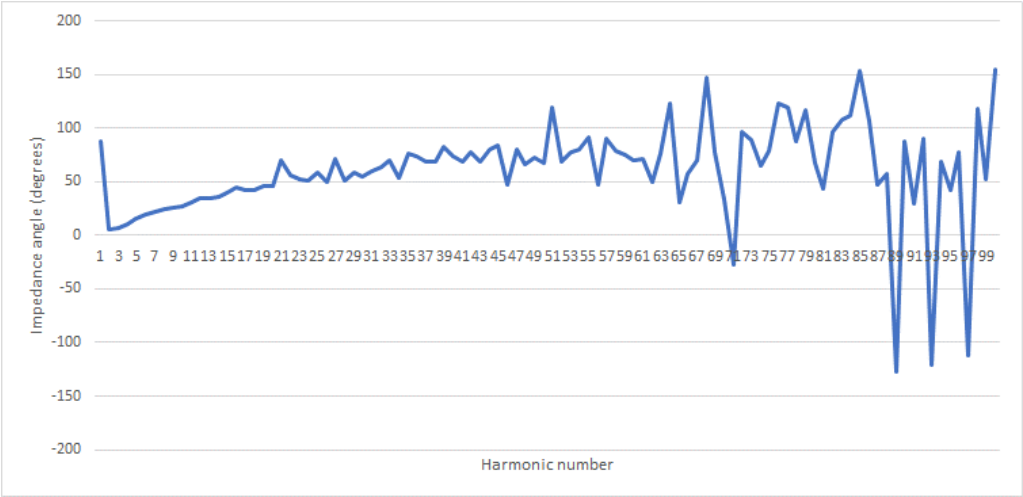

Figure 41. *STATCOM's impedance angle measured at PCC in zero current operating point with fundamental voltage feedforward.*

Phasor diagrams were drawn according to the equation 4.3 assuming capacitive grid impedance. In the first diagram STATCOM produced harmonic current is inductive-resistive and in the second diagram it is capacitive-resistive. The diagrams are presented in Figure 42.

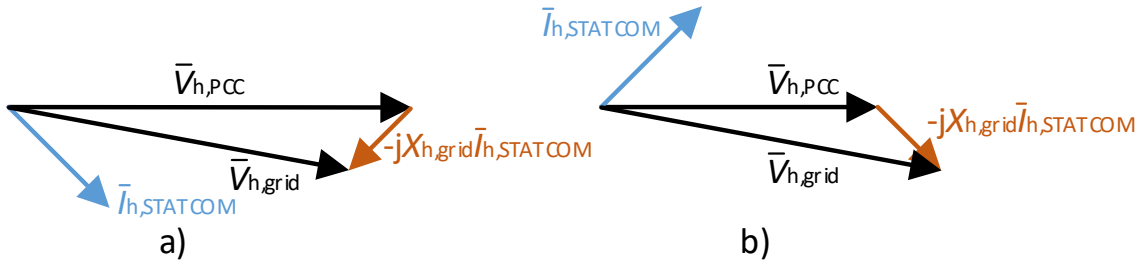

Figure 42. *Phasor diagram of grid and PCC harmonic voltages in capacitive grid, when STATCOM's harmonic current is a) inductive-resistive, b) capacitive-resistive.*

The situation is now opposite compared to inductive grid. When STATCOM's current is inductive-resistive, the voltage drop in capacitive grid impedance $-jX_{h,grid}$ causes larger harmonic voltage magnitude at PCC than in the supplying grid. When the current is capacitive-resistive, PCC harmonic voltage magnitude is smaller than the voltage magnitude in grid.

Simulation with same parameters was done also with instantaneous voltage feedforward. Harmonic current spectrum at PCC is presented in Figure 43.

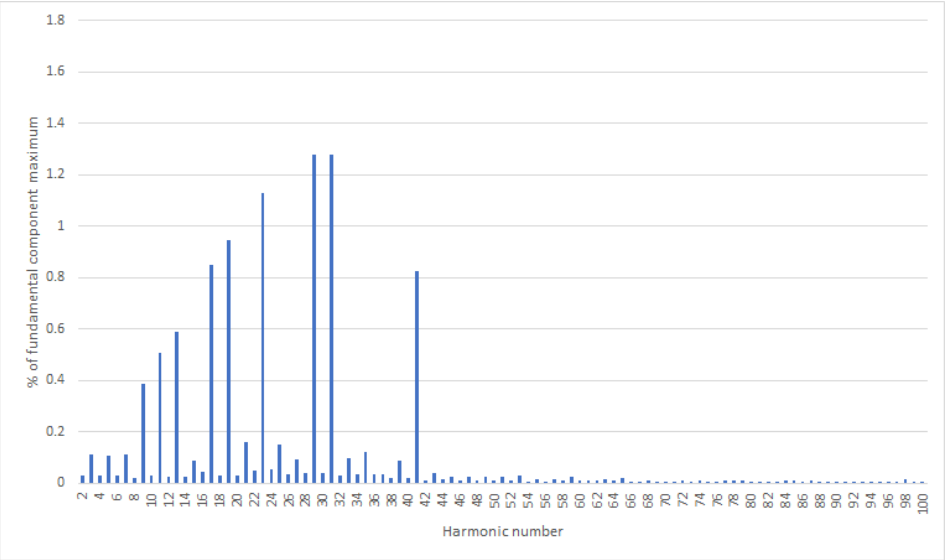

Figure 43. *Harmonic spectrum of PCC current in zero current operating point in capacitive-resistive grid with instantaneous voltage feedforward.*

Harmonic currents are increased at those frequencies where harmonic voltages were increased. Low-order harmonic currents are mitigated well due to harmonic voltage feedforward but harmonics around 30th order not much. Still, current TDD was 2.78 % which is smaller than with fundamental voltage feedforward. Resulting harmonic voltages in grid and at PCC are presented in Figure 44 and Figure 45.

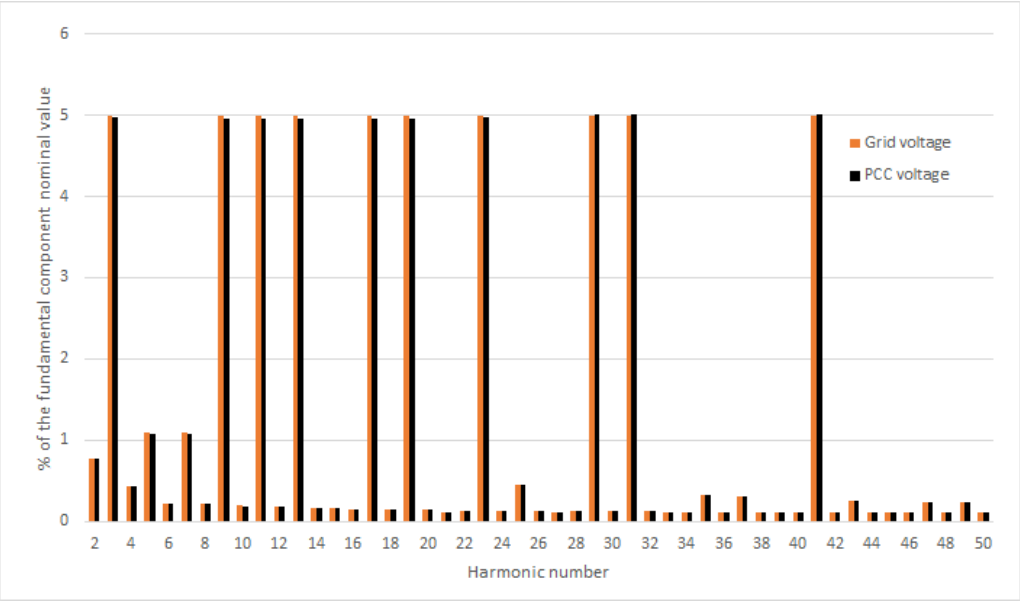

Figure 44. *A-phase harmonic voltages from 2nd to 50th in grid and PCC with instantaneous voltage feedforward when grid is capacitive-resistive.*

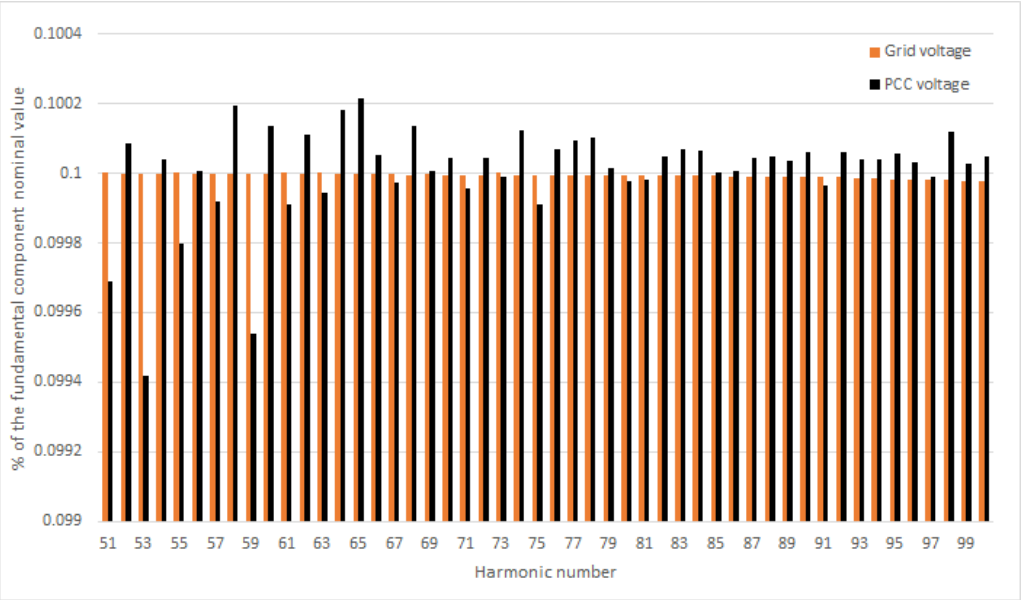

Figure 45. *A-phase harmonic voltages from 51st to 100th in grid and PCC with instantaneous voltage feedforward when grid is capacitive-resistive.*

Low-order harmonic voltages are decreased a bit at PCC but 29th, 31st and 41st harmonics are increased compared to grid. The reason can be found from STATCOM's impedance measured at PCC whose magnitude is shown in Figure 46 and angle in Figure 47.

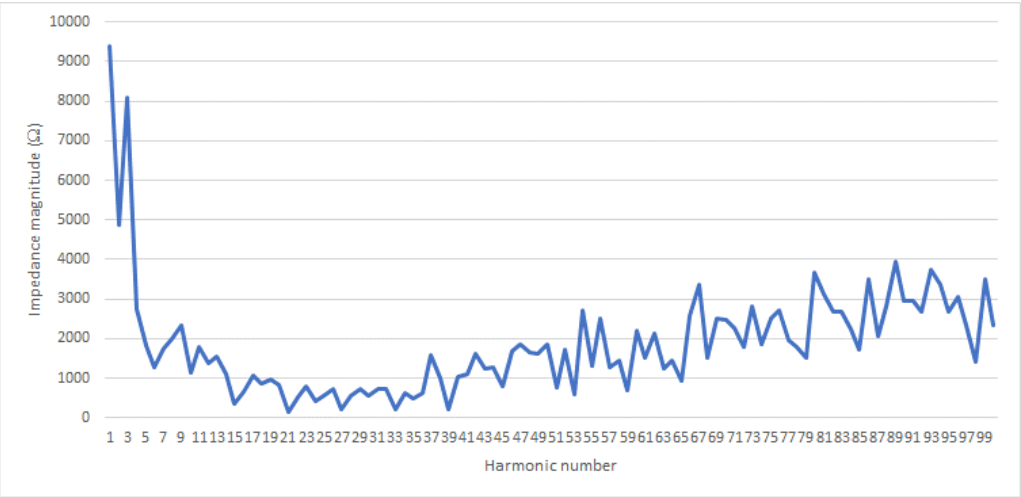

Figure 46. *STATCOM's impedance magnitude measured at PCC in zero current operating point with instantaneous voltage feedforward.*

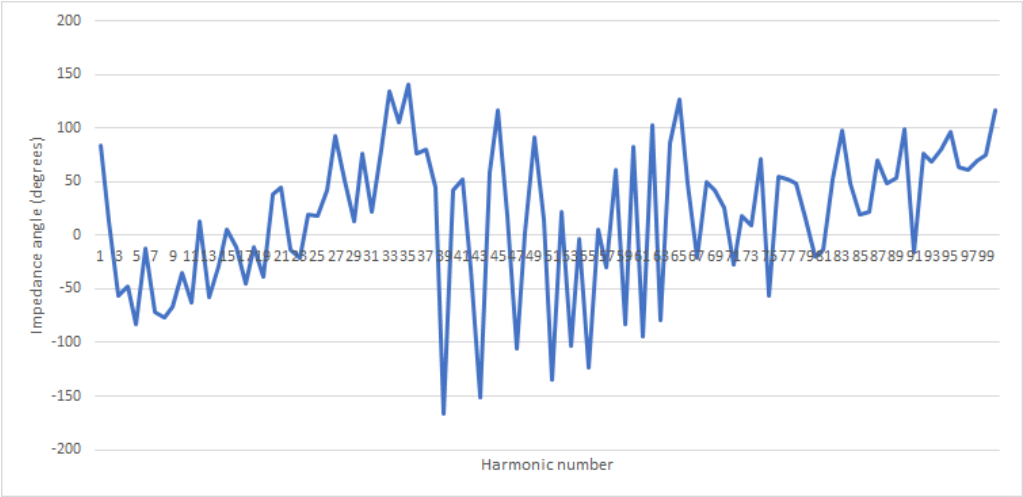

Figure 47. *STATCOM's impedance angle measured at PCC in zero current operating point with instantaneous voltage feedforward.*

It seems that STATCOM's impedance decreases up to 30th harmonic and starts to increase after that. It explains that the highest harmonic currents are around the 30th harmonic. The impedance also changes quite randomly between inductive-resistive and capacitive-resistive which explains that at some frequencies harmonic voltages increase at PCC and at some frequencies they decrease.

4.5 Comparison of voltage feedforward options

Based on the simulation results presented in the earlier subchapters voltage feedforward options were compared. When instantaneous value of measured secondary busbar voltage with all the harmonics is used as feedforward, STATCOM's impedance is quite high at low-order harmonics. However, the impedance seems to have a dip around 30th harmonic. That means relatively high harmonic current emissions at those frequencies if there are harmonic voltages present. High currents at high-order harmonics cause large harmonic voltage drops in inductive grid where impedance increases as function of frequency. The impedance angle is also very unpredictable so it can not be predicted if the harmonic voltage drop causes PCC harmonic voltage to rise or decrease even if grid impedance was known. Moreover, measuring harmonic voltages might be inaccurate which would deteriorate the performance and cause unpredictability even more.

When fundamental component of secondary busbar voltage is used as feedforward, STATCOM's impedance is quite predictable. It seems to be inductive-resistive at least up to 70th harmonic and increases as function of frequency. Impedance is lowest at low-order harmonics and thus highest harmonic currents appear at those frequencies. However, low-order harmonic currents can be mitigated by means of current control which is shown in chapter 5.2. The impedance around 30th harmonic is higher than with instantaneous feedforward so the high-order harmonic currents are mitigated more efficiently. On the other hand, if harmonic voltage feedforward was used for low-order harmonics only,

low-order harmonic currents could be reduced compared to fundamental feedforward and still good current mitigation at high-orders would be obtained also. This is studied in the next subchapter by using a low-pass filter for the measured voltage.

According to IEC/TR 61000-3-6, harmonic voltages from several sources can be added together to get statistical value for total harmonic voltage $V_{\mathrm{h,total}}$ as per

$$V_{\mathrm{h,total}} = \sqrt[\gamma]{\sum_{\mathrm{i}} {V_{\mathrm{hi}}}^{\gamma}}, \tag{4.4}$$

where V_{hi} is harmonic voltage caused by source i. Factor γ depends on the chosen probability level that actual value will not exceed the calculated value and, if known, on the degree how harmonic voltages from different sources vary on magnitude and phase. In reality, γ varies between 1 and 2. [20] The lowest value for V_{h} is got by exponent value 2 (geometrical sum) and the highest value is got by exponent 1 (arithmetic sum). According to the calculation procedure existing grid harmonic voltages and STATCOM produced harmonic voltages in grid impedances are added together. This means that if existing harmonic voltages are almost at the allowed limit, STATCOM should not produce any additional harmonic voltages. Transmission operators usually provide limits for harmonic voltages at PCC caused by the harmonic current emissions of STATCOM or define that harmonic voltages are calculated as in the standard described above.

Based on the simulations, when grid is inductive-resistive and fundamental voltage feedforward is used, produced inductive-resistive harmonic currents mitigate harmonic voltages at PCC. However, when grid is capacitive-resistive, harmonic voltages increase at PCC. Typically grid impedance is inductive but other loads such as power factor correction capacitors may change it to capacitive [39]. As explained in chapter 3.2, grid impedances change over time and thus they are often specified as sector or circle diagrams to include all possible values. They often include both inductive and capacitive values [25]. STATCOM should comply with harmonic voltage limits in every grid contingency, so the harmonic voltage filtering capability in inductive grid can not be utilized in system design.

A better approach to keep harmonic voltages at PCC in standard and specification limits in all situations is to minimize the produced harmonic currents and thus the harmonic voltage components that they cause to PCC. This approach works also if the grid is capacitive at some or all harmonics. The rest of the thesis concentrates on the minimization of harmonic current emissions.

4.6 Harmonic current emissions with filtered voltage feedforward

It was observed that instantaneous voltage feedforward performs better at low-order harmonics than fundamental voltage feedforward. However, it can not be used in reality because all measurement noise would be fed also forward. Therefore, a low-pass filter was designed for the measured voltage to reject high frequency noise. It was also noticed that instantaneous feedforward increases harmonic current emissions at orders from 20 to 40 compared to fundamental feedforward. Thus, those frequencies were tried to be filtered additionally.

Disadvantage of the filter is that it affects fundamental frequency also. As the feedforward's purpose is to make the fundamental frequency control response faster, filter should disturb fundamental component as little as possible. Thus, a filter with low cut-off frequency can not be used because it shifts fundamental frequency phase too much.

Filter was designed with MATLAB's Filter Designer tool. Butterworth low-pass filter was chosen because of its quite flat magnitude response at passband. First-order filter was selected to have as small effect on phase behavior as possible because the feedforward is very sensitive to phase delay. A cut-off frequency of 1500 Hz was chosen as then filter affects fundamental frequency phase only 1.79 degrees. Also -3 dB mitigation is achieved at 30th harmonic where the impedance dip was observed with instantaneous feedforward. The magnitude and phase of the designed filter are shown in Figure 48.

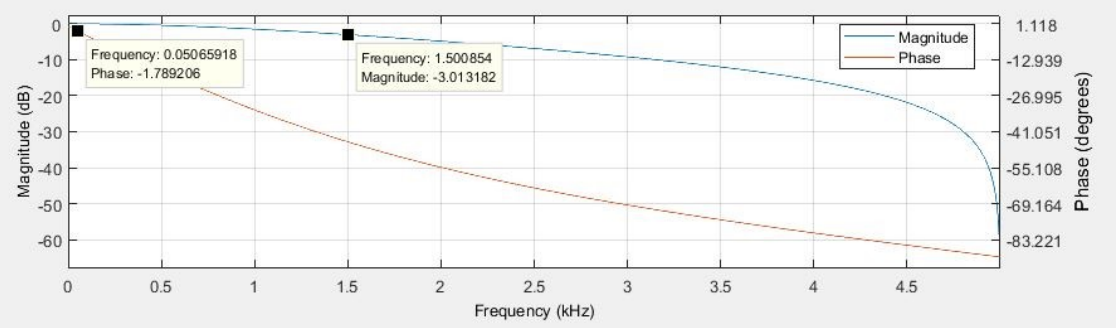

Figure 48. *Magnitude and phase of the designed low-pass filter.*

The discrete time coefficients of the filter were calculated by the tool. These coefficients were fed to a filter block implemented earlier in PSCAD. The block calculates the filter output from the present and previous input and output values of the filter using the coefficients. This filter block was then added to feedforward path. Simulation was done with same parameters as first simulation of chapter 4.2. Simulated harmonic current spectrum at PCC is presented in Figure 49.

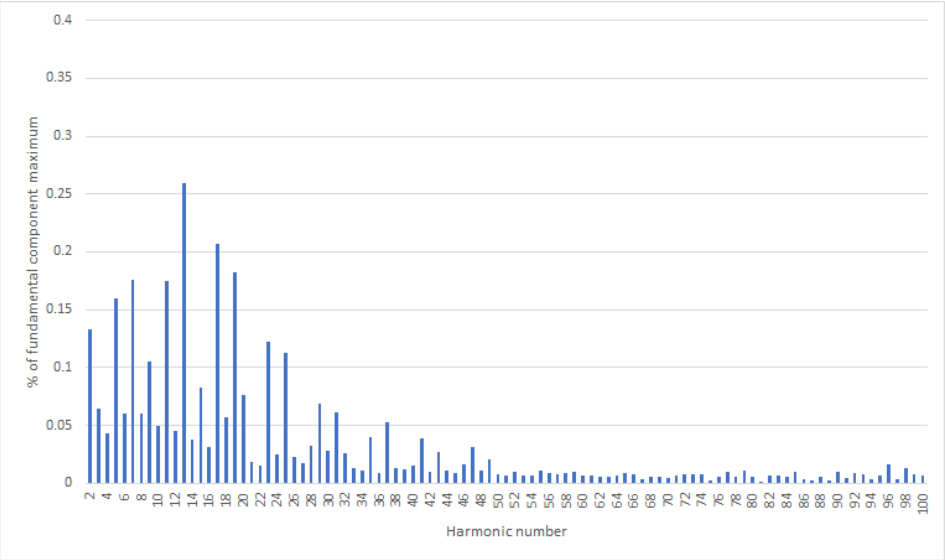

Figure 49. *Harmonic spectrum of PCC current in capacitive operating point with low-pass filtered voltage feedforward.*

Calculated current TDD was 0.589 % which is larger than with instantaneous voltage feedforward but clearly smaller than with fundamental voltage feedforward. Low-order harmonics are quite well mitigated but not as well as with instantaneous feedforward. The phase delay of the filter deteriorates the harmonic performance when the frequency increases. Due to delay, harmonic currents of orders from 10 to 20 have increased substantially compared to instantaneous feedforward. However, at high frequencies the magnitude of the filter decreases and thus the feedforward effect decreases. That is desirable because at harmonics around 30th order instantaneous feedforward effect was negative as it increased harmonics compared to fundamental feedforward. Now, harmonics around 30th order are considerably smaller than with instantaneous feedforward. Still, accurate harmonic voltage measurement in filter's passband is needed to achieve this performance.

STATCOM's impedance magnitude with filtered voltage feedforward is presented in Figure 50 and angle in Figure 51. Impedance magnitude has increased at low-orders compared to fundamental feedforward and around 30th order compared to instantaneous feedforward. However, it has decreased at low-order harmonics up to 20th order in comparison with instantaneous feedforward. Impedances are capacitive at low-order harmonics so in inductive grid they would cause increased harmonic voltages to PCC.

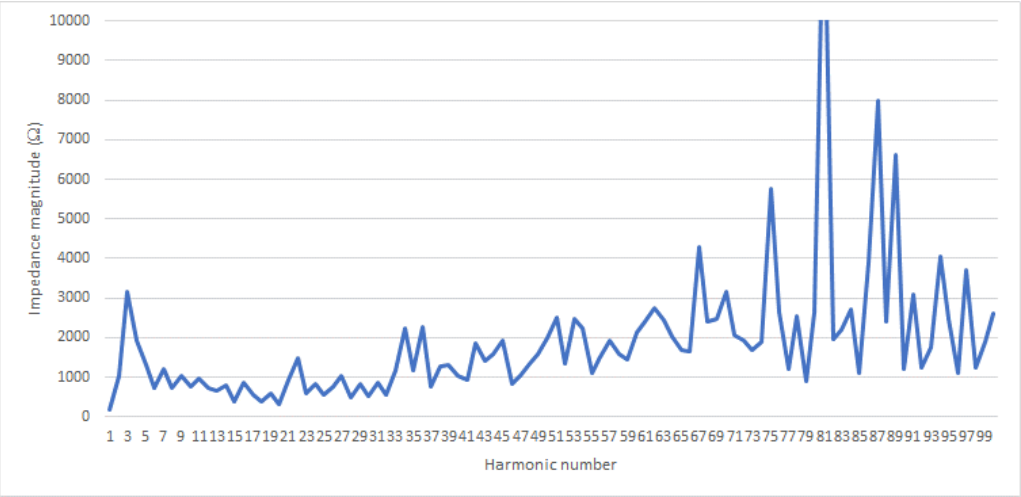

Figure 50. *STATCOM's impedance magnitude measured at PCC in capacitive operating point with low-pass filtered voltage feedforward.*

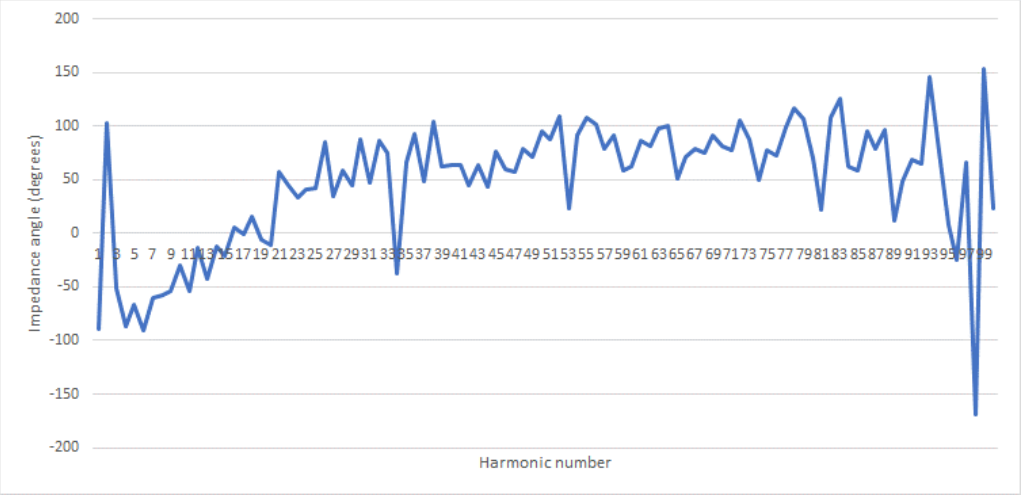

Figure 51. *STATCOM's impedance angle measured at PCC in capacitive operating point with low-pass filtered voltage feedforward.*

4.7 Harmonic current emissions with increased reactance

Harmonic current emissions can be decreased by increasing the impedance of STATCOM. The effect of increasing the impedance of STATCOM's passive components is studied in this chapter. First, transformer's reactance was increased by 50 % to 0.1725 p.u. Other parameters were same as in the first simulation of chapter 4.2. The harmonic spectrum of current measured at PCC is shown in Figure 52.

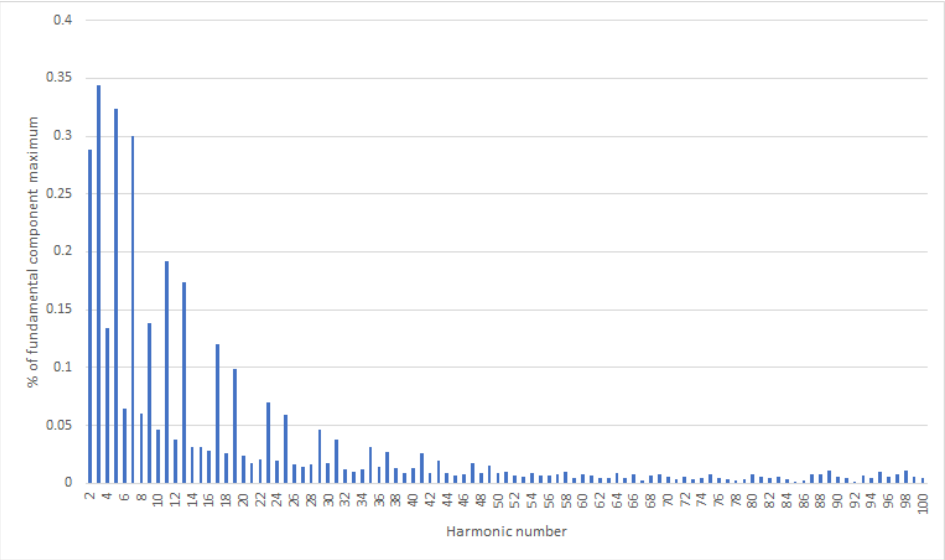

Figure 52. *Harmonic spectrum of PCC current with higher transformer's reactance.*

Compared to Figure 22, harmonic currents have decreased only slightly. Calculated current TDD was 0.749 % which is only a bit lower than with original reactance value.

Next, transformer's reactance was changed back to its original value and coupling reactor's inductance was increased by 50 % to 16.5 mH. Other parameters were not changed. The harmonic spectrum of current measured at PCC is presented in Figure 53.

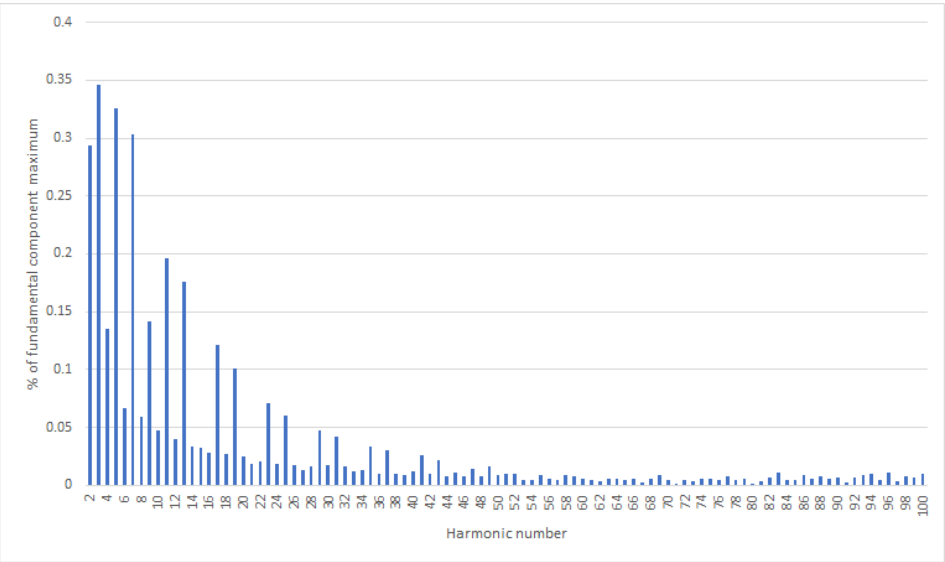

Figure 53. *Harmonic spectrum of PCC current with higher coupling reactor's inductance.*

Calculated current TDD was 0.758 %. Harmonic currents have decreased only a little. However, as inductance is increased, changing speed of STATCOM's output current is slowed down as equation for inductor shows:

$$\frac{di_L}{dt} = \frac{v_L}{L}, \tag{4.5}$$

where i_L is inductor current, v_L inductor voltage and L inductance. The increase of inductance can be compensated by increasing the P-gain (proportional gain) of current controller also by 50 %. That causes 50 % higher voltage component over inductor for same error between current reference and measured current and thus results in same current changing speed. Therefore, same dynamic performance is achieved as with original reactor and lower P-gain. The simulated harmonic spectrum of PCC current with increased P-gain and reactance is presented in Figure 54.

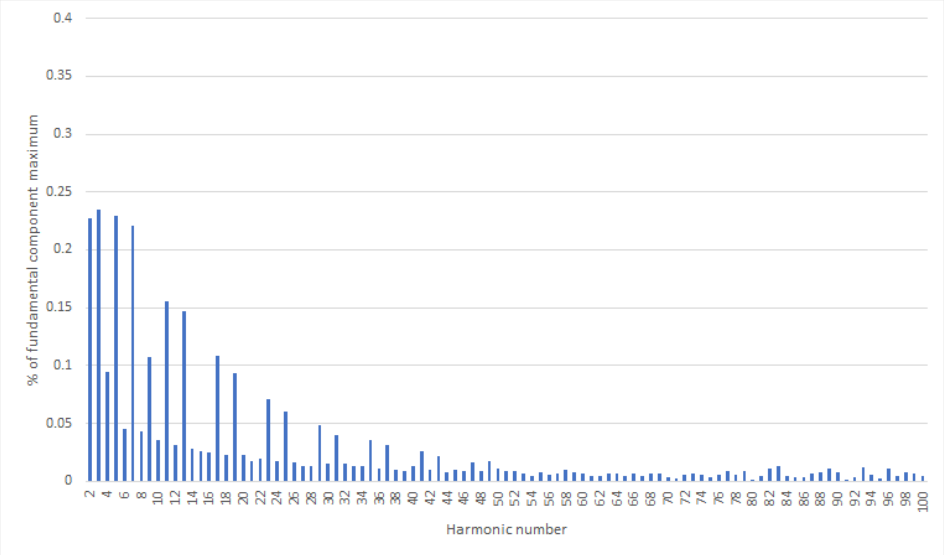

Figure 54. *Harmonic spectrum of PCC current with higher coupling reactor's inductance and P-gain.*

Calculated current TDD was 0.571 % so the increase of both factors reduces harmonic currents considerably. The increase of reactor's inductance is not an effective way to decrease harmonic currents itself but when it is combined with increase of P-gain, effect is significant.

The disadvantage of increasing the reactance of the components is that more material is needed and thus costs are increased. Moreover, as reactance is increased, higher converter voltage is needed to produce same capacitive current as equation 3.18 states. To produce higher converter voltage more submodules are needed in series which also raises costs.

Increasing current controller's P-gain without changing any component values was studied for voltage-source converter connected to grid through an LCL-filter [36]. It was observed that increase of P-gain decreases harmonic currents but makes the converter current more oscillatory in transient situations [36]. That would happen for STATCOM too because higher P-gain causes higher voltage reference and thus higher voltage over coupling reactor for same current error. According to equation 4.5, that increases the current changing speed.

5. SOURCES OF HARMONIC CURRENTS

In the earlier chapter secondary busbar voltage feedforward options were compared. Advantages of fundamental voltage feedforward were quite predictable behavior of STATCOM's impedance, good mitigation of high-order harmonic currents and no need for harmonic voltage measurement which might be inaccurate. Disadvantages were higher harmonic currents at low frequencies. However, it is shown in this chapter that at least in simulations with ideal current measurement they can be controlled to very small values by means of current control. Advantage of instantaneous voltage feedforward was better mitigation of low-order harmonic currents. However, harmonic currents of orders from 20 to 40 were larger than with fundamental feedforward. In addition, exact harmonic voltage measurement is required. Low-pass filtered voltage feedforward combined the good mitigation of low-order harmonics and harmonics around 30^{th} order but increased harmonic currents of orders from 10 to 20. Effect of harmonic currents on PCC harmonic voltages was studied but it was concluded that this information can not be utilized as the effect depends on grid impedance which changes over time. It was also shown that harmonic currents could be decreased by increasing the coupling reactor's reactance. Its effect is small itself but when combined with increased current controller's P-gain the harmonics could be decreased considerably. The disadvantage is that more reactor material and converter submodules are needed and therefore costs increase.

In this chapter, it is investigated if modulator or different controllers have effect on STATCOM's harmonic current emissions. Simulations are done where modulator or control block is made ideal and the produced harmonic current spectrum is compared to the spectrum of reference case. The reference case is the first simulation in chapter 4.2 whose current spectrum is shown in Figure 22. Moreover, solutions to decrease harmonics in the viewpoint of each control function are proposed or developed. First, the effect of modulator is investigated. Then, current controller and DC-link voltage controller impacts are studied. Last, manual current q-component control is changed to voltage control and the changes in harmonic spectrum are investigated. Synchronization to secondary busbar voltage is simplified in this simulation model so its effect is not studied. In this model it is implemented as Fast Fourier Transform which extracts the phase angles of secondary busbar's fundamental frequency line-to-line voltages.

5.1 Modulator effect

An ideal modulator produces exactly the reference voltage. It also balances submodule voltages so well that their voltages stay constant. That is impossible in a real system but this way additional harmonic voltages that are caused by the operation of modulator can

be eliminated. Still, produced voltage is not necessarily sinusoidal because reference voltage may contain harmonic components. It is investigated if producing the exact reference voltage decreases harmonic currents of STATCOM. In that case, other modulator schemes could be considered to improve performance.

Ideal modulator was implemented by setting the output voltage of converter equal to reference voltage. Submodule voltages were forced to stay at their nominal value. Figure 55 presents simulated harmonic current spectrum measured from PCC when ideal modulator was used and other parameters were same as in the reference case.

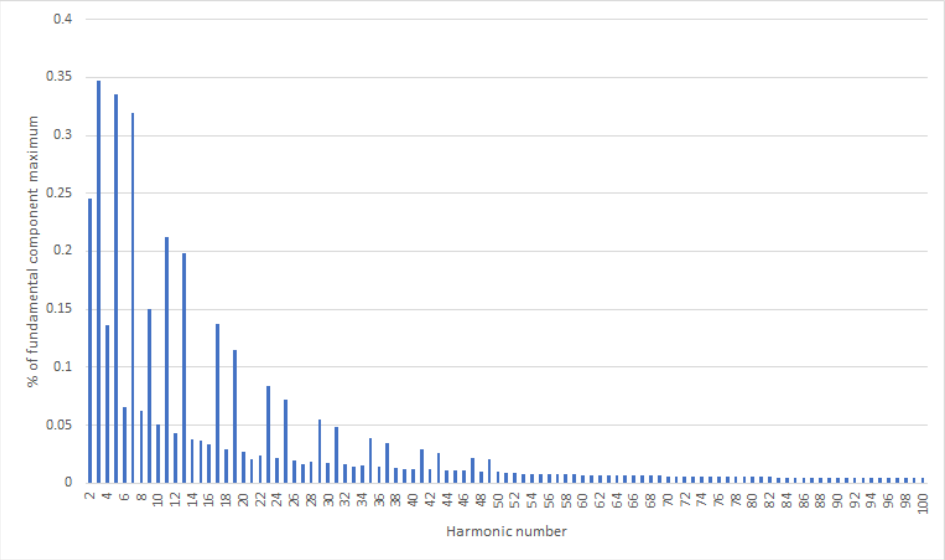

Figure 55. *Harmonic spectrum of PCC current with ideal modulator.*

Calculated current TDD was 0.774 % which is slightly lower than with original modulator. Harmonic currents are not decreased much but they are more predictable. It seems that if there are equal voltage magnitudes at some harmonics in grid, the magnitudes of those harmonic currents decrease linearly as function of frequency. The effect can be seen at harmonics from 51st to 100th where grid harmonic voltages are equal magnitude (0.1 % of the fundamental). Produced harmonic currents decrease quite linearly as function of frequency because the inductive reactances of passive components increase. When the original modulator was used, these higher frequency harmonics were more unpredictable. Another example are the harmonics 3, 5 and 7 which also have equal magnitudes in grid voltage but the current magnitudes decrease linearly when the frequency increases.

Next, harmonic current emissions were simulated using the ideal modulator with sinusoidal grid voltage. The harmonic spectrum of current at PCC is shown in Figure 56.

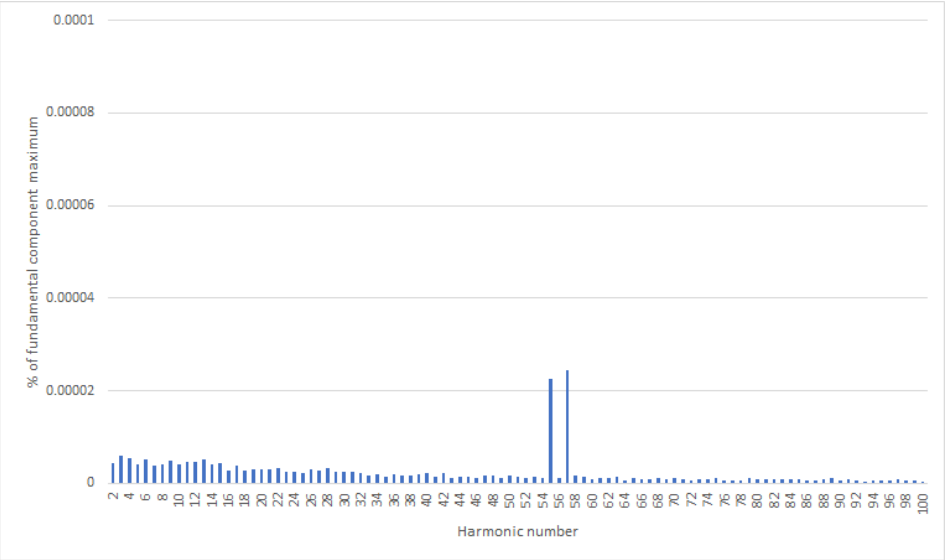

Figure 56. *Harmonic spectrum of PCC current with ideal modulator and sinusoidal grid voltage.*

Calculated current TDD was only 0.00004 %. It seems that when grid voltage is sinusoidal, modulator causes all the harmonic current emissions. However, the emissions are already very low with original modulator in that situation (Figure 18) and not usually a problem.

The original modulator is a modification of nearest-level control modulation scheme. In this kind of modulator, the spectrum of voltage is spread to all harmonics [34]. If grid voltage is sinusoidal, those harmonic components appear in current also. In some other modulator schemes harmonic voltages could be centered to higher frequencies. In phase-shifted carrier modulation the lowest order harmonics would appear at the sidebands of the harmonic whose order is the number of submodules in one phase multiplied by the ratio of carrier frequency to fundamental frequency [34]. If the number of submodules is high enough, low-order harmonics are decreased a lot [34]. Same voltage waveform and thus harmonics could also be achieved with level-shifted carrier modulation having an alternative phase opposition disposition between adjacent two levels [34]. This could be beneficial if producing currents at some low-order harmonics is forbidden and grid voltage does not have those harmonic components. As observed in Figure 55 for ideal modulator, if there are harmonic voltages in grid voltage, also harmonic currents of same orders appear so the modulator scheme does not really make a difference.

In the earlier chapter, it was concluded that the instantaneous voltage feedforward does not work as it is planned to. Now, simulation was done to see if using ideal modulator without delays would improve the harmonic performance when instantaneous feedforward is used. Grid's harmonic voltages were set back to reference case values. The harmonic spectrum of current measured at PCC is shown in Figure 57.

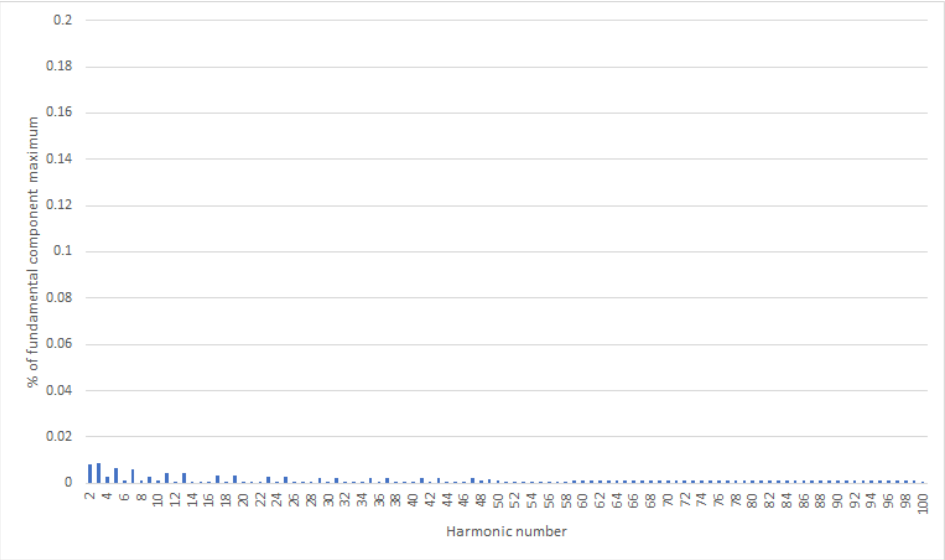

Figure 57. *Harmonic spectrum of PCC current with ideal modulator and instantaneous voltage feedforward.*

Current TDD was only 0.020 %. It seems that modulator causes the performance of instantaneous feedforward to deteriorate. The most probable reason is the delay introduced since modulator algorithm is executed once in 100 µs.

The delay effect of original modulator on harmonic performance of instantaneous feedforward was studied by using the original modulator and changing modulator algorithm execution interval to 1 µs. In reality, algorithm can not be executed so often. Submodule voltages were balanced according to the modulator algorithm and thus they were not constant as with ideal modulator. Resulting PCC current spectrum is shown in Figure 58.

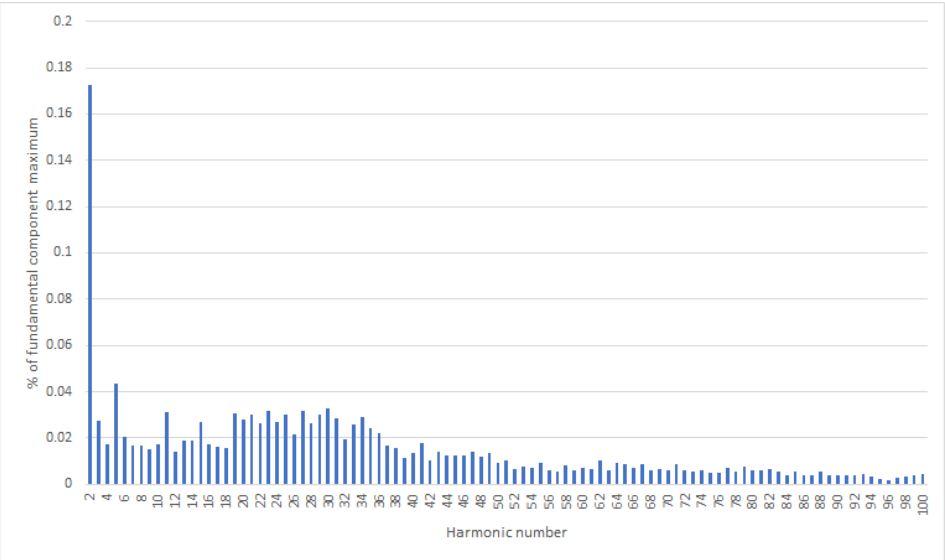

Figure 58. *Harmonic spectrum of PCC current with instantaneous voltage feedforward and modulator algorithm executed once in 1 µs.*

Current TDD was 0.236 %. Current distortion is larger than with ideal modulator but still very low except for second harmonic. A more realistic interval of 50 µs was simulated next and the harmonic spectrum of current is presented in Figure 59.

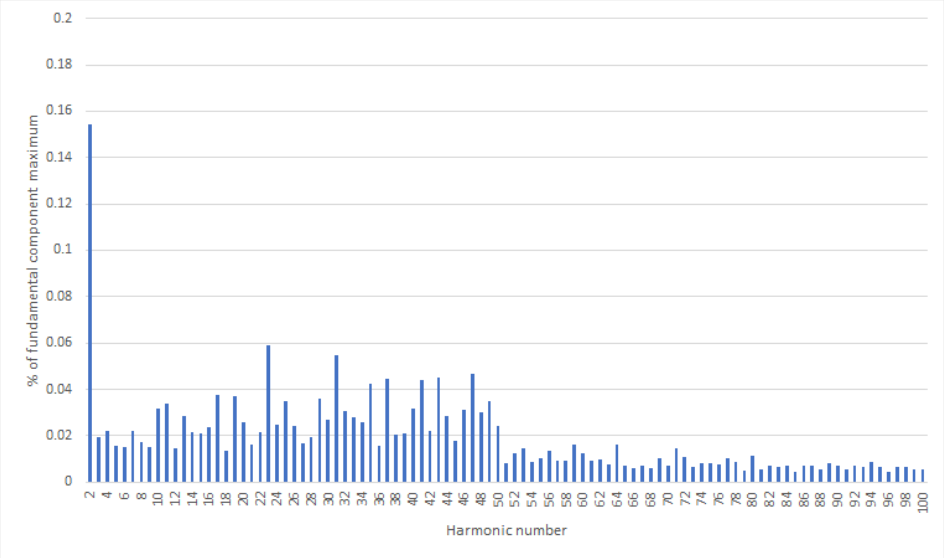

Figure 59. *Harmonic spectrum of PCC current with instantaneous voltage feedforward and modulator algorithm executed once in 50 µs.*

Calculated current TDD was 0.265 % which is a bit more than half of the TDD with 100 µs interval. So, by increasing the modulator's execution frequency, the harmonic performance with instantaneous feedforward could be improved a lot. However, as modulator algorithm is performed with double frequency, switching frequency is doubled and losses increase considerably. In addition, the simulation model does not include other delays and harmonic voltage measurement errors. Thus, the performance of instantaneous feedforward may be worse than simulated.

5.2 Current control effect

An ideal current controller would make the current follow its reference exactly. A controller more ideal than the original was implemented by increasing controller's gain at some harmonics.

Current control can be implemented in various ways. To track a sinusoidal current reference PI-controller (proportional-integral controller) can not be used because it can not remove the steady-state error. One possibility is to transform three-phase current signals to synchronous reference frame (dq-frame) where they are DC-values and PI-controllers can be used. Another way is to use PR-controllers (proportional-resonant controllers). In stationary reference frame for three-phase systems two PR-controllers can be used to control separately α- and β-components. In single-phase systems conventional transformation to synchronous frame can not be applied but PR-controllers can still be used. [35]

Transfer function for ideal PR-controller is

$$G_{\mathrm{PR,ideal}}(s) = K_{\mathrm{P}} + \frac{2K_{\mathrm{I}}s}{s^2+{\omega_{res}}^2}, \tag{5.1}$$

where K_{P} is proportional gain, K_{I} integral gain, ω_{res} resonance frequency and s Laplace transform variable [35]. Non-ideal PR-controller's transfer function is

$$G_{\mathrm{PR,non-ideal}}(s) = K_{\mathrm{P}} + \frac{2K_{\mathrm{I}}\omega_{\mathrm{c}}s}{s^2+2\omega_{\mathrm{c}}s+{\omega_{res}}^2}, \tag{5.2}$$

where ω_{c} is cut-off frequency which is much smaller than ω_{res} [35]. When resonance frequency is chosen to fundamental frequency and proportional gain is 1, ideal PR-controller's gain is infinite at that frequency and zero decibel at other frequencies. Non-ideal PR-controller's gain at resonance frequency is high but finite. The peak is wider around the resonance frequency so frequencies near resonance frequency get magnified also. The non-ideal controller can therefore control the current even though its frequency changes slightly which is the case in a utility grid. The width of the resonance peak can be modified by changing the cut-off frequency. [35] Figure 60 presents the frequency responses of ideal and non-ideal PR-controllers with parameters $K_{\mathrm{P}} = 1$, $K_{\mathrm{I}} = 20$, $\omega_{\mathrm{res}} = 314$ rad/s and $\omega_{\mathrm{c}} = 10$ rad/s.

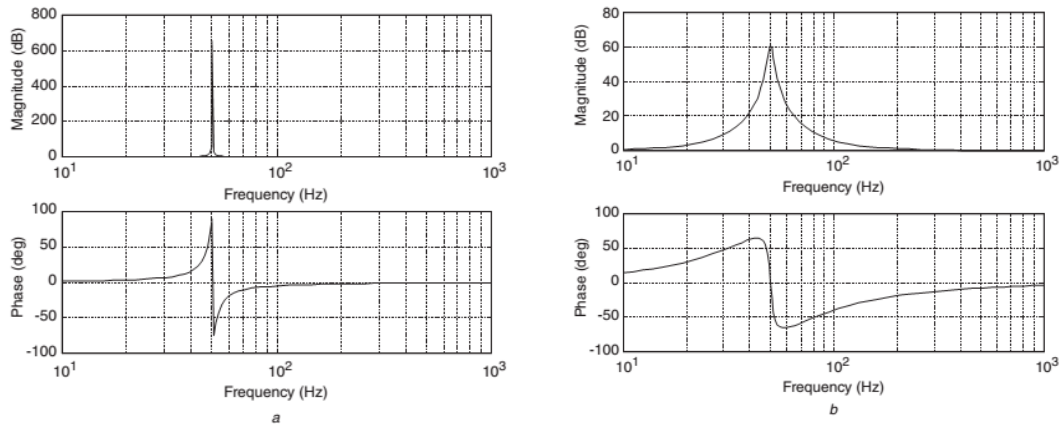

Figure 60. *PR-controller transfer functions, a) ideal, b) non-ideal [35].*

In addition to fundamental frequency current control, branches for harmonics can be added to control them. They do not affect fundamental frequency control because they are tuned to magnify only controlled harmonics and frequencies near them. To control harmonics the following transfer function is added to the ideal control function 5.1:

$$G_{\mathrm{h,ideal}}(s) = \sum_{\mathrm{h}} \frac{2K_{\mathrm{Ih}}s}{s^2+(h\omega_{\mathrm{res}})^2}, \tag{5.3}$$

and the following to the non-ideal transfer function 5.2:

$$G_{\mathrm{h,non-ideal}}(s) = \sum_{\mathrm{h}} \frac{2K_{\mathrm{Ih}}\omega_{\mathrm{c}}s}{s^2+2\omega_{\mathrm{c}}s+(h\omega_{\mathrm{res}})^2}, \tag{5.4}$$

where sum is taken from the harmonics h that are controlled [35]. K_{Ih} is integral gain at harmonic order h. Integral gains for harmonics should be tuned to relatively high but within stability limit [35].

In s-domain, the transfer function of ideal PR-controller for fundamental frequency and harmonics is the sum of equations 5.1 and 5.3. Because real-time control systems are discrete, the transfer function needs to be discretized to the z-domain. Common method for discretization is the Tustin method or bilinear transform. In the Tustin method, continuous-time transfer function is discretized by substituting the Laplace transform variable s with:

$$s \rightarrow \frac{2}{T_s}\frac{z-1}{z+1}, \tag{5.5}$$

where T_s is the sampling period and z is the Z-transform variable [40, 41]. However, original version of Tustin method causes error between continuous-time and discretized versions of the transfer function at higher frequencies. To eliminate the error at a desired frequency, prewarped version of the same method can be used. The idea is that the continuous-time transfer function is first prewarped at a desired frequency ω_{pw} and then discretized by the original Tustin substitution. Prewarping ensures that at the prewarp frequency the magnitudes of the continuous-time and discrete-time transfer functions are equal. At other frequencies, the errors remain. [40, 41] Still, as control is done at the desired prewarp frequency, that is not a problem. The prewarping and discretization together result in the following substitution [41]:

$$s \rightarrow \frac{\omega_{pw}}{\tan(\frac{\omega_{pw}T_s}{2})}\frac{z-1}{z+1}. \tag{5.6}$$

When s-domain transfer function for one harmonic is discretized (equation 5.3 or 5.4), the z-domain transfer function has the following form:

$$G_h(z) = \frac{N_0+N_1z^{-1}+N_2z^{-2}}{1+D_1z^{-1}+D_2z^{-2}}. \tag{5.7}$$

where N_0, N_1, N_2, D_1 and D_2 are the numerator and denominator coefficients, z^{-1} means previous sample value and z^{-2} value before that. In z-domain controller output for one harmonic y_h at time instant k is

$$y_h(k) = G_h(z)u_h(k), \tag{5.8}$$

where u_h is controller input at the harmonic component. Therefore, output of controller for one harmonic can be calculated from output's previous values and input's present and previous values.

In STATCOM three single-phase PR-controllers are used which try to control each phase current to the desired reference value. R-branches of the ideal form were added for the

harmonics from 2nd to 15th to make them also follow their references better. Original controller in PSCAD-model was updated to include these branches. The z-domain numerator and denominator coefficients for every branch were calculated by MATLAB's continuous-to-discrete function with prewarped Tustin as discretization method. Controlled harmonic frequencies were used as prewarp frequencies. The coefficients were used to calculate output for each controlled harmonic. These outputs were added to the sum of fundamental component R-branch output and P-term output which magnifies the inputs of all frequencies equally.

Simulation was done with added R-branches and same parameters as in the reference case. Fundamental voltage feedforward was used where largest harmonic currents appeared at low frequencies. Proportional gain of 110 and integral gain of 10 for fundamental component were used as in all simulations earlier. Integral gain of 500 was chosen for all controlled harmonics. Bode plot of the used controller is presented in Figure 61.

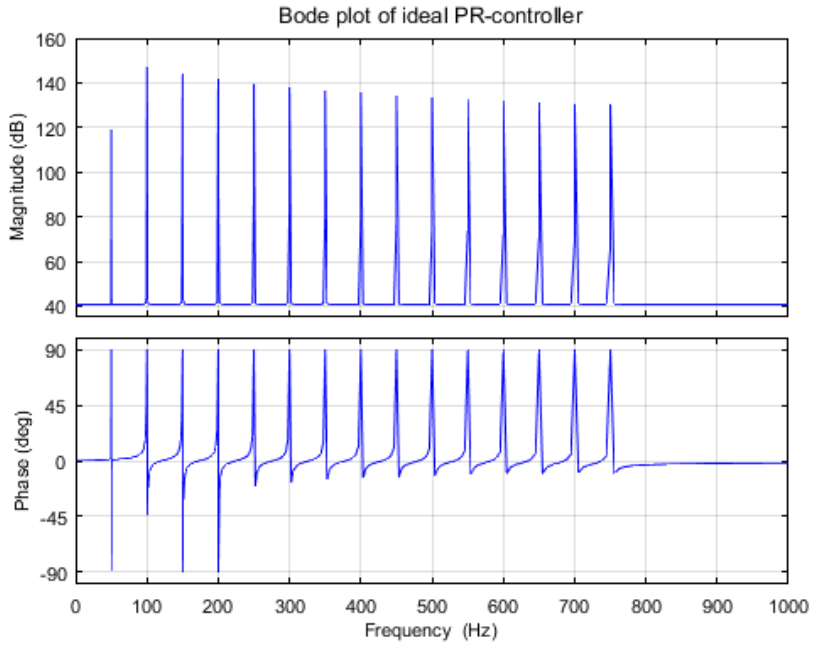

Figure 61. *Bode plot of the designed ideal PR-controller.*

Magnitudes at controlled harmonic frequencies are high so the harmonic currents should follow their references well. However, due to high magnitudes there might be a risk of oscillatory response in transient situations. Simulated harmonic spectrum of PCC current is shown in Figure 62 after 10 seconds of simulation.

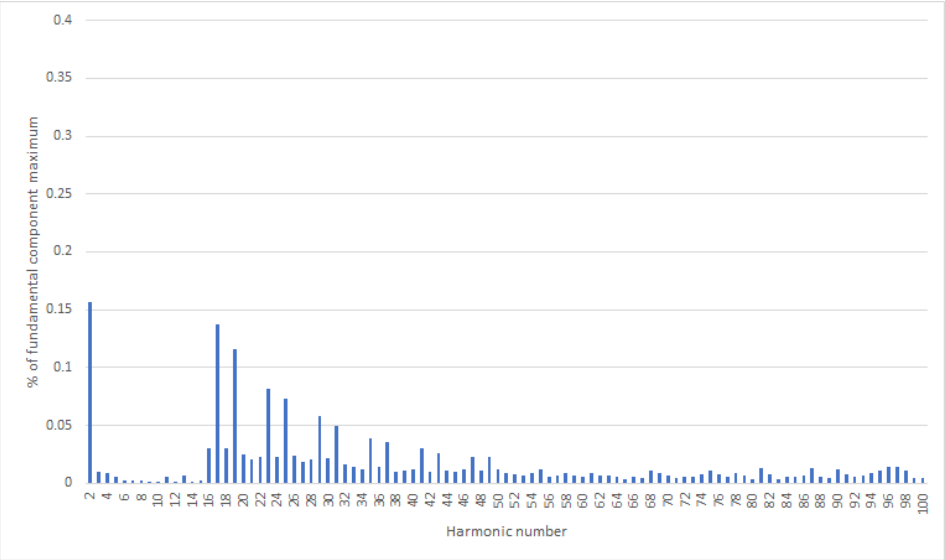

Figure 62. *PCC harmonic current spectrum with ideal control of low-frequency harmonic currents.*

Compared to the reference case (Figure 22), controlled harmonic currents from 3rd to 15th have decreased significantly. The second harmonic current has been mitigated almost to half of its original value. Other harmonics have stayed quite same. Calculated current TDD was 0.302 % which is considerably smaller than in the reference case.

The PR-controller tries to make current follow its reference. As there is now higher gain at harmonics up to 15th, also these harmonic currents are forced to follow their references. This implies that there is a second harmonic component in current reference. Thus, the harmonic spectrum of current reference in delta branch between phases a and b was simulated. It is presented in Figure 63.

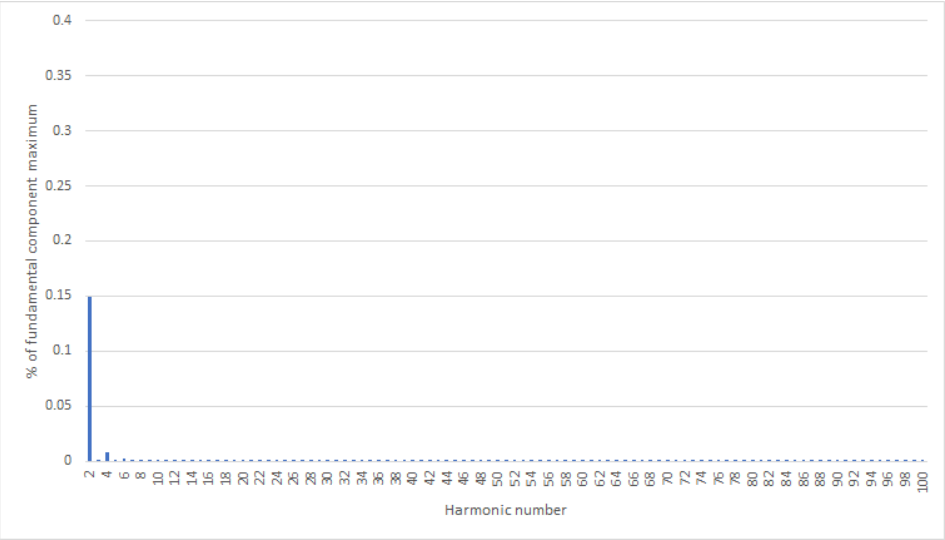

Figure 63. *Harmonic spectrum of current reference in ab-branch with ideal control of low-frequency harmonic currents.*

As expected, there is second harmonic component in current reference which is almost as large as the produced second harmonic current at PCC. There is also a small fourth harmonic component in the reference which can be seen in the produced current also. Produced current has some of the controlled harmonics that are not present in the reference. Their magnitudes are still very small. As observed in the earlier subchapter, modulator affects harmonic currents slightly so it may cause the small deviations.

The performance of non-ideal PR-controller was also investigated. In s-domain, the transfer function of the controller for fundamental and harmonics is the sum of equations 5.2 and 5.4. Harmonics up to 15th order were controlled as with ideal PR-controller. Proportional gain of 110 was used as earlier. Integral gain of 500 and cut-off frequency of 3 Hz were chosen for fundamental component and harmonics. Bode plot of the designed controller is shown in Figure 64.

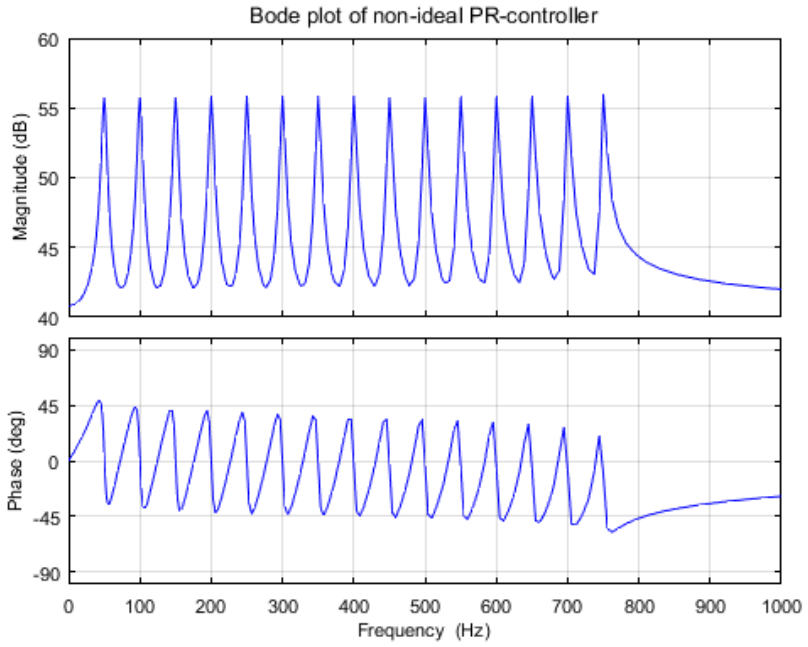

Figure 64. *Bode plot of the designed non-ideal PR-controller.*

Magnitudes at fundamental frequency and harmonics are considerably smaller than with ideal controller. Therefore, harmonic currents might not be so well mitigated and fundamental frequency control might be more inaccurate and slower than with ideal controller. However, transient response should not be so oscillatory as with ideal controller due to smaller gains.

Each harmonic R-branch of the designed controller was discretized by prewarped Tustin method using the respective harmonic frequencies as prewarp frequencies. Calculated discrete coefficients were fed to the PSCAD model. Simulation was done with designed

controller and same parameters as in the reference case. Simulated PCC current is presented in Figure 65.

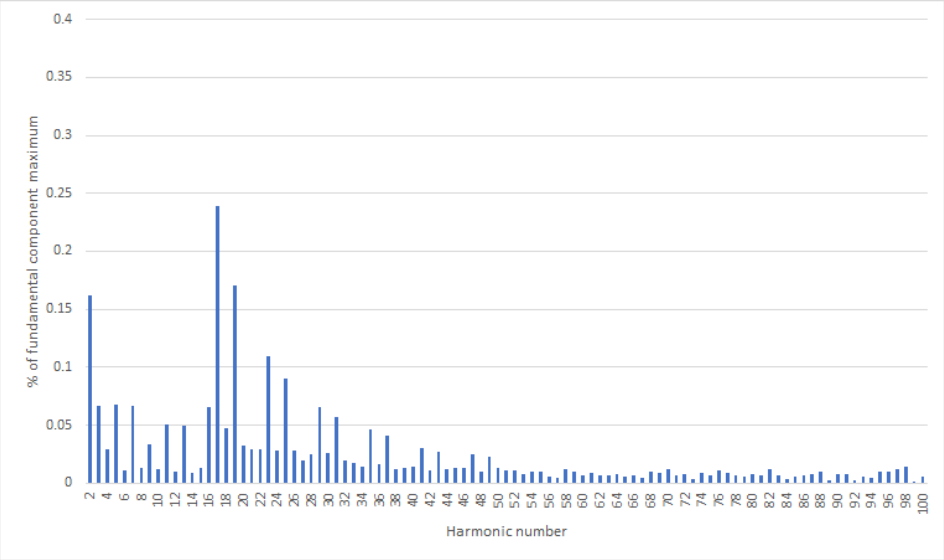

Figure 65. *PCC harmonic current spectrum with non-ideal control of low-frequency harmonic currents.*

Controlled harmonic currents have decreased significantly compared to the reference case. Still, mitigation is not as good as with ideal PR-controller. Produced second harmonic current is almost as large as with ideal control and it results from the second harmonic in current reference as observed earlier. Other harmonic currents which were not controlled have increased a bit. Current TDD was 0.432 % which is 43 % higher than with ideal control. Used integral gain for harmonics was chosen to be same as with ideal control for comparison. It was not optimized with respect to harmonic performance so it may still be possible to increase gains at harmonics to decrease currents.

Theoretically, all harmonic currents could be removed by adding R-branches to current controller for all harmonics. Exceptions are the second and fourth harmonic which are present in the reference and the small harmonic currents caused by modulator. However, in reality the measurement for harmonics may not be so accurate as for fundamental component which may deteriorate the performance of current control. Harmonic currents are tried to be controlled to zero or at least almost to zero so the sensor should be very sensitive at harmonics. At the same time, the sensor should accurately measure small DC-component and the fundamental component which can be up to 1000 A RMS. Currently used LEM ITL-4000-S fluxgate current transducer's sensitivity is almost 0 dB up to 10 kHz as can be seen from Figure 66 [42]. However, the sensitivity is measured with 40 A RMS primary current so characteristics might be worse for smaller currents.

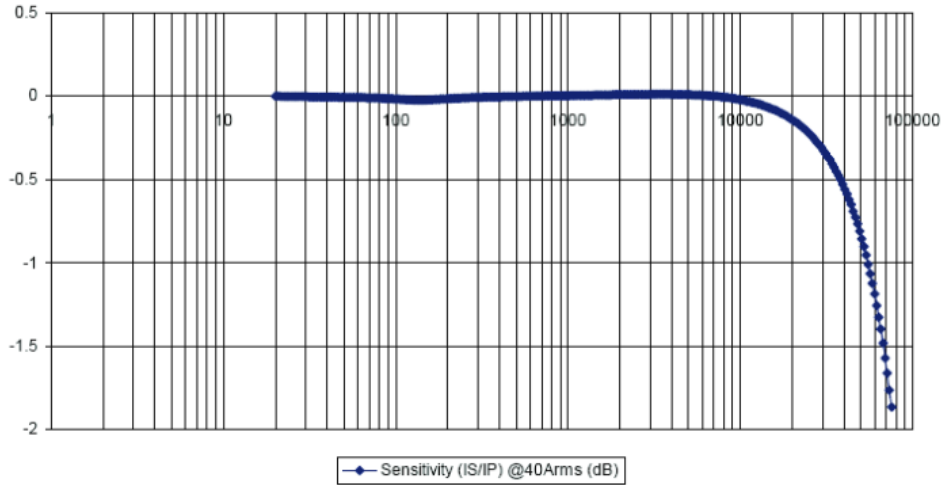

Figure 66. *LEM ITL-4000-S current transducer's sensitivity in decibels as function of frequency [42].*

5.3 DC-link voltage control effect

In the earlier subchapter it was found out that there are second and fourth harmonic components in current reference. As manual current q-component control is used and q-component reference is kept constant, the harmonics must come either from the synchronization to secondary busbar voltage or the controllers which control total DC-voltages of MMC branches to nominal values.

Effect of DC-link voltage control can be removed by setting all submodule voltages constant. Then, total DC-voltages of each branch stay constant all the time and controlling of branch voltages is not needed. This affects modulator a bit also because DC-voltages of submodules do not change and thus they are not needed to be balanced either.

Submodule voltages were forced to stay at their nominal values and current control with ideal PR-controller for harmonics from 2^{nd} to 15^{th} was used with same parameters as before. Simulated PCC current harmonic spectrum is presented in Figure 67.

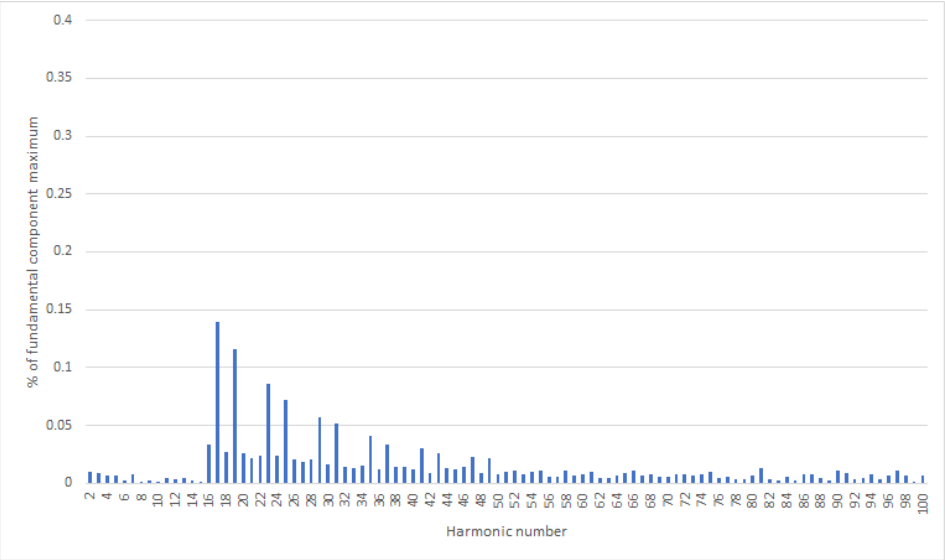

Figure 67. *Harmonic spectrum of PCC current with constant DC-voltages and low-frequency harmonic current control.*

Second harmonic current has decreased to same order of magnitude as other low-order harmonics. This result confirms that controlling of branch DC-voltages causes the second harmonic to increase. Harmonic spectrum of current reference in ab-branch in this case is shown in Figure 68.

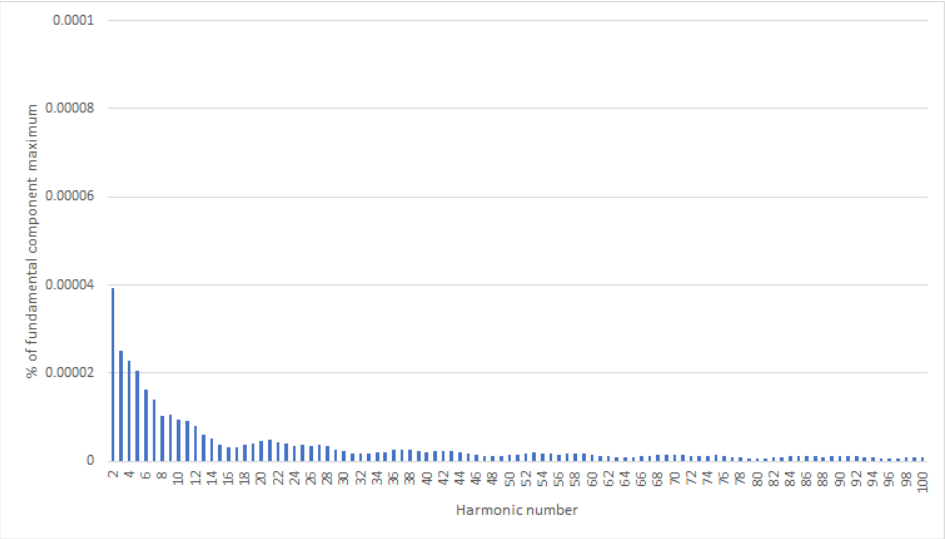

Figure 68. *Harmonic spectrum of current reference with constant DC-voltages and low-frequency harmonic current control.*

Second and fourth harmonic components have disappeared from the reference. Rest of the harmonics from 2nd to 15th order appearing in PCC current are thus result of modulator operation or errors in current control.

DC-link voltage control consists of two controllers so the exact origin of second harmonic current was investigated. In the current reference, second harmonic could be any sequence. However, second harmonic appears in PCC current also. Therefore, it can not be zero sequence since zero sequence current can not escape the delta connected STATCOM or flow through the star-delta connected transformer. Thus, second harmonic should be a result of control which balances the average of DC-voltages in three branches and produces current d-component reference. Consequently, simulation with ideal PR-control for harmonics up to 15th order was repeated and the spectrum of current d-component reference transformed to the stationary frame was recorded. The reference current term in stationary frame $i_{\mathrm{d,ab,ref}}$ due to current d-component reference $i_{\mathrm{d,ref}}$ is calculated as follows:

$$i_{\mathrm{d,ab,ref}} = \sqrt{2} i_{\mathrm{d,ref}} \sin(\omega_1 t + \theta), \tag{5.9}$$

where ω_1 is the fundamental angular frequency, t time and θ angle provided by synchronization to secondary busbar. The spectrum of the reference is shown in Figure 69.

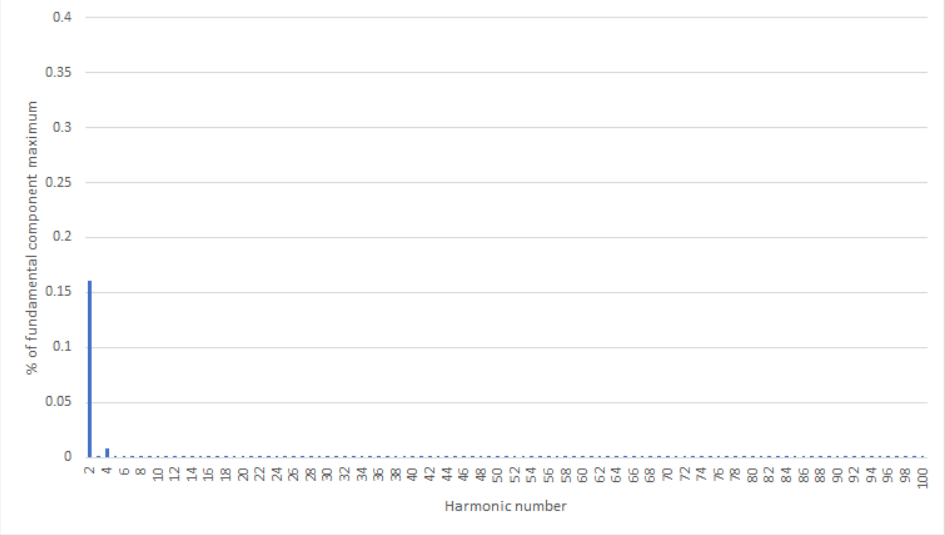

Figure 69. *Harmonic spectrum of current d-component reference in stationary frame with low-frequency harmonic current control.*

Second and fourth harmonics are almost same magnitude as in the total current reference. These harmonics are therefore a result of controlling the average of DC-voltages in three MMC branches to the nominal value. As the harmonics participate in DC-link voltage control in STATCOM, it may be difficult to remove them.

However, it was observed in chapter 4.1 that when grid voltage is sinusoidal, second harmonic current is very small. So, it seems that DC-link voltage control does not increase second harmonic current when there are not harmonic voltages present in grid. It was further studied by repeating the simulation in capacitive operating point with sinusoidal grid voltage. Simulated current reference in ab-branch is shown in Figure 70.

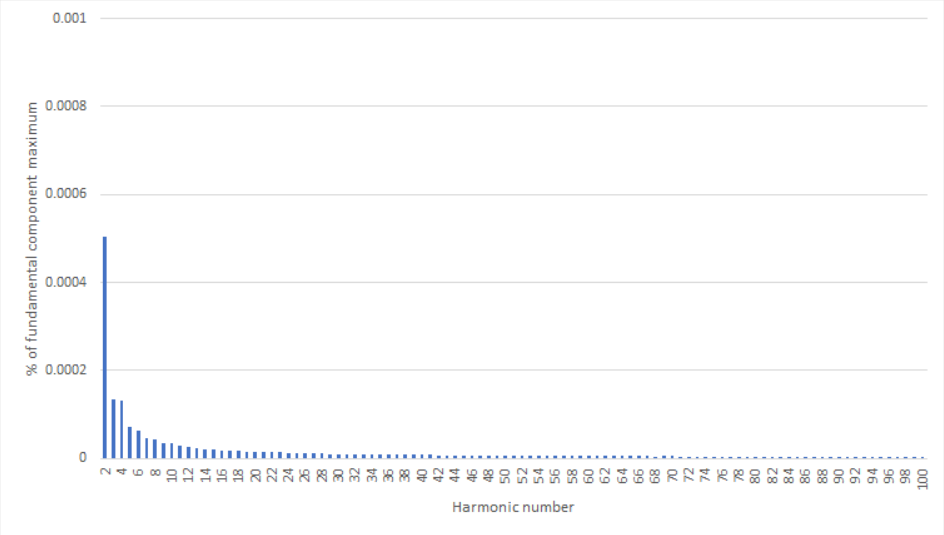

Figure 70. *Harmonic spectrum of current reference with sinusoidal grid voltage.*

Second harmonic current is negligible in the reference. It can be concluded that second harmonic current increases due to combined effect of harmonic voltages in grid and control of average DC-voltage in three MMC branches.

5.4 Voltage control effect

Investigation of voltage control effect on harmonic current emissions is quite simple. In all previous simulations manual current q-component control was used. It is only needed to switch on the voltage control function which provides the current q-component reference. First, simulation was done with voltage reference of 1.05 p.u which resulted in 993 A capacitive current in STATCOM's delta branch. The operating point is thus almost same as in the reference case. Harmonic current spectrum at PCC is shown in Figure 71.

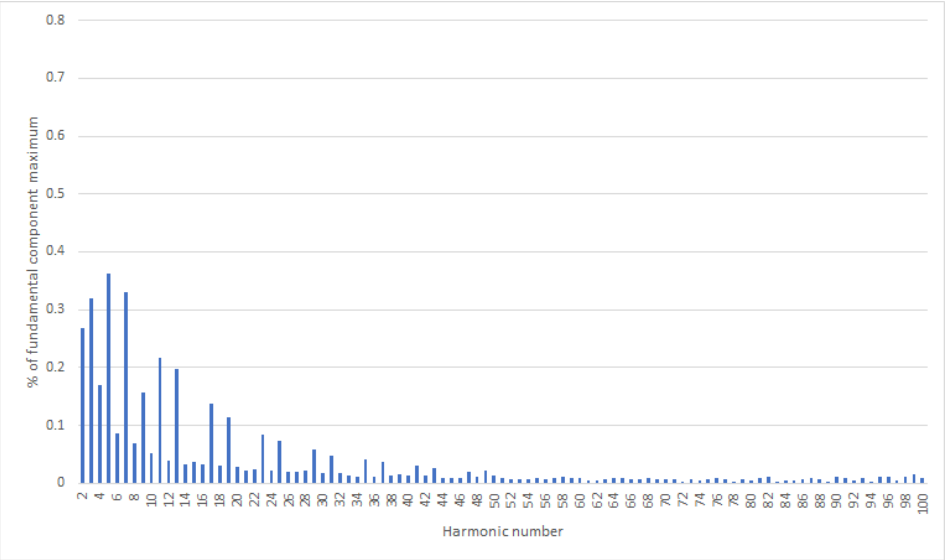

Figure 71. *Harmonic spectrum of PCC current with voltage control (1.05 p.u voltage reference).*

Calculated current TDD was 0.800 % which is almost same as in the reference case. Moreover, the spectrum resembles reference case spectrum. Low-order harmonics have increased or decreased slightly compared to it.

However, voltage controller provides current q-component reference and can add harmonics to it. These harmonics are not seen well in the output current because current controller's gain is low at harmonics. Therefore, also the harmonic spectrum of current reference in ab-branch was recorded. It is presented in Figure 72.

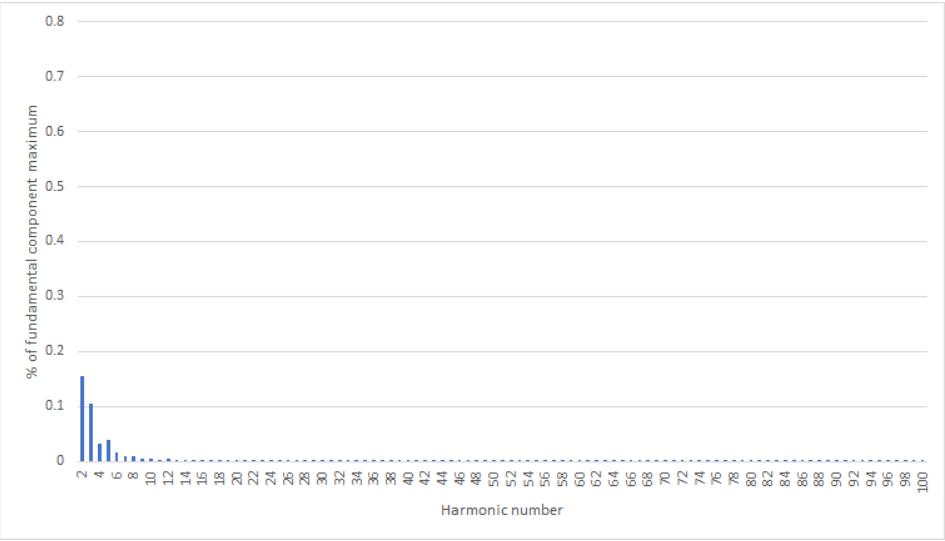

Figure 72. *Harmonic spectrum of current reference with voltage control (1.05 p.u voltage reference).*

Low-order harmonics, especially the third harmonic, have increased in the reference compared to manual current q-component control. However, second harmonic has increased

only little since there was already a second harmonic component in the reference with manual current q-component control. As the other low-order harmonics increased but second harmonic did not, harmonic spectrums of the d-, q- and zero-component references were investigated to understand the phenomenon. Current d-component in stationary frame was calculated according to equation 5.9 and q-component reference in stationary frame $i_{\mathrm{q,ab,ref}}$ was calculated as follows:

$$i_{\mathrm{q,ab,ref}} = \sqrt{2} i_{\mathrm{q,ref}} \cos(\omega_1 t + \theta), \tag{5.10}$$

where $i_{\mathrm{q,ref}}$ is current q-component reference in synchronous frame. Spectrums of the reference components up to 10^{th} harmonic are presented in Figure 73.

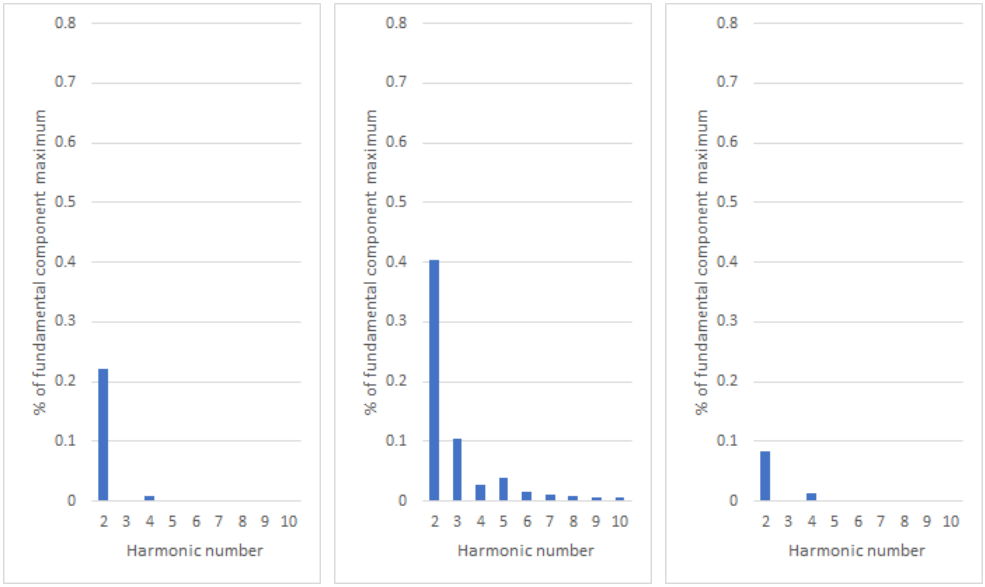

a) d-component reference b) q-component reference c) zero-component reference

Figure 73. *Harmonic spectrums of current d-, q-, and zero-component references with voltage control (1.05 p.u voltage reference).*

Second harmonic is substantially larger in q-component reference than in the total current reference. It seems that the second harmonic reference components cancel each other partly so that the total second harmonic reference is smaller than the q-component reference.

Next, effect of voltage control was studied in another operating point. Simulation was done with voltage reference of 1.0 p.u which resulted in 20 A inductive-resistive current in STATCOM's delta branch. Harmonic current spectrum at PCC is shown in Figure 74.

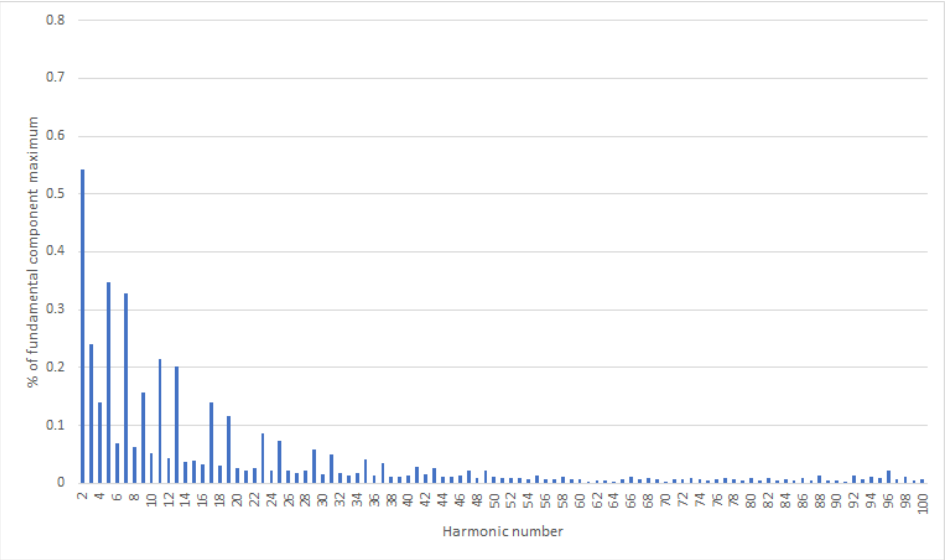

Figure 74. *Harmonic spectrum of PCC current with voltage control (1.0 p.u voltage reference).*

The second harmonic current has increased considerably compared to capacitive operating point. Third harmonic has decreased a bit but other harmonics have stayed quite same. Large second harmonic component can be seen in the current reference of ab-branch also which is shown in Figure 75. As there is a considerable component in current reference, the second harmonic can not be mitigated by harmonic current control.

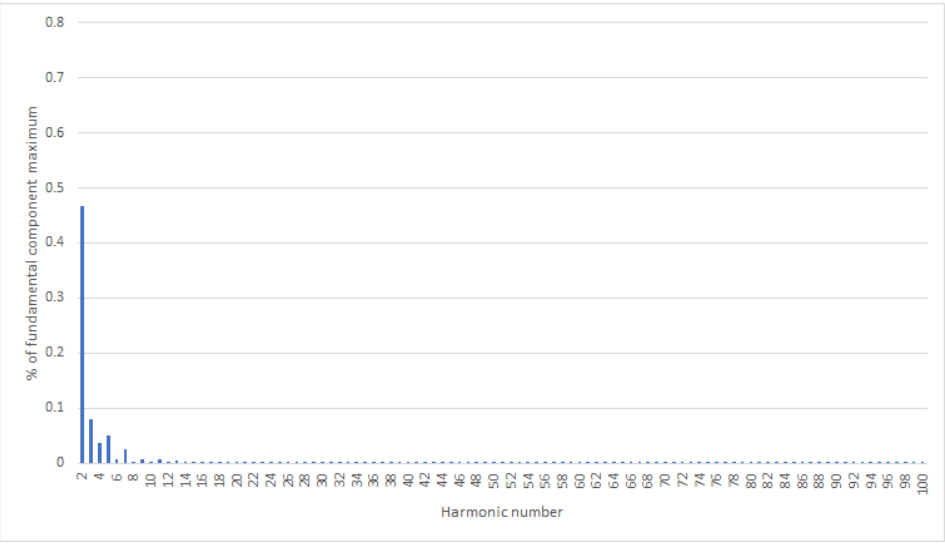

Figure 75. *Harmonic spectrum of current reference with voltage control (1.0 p.u voltage reference).*

To understand why the second harmonic component increases in the reference, harmonic spectrums of all reference components were recorded up to 10th harmonic. The spectrums of d-, q- and zero-sequence current references are presented in Figure 76.

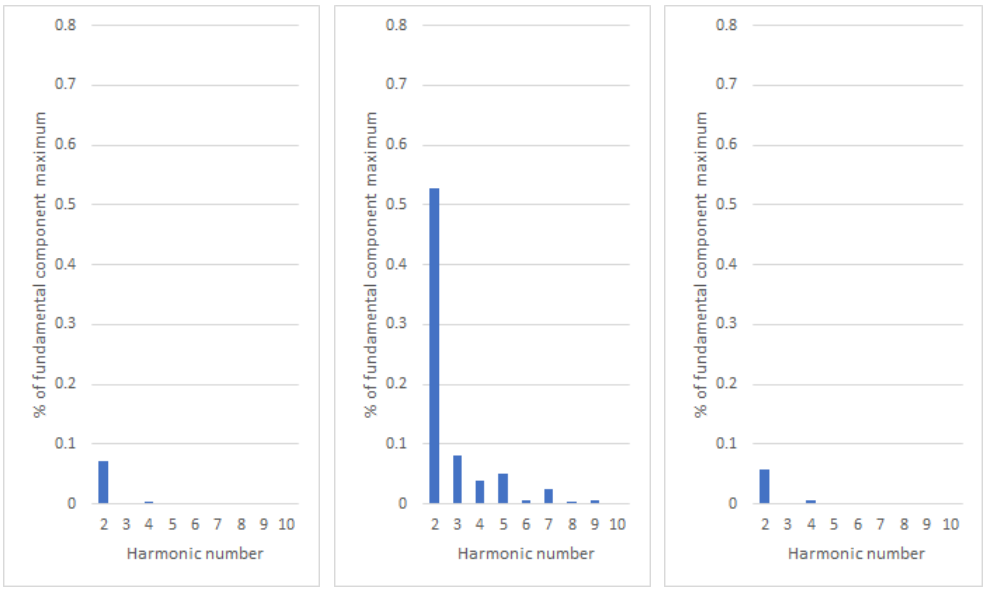

Figure 76. *Harmonic spectrums of current d-, q-, and zero-component references with voltage control (1.0 p.u voltage reference).*

Second harmonic in current q-component reference has increased a bit compared to capacitive operating point. Second harmonic has decreased significantly in current d-component and a bit in zero-component reference. It seems that the total second harmonic current reference increases because other reference components cancel smaller part of the q-component reference second harmonic than in the capacitive operating point.

Simulation was done also with 0.95 p.u voltage reference. It resulted in 954 A inductive current in delta branch. Harmonic current spectrum at PCC is presented in Figure 77 and reference current spectrum in Figure 78.

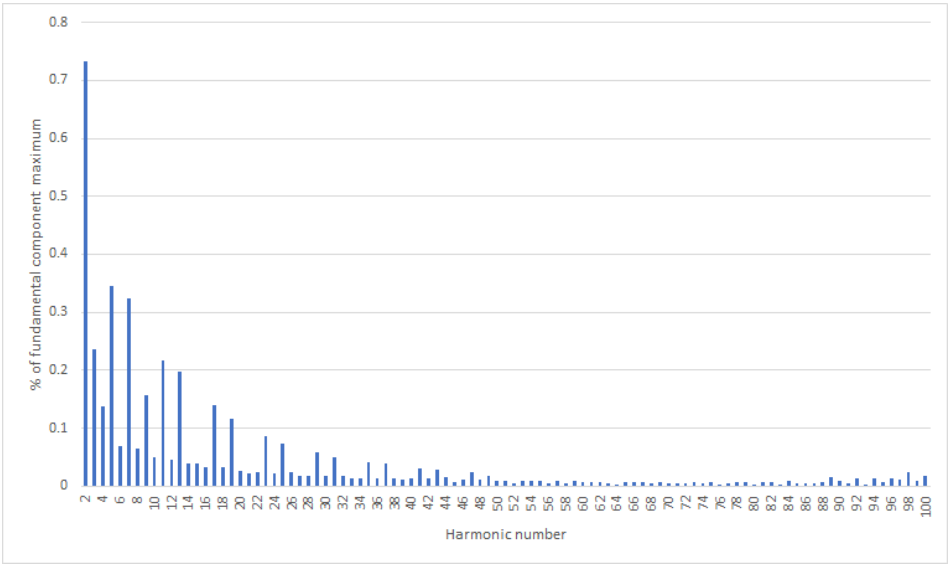

Figure 77. *Harmonic spectrum of PCC current with voltage control (0.95 p.u voltage reference).*

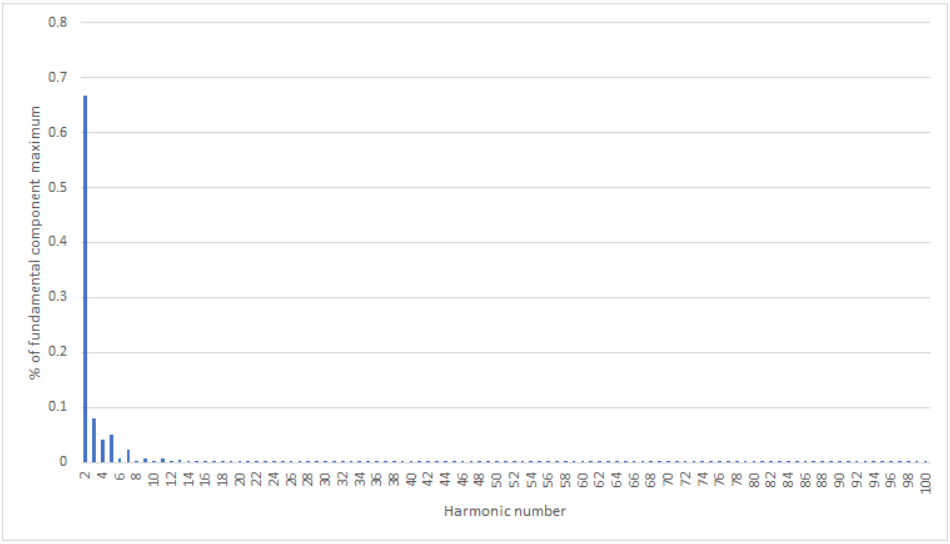

Figure 78. *Harmonic spectrum of current reference with voltage control (0.95 p.u voltage reference).*

Second harmonic current and its reference are even larger in this operating point. Again, all reference component harmonic spectrums were recorded up to 10th harmonic to see the composition of total second harmonic reference. They are shown in Figure 79.

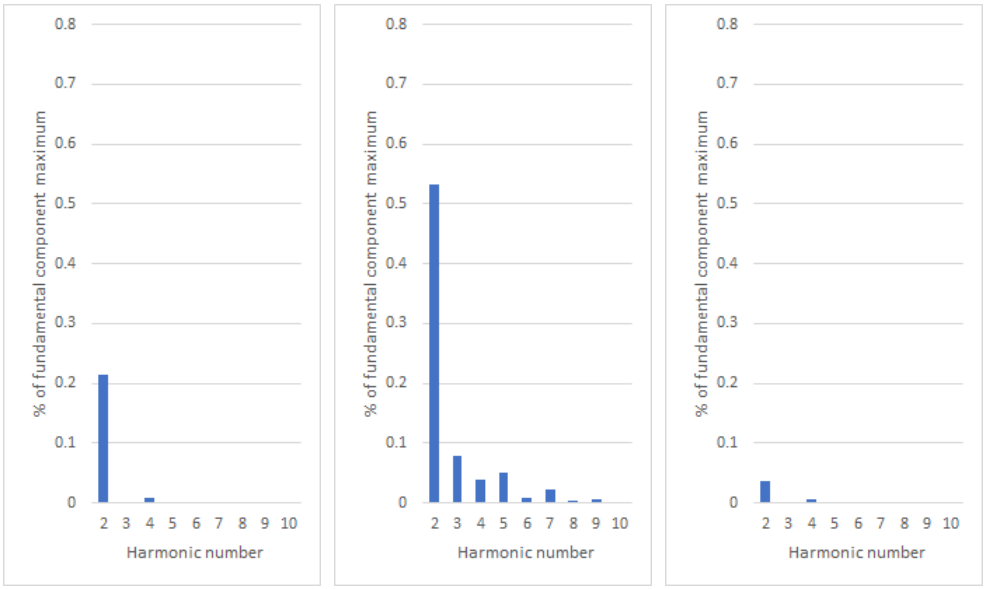

a) d-component reference b) q-component reference c) zero-component reference

Figure 79. *Harmonic spectrums of current d-, q-, and zero-component references with voltage control (0.95 p.u voltage reference).*

Second harmonic in d-component reference has increased to same level as in capacitive operating point. Second harmonic in q- and zero- components have stayed quite same as in the previous operating point. It seems that in this inductive operating point second harmonic reference components do not cancel each other like in capacitive operating

point. Now they add together partly so that the second harmonic in total reference is larger than in individual components.

It seems that the second harmonic current increases when voltage reference magnitude is decreased and STATCOM's current is changed from capacitive to inductive. A simulation was made to see if the growth is due to decreasing voltage or change of STATCOM's current. The magnitude of grid's voltage source was set to 1.10 p.u and the reference for PCC voltage was set to 1.05 p.u. These options resulted in 953 A inductive current in STATCOM's delta branch. The harmonic spectrum of PCC current is presented in Figure 80.

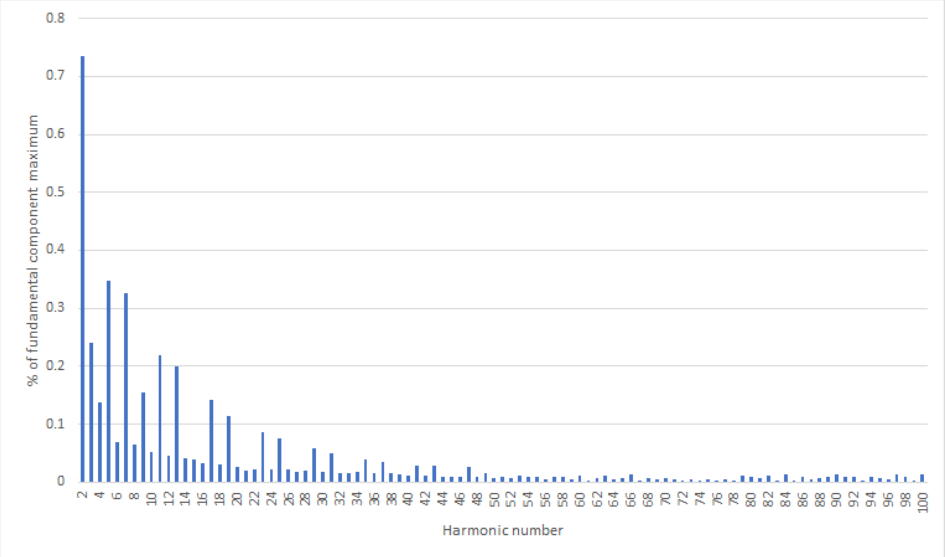

Figure 80. *Harmonic spectrum of PCC current with voltage control (1.05 p.u voltage reference) and grid voltage magnitude of 1.10 p.u.*

Second harmonic current is as large as in the previous case. It can be concluded that its growth is not related to voltage. Second harmonic current increases when STATCOM's fundamental current is shifted from capacitive to inductive. It is due to the combined effect of second harmonic reference components. Still, second harmonic is largest in q-component reference so its reduction would decrease the total second harmonic the most.

In the previous simulations the second harmonic voltage was positive sequence. In positive sequence fundamental frequency synchronous reference frame, it is a 50 Hz component since the frame rotates to same direction at 50 Hz frequency. If 50 Hz voltage component can pass through the PCC synchronization block, it is in the voltage d-component reference. As voltage difference between reference and produced voltage magnitude is controlled to zero, 50 Hz component appears in the current q-component reference also. When current q-component reference is transformed to stationary frame, the 50 Hz component changes back to 100 Hz component. That explains the second harmonic in current q-component reference when it is studied in stationary frame.

Synchronization includes a first-order low-pass filter for produced voltage d-component. Used time constant of the filter was 0.01 seconds in the simulations. Transfer function of the used filter is therefore

$$LPF(s) = \frac{1}{1+0.01s}. \tag{5.11}$$

Its magnitude is

$$|LPF(\omega)| = \frac{1}{\sqrt{1+0.0001\omega^2}}. \tag{5.12}$$

Magnitude at 50 Hz, which corresponds to positive sequence second harmonic in the synchronous frame, is

$$|LPF(50Hz)| = \frac{1}{\sqrt{1+0.0001*(2\pi*50)^2}} = 0.303. \tag{5.13}$$

Therefore, part of the 50 Hz component can pass through the low-pass filter. The 50 Hz component in voltage d-component and the second harmonic in current q-component reference can be decreased by increasing the low-pass filter's time constant and thus decreasing its gain at 50 Hz. However, increasing the time constant slows down the transient response of the synchronization [43].

If second harmonic voltage is negative sequence, it rotates to another direction as positive sequence fundamental synchronous reference frame. In the frame, it is thus a 150 Hz component. As the frequency is higher, the low-pass filter for voltage d-component should mitigate the component better. Figure 81 presents the harmonic spectrum of simulated PCC current when all grid harmonic voltages were same magnitude as before but negative sequence. Grid voltage was 1.0 p.u and reference for PCC voltage was 0.95 p.u as in the worst case simulated for positive sequence harmonics.

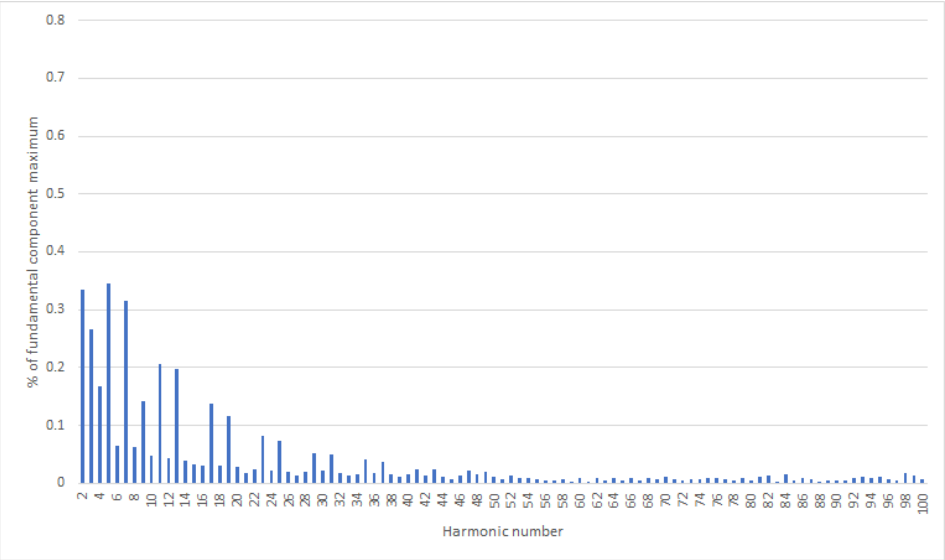

Figure 81. *Harmonic spectrum of PCC current with voltage control (0.95 p.u voltage reference) and negative sequence harmonic voltages.*

Second harmonic current is substantially smaller than with positive sequence harmonic voltages. Magnitudes of other harmonic currents are quite same as with positive sequence harmonics. Current reference in ab-branch is shown in Figure 82.

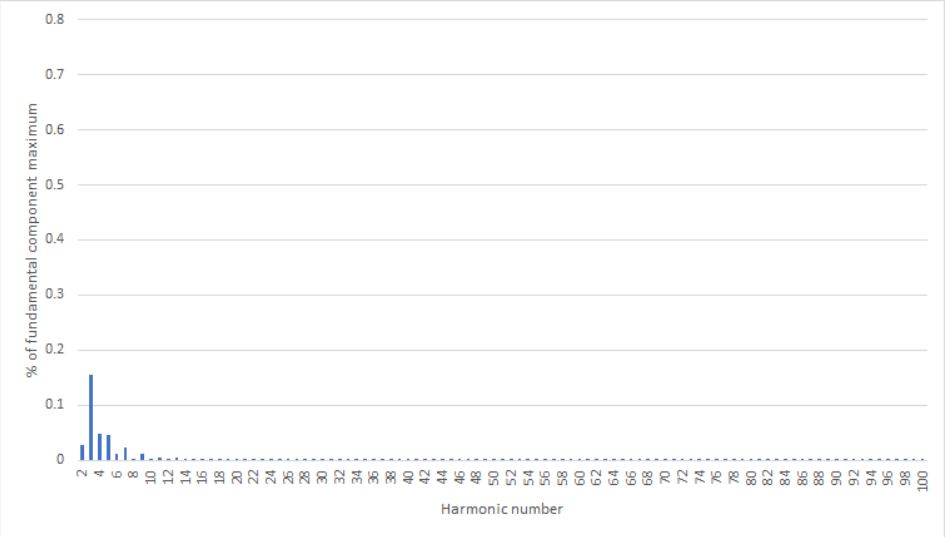

Figure 82. *Harmonic spectrum of current reference with voltage control (0.95 p.u voltage reference) and negative sequence harmonic voltages.*

The second harmonic has decreased considerably in the reference also. The third harmonic has increased over 50 % compared to positive sequence case but its magnitude is still quite low.

In perfectly balanced three-phase system second harmonic voltage is negative sequence [4]. According to previous simulation, it would not be a problem then. However, in unbalanced system, the second harmonic voltage may appear at any sequence. As observed,

large positive sequence second harmonic voltage causes large current at same frequency in inductive operating point. That may cause noncompliance with standards or specifications.

A solution was developed to decrease the second harmonic in current q-component reference and thus in produced current. A band-stop filter was designed for the voltage d-component that synchronization produces. Design was done with MATLAB's Filter Designer tool. Positive sequence second harmonic voltage appears in fundamental frequency synchronous frame as 50 Hz component so filter's lowest magnitude was designed to 50 Hz. Butterworth 2nd order filter was chosen with lower cut-off frequency of 40 Hz and higher cut-off frequency of 62 Hz. The magnitude response of the filter is shown in Figure 83.

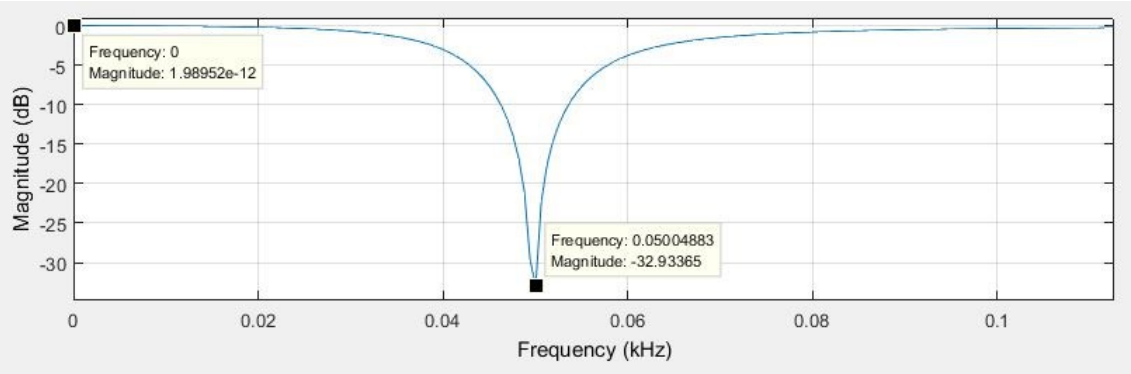

Figure 83. *Magnitude response of the designed band-stop filter.*

The most important restriction for the filter is that it should not affect voltage DC-component at all because that would deteriorate the accuracy of fundamental voltage control. As can be seen from the magnitude response, the magnitude of the designed filter is very close to zero decibel at 0 Hz. In addition, filter offers over 30 dB attenuation at 50 Hz.

A simulation was done with the designed filter in the worst-case operation point with respect to second harmonic current generation. Voltage reference was set to 0.95 p.u, grid voltage magnitude to 1.0 p.u and positive sequence harmonic voltages were added in grid. The simulated harmonic spectrum of PCC current is presented in Figure 84 and spectrum of reference current in ab-branch in Figure 85.

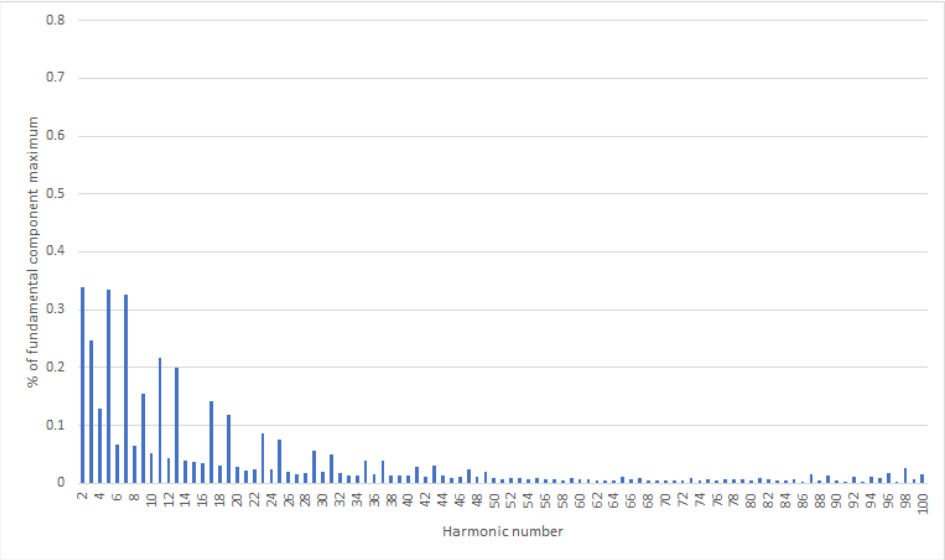

Figure 84. *Harmonic spectrum of PCC current with voltage control (0.95 p.u voltage reference) and band-stop filter.*

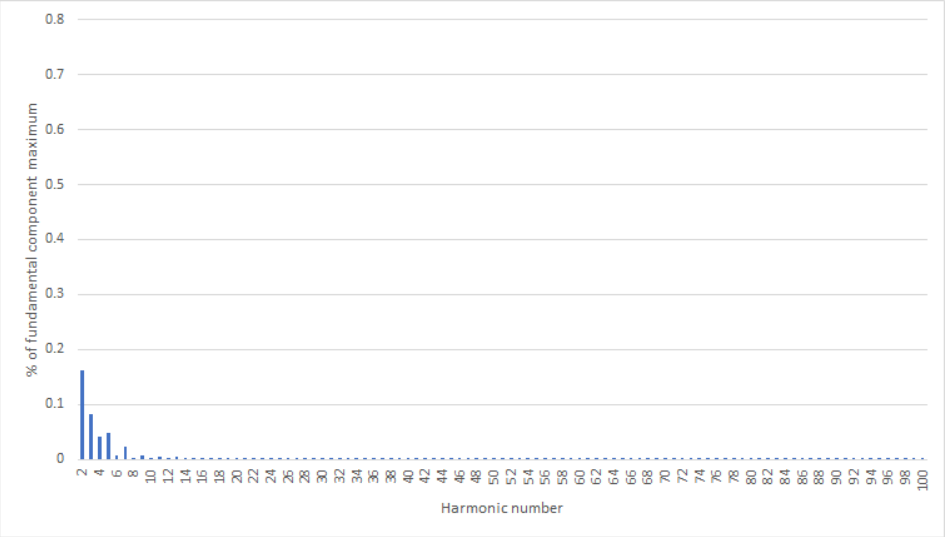

Figure 85. *Harmonic spectrum of current reference with voltage control (0.95 p.u voltage reference) and band-stop filter.*

Second harmonic has decreased considerably both in PCC and reference currents. Produced second harmonic current is almost as small as in capacitive operating point without filter. The remaining second harmonic current in the reference was identified earlier to be result of DC-link voltage control. Now, second harmonic current could be also further attenuated by current control as its reference is smaller than produced current.

Since filter was added to voltage control path, delay was introduced. Therefore, filter's effect on dynamic performance of voltage control was investigated. A step test was done where voltage reference was changed from 0.95 p.u to 1.05 p.u after 0.5 seconds of simulation. Measured voltage d-component magnitude at PCC during step test without and with filter are presented in Figure 86.

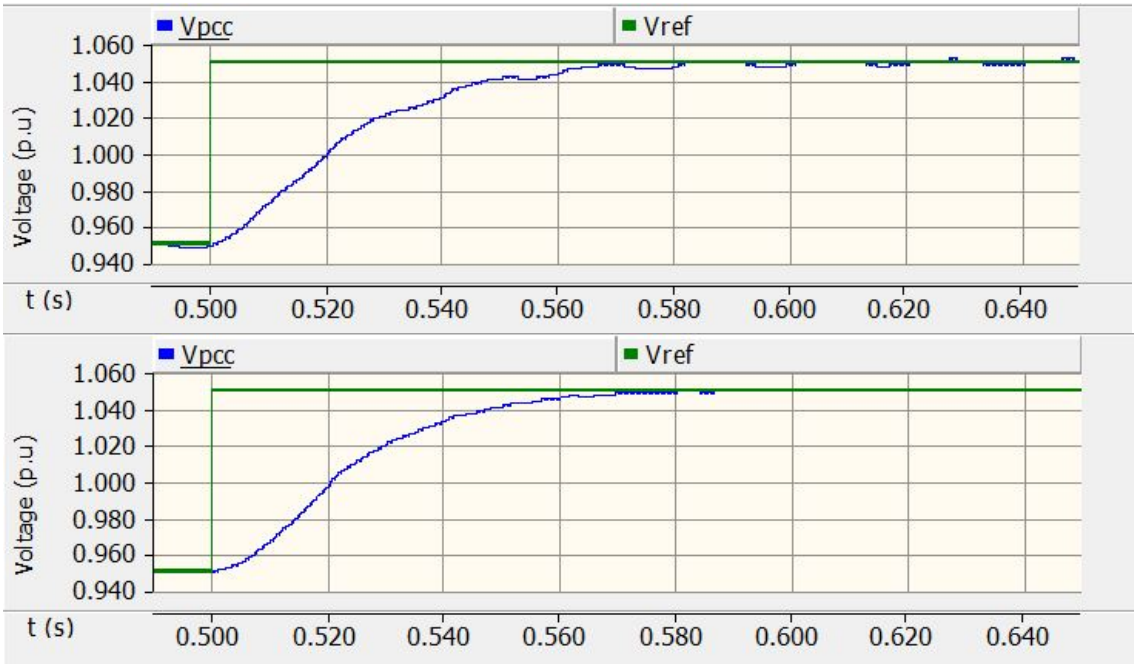

Figure 86. *Dynamic behavior of measured voltage d-component magnitude during step test without (upper figure) and with (lower figure) band-stop filter.*

Control delay is so small that it can not be seen from the figure. In the figure, measured voltage d-component is smoother with filter because second harmonic is filtered from the voltage. Alternative option for 50 Hz component filtering would have been a low-pass filter with lower cut-off frequency than currently used. To achieve same attenuation at 50 Hz with it, very small cut-off frequency and higher filter order should have been used. That would have decreased the filter's gain at lower frequencies also and slowed down the voltage response more.

6. FUTURE WORK

There are still some ideas to improve harmonic performance which were not possible to test in the given time frame or were decided not to be included in the thesis. These ideas are introduced in this chapter.

Harmonic voltages at PCC can be reduced by actively filtering them. The idea of active filtering is to inject harmonic currents from the converter so that they cause harmonic voltage drops in grid impedances which cancel the harmonic voltages at PCC [39]. It is important to know the grid impedance angles at controlled harmonics as they determine the phase differences between produced currents and voltage drops [39].

Secondary busbar synchronization effect on harmonic currents was not studied in the thesis because the synchronization implementation had been simplified in the used PSCAD model. Its effect could be studied by building the real synchronization block to the model and comparing the results with the quite ideal one used in this model.

Modulator's effect on harmonic currents was observed to be small if there are harmonics of same order in grid voltage. However, if there is not a voltage component at some harmonic present, modulator causes still some current at that frequency. The problem of the modulator is that it produces small currents at all harmonics. If there are some frequencies where current should not be produced, the modulator prevents that possibility. As explained before there are some alternative modulator schemes where harmonic currents caused by the modulator could be shifted to higher frequencies and thus zero current emissions at some harmonics could be achieved.

Non-ideal current controller, introduced in chapter 5.2, can control harmonic currents even though frequencies of harmonic components change a bit. Harmonic performance of the STATCOM system with non-ideal controller could be tested when harmonic frequencies are varied slightly.

7. CONCLUSIONS

The studied problem in this thesis was that harmonic currents of STATCOM increase considerably when harmonics are added to grid voltage. These harmonic currents cause harmonic voltages at impedances of grid components. The limits for harmonic currents in reactive power compensation applications originate usually from the limits for PCC harmonic voltages which are stated in standards and transmission operators' specifications. The harmonic voltages caused by STATCOM are usually added to existing harmonic voltages at PCC. If the existing harmonic voltages are large, the limits for STATCOM produced harmonic voltages and currents are strict. The problem, its reasons and solutions were investigated by simulations in PSCAD.

One major topic studied was the comparison of secondary busbar voltage feedforward options. The considered options are instantaneous value of the voltage or the fundamental component of it. The fundamental component feedforward seemed to have some desirable characteristics such as predictability of the produced harmonic current spectrum, better current mitigation at harmonic orders from 20 to 40 and no need for harmonic voltage measurement. Its disadvantage is that low-order harmonic currents are large if there are large low-order harmonic voltages in grid. With fundamental feedforward, produced harmonic currents decreased harmonic voltages at PCC at most frequencies but only if grid is inductive-resistive. Grid's harmonic impedances change over time and have also capacitive values. In that case, produced currents cause increasing harmonic voltages at PCC. Although grid impedances might be mostly inductive, harmonic limits must be respected in every grid contingency.

The idea of instantaneous voltage feedforward is that harmonic voltages over coupling reactor would be zero and harmonic currents would not be induced. As observed, used modulator execution frequency causes too much delay so that the feedforward would work as planned for higher order harmonics. Still, harmonic currents up to 20^{th} order were smaller than with fundamental feedforward. Harmonic currents decreased considerably when modulator execution frequency was doubled and instantaneous feedforward was used. However, switching frequency was doubled and thus losses were increased substantially. Moreover, real life harmonic voltage measurement can be inaccurate and other possible delays can deteriorate the performance more.

The advantages of feedforward options were tried to be combined by using a low-pass filter for the voltage feedforward. A low-pass filter was designed to reject high frequency noise and reduce the effect of feedforward at high-order harmonics. As a result, low-order harmonics were mitigated compared to fundamental feedforward and harmonics around 30^{th} decreased compared to instantaneous feedforward. Still, low-order harmonics up to 20^{th} order increased in comparison with instantaneous feedforward due to filter delay.

One simple solution to decrease harmonic currents is to increase the coupling reactor's inductance. Current controller's proportional gain must be increased with same amount in percent to have considerable effect on harmonics and same dynamic performance as with original reactor. Disadvantage of the higher inductance is that more reactor material and more submodules in converter are needed so costs are increased.

The effect of modulator on harmonics was studied by idealizing it. Ideal modulator produces exactly the reference voltage every simulation step and keeps submodule voltages constant. It was observed that with fundamental voltage feedforward all harmonic currents could be removed if grid voltage was sinusoidal. However, when there were harmonic voltages in grid, modulator had only a minor effect on harmonic currents. With instantaneous feedforward and ideal modulator all harmonic currents could be removed even if harmonic voltages appeared in grid. So, modulator's effect on harmonics is mainly its delay which deteriorates the feedforward of harmonic voltages. Moreover, it causes small currents at all harmonics even though grid voltage is sinusoidal.

Current control with added resonant branches for harmonics seemed to work very well for low-order harmonics when current measurement was ideal. Better mitigation was achieved with ideal resonant branches but non-ideal branches should be more stable and work even if frequencies vary a bit. Fundamental voltage feedforward can be used so harmonic voltage measurement is not needed. Measuring the quite small harmonic components accurately from large total current might still be a challenge in a real system.

Harmonic current control could not remove the second harmonic component. This component was present in current reference and thus the second harmonic was controlled to the reference value. Origin of this component in the reference was identified to be the control function which controls the average of DC-voltages in three STATCOM delta branches to the nominal value. However, second harmonic current was not present in the reference when grid voltage was sinusoidal. Therefore, the second harmonic is due to the combination of harmonic voltages in grid and DC-link voltage control.

Voltage control had no significant effect on produced harmonic currents except for second harmonic. It was observed that second harmonic current increases when the operating point is shifted from capacitive to inductive. Voltage controller caused quite large second harmonic to current q-component reference when there was a positive sequence second harmonic voltage in grid. In capacitive point, d- and zero-components canceled the second harmonic in q-component partly so that the total reference was smaller than the q-component. In inductive point, reference components were partly summed together so the total second harmonic current reference increased. When second harmonic voltage in grid was negative sequence, produced second harmonic current was significantly smaller. The problem was solved by adding a band-stop filter for voltage d-component at 50 Hz which efficiently mitigated the second harmonic current.

REFERENCES

[1] B. Singh, A. Chandra, K. Al-Haddad, Power Quality : Problems and Mitigation Techniques, John Wiley & Sons, New York, 2014, 599 p.

[2] CIGRE Working Group 14.19, Static Synchronous Compensator (STATCOM), CIGRE, 2000, 211 p.

[3] E. Fuchs, M.A.S. Masoum, Power Quality in Power Systems and Electrical Machines, Elsevier Science, San Diego, 2008, 659 p.

[4] S. Santoso, M.F. McGranaghan, R.C. Dugan, H.W. Beaty, Electrical Power Systems Quality, Third Edition, McGraw-Hill Education, 2012, 528 p.

[5] T. Dao, B.T. Phung, T. Blackburn, Effects of voltage harmonics on distribution transformer losses, Proceedings of the Power and Energy Engineering Conference (APPEEC), 2015 IEEE PES Asia-Pacific, Brisbane, Australia, November 15–18, 2015, IEEE, pp. 1-5.

[6] M.A. Prša, K.K. Kasaš-Lažetić, N.D. Mučalica, Skin effect and proximity effect in a real, high voltage, double three-phase system, Proceedings of the EUROCON - International Conference on Computer as a Tool (EUROCON), Lisbon, Portugal, April 27–29, 2011, IEEE, pp. 1-4.

[7] K.D. Patil, W.Z. Gandhare, Threat of harmonics to underground cables, Proceedings of the 2012 Students Conference on Engineering and Systems, Allahabad, India, March 16-18, 2012, IEEE, pp. 1-6.

[8] Sumaryadi, H. Gumilang, A. Suslilo, Effect of power system harmonic on degradation process of transformer insulation system, Proceedings of the 9th International Conference on the Properties and Applications of Dielectric Materials, Harbin, China, July 19–23, 2009, IEEE, pp. 261-264.

[9] S. Chattopadhyay, M. Mitra, S. Sengupta, Electric Power Quality, Springer Netherlands, 2011, 179 p.

[10] De La Rosa, Harmonics and Power Systems, CRC Press, 2006, 179 p.

[11] F. Lin, S. Zuo, W. Deng, S. Wu, Modeling and Analysis of Electromagnetic Force, Vibration, and Noise in Permanent-Magnet Synchronous Motor Considering Current Harmonics, IEEE Transactions on Industrial Electronics, Vol. 63, Iss. 12, 2016, pp. 7455-7466.

[12] M. Ertl, S. Voss, The role of load harmonics in audible noise of electrical transformers, Journal of Sound and Vibration, Vol. 333, Iss. 8, 2014, pp. 2253-2270.

[13] A. Fidigatti, E. Ragaini, Effect of harmonic pollution on low voltage overcurrent protection, Proceedings of the 14th International Conference on Harmonics and Quality of Power - ICHQP, Bergamo, Italy, September 26–29, 2010, IEEE, pp. 1-4.

[14] IEEE 519, Recommended Practice and Requirements for Harmonic Control in Electric Power Systems, IEEE, 2014, 29 p.

[15] IEC 61000-2-2, Compatibility levels for low-frequency conducted disturbances and signalling in public low-voltage power supply systems, IEC, 2017, 36 p.

[16] IEC 61000-2-4, Compatibility levels in industrial plants for low-frequency conducted disturbances, IEC, 2002, 75 p.

[17] IEC 61000-2-12, Environment – Compatibility levels for low-frequency conducted disturbances and signalling in public medium-voltage power supply systems, IEC, 2003, 55 p.

[18] IEC 61000-3-2, Limits – Limits for harmonic current emissions (equipment input current ≤ 16 A per phase), IEC, 2014, 34 p.

[19] IEC 61000-3-12, Limits – Limits for harmonic currents produced by equipment connected to public low-voltage systems with input current >16 A and ≤75 A per phase, IEC, 2011, 25 p.

[20] IEC/TR 61000-3-6, Limits – Assessment of emission limits for the connection of distorting installations to MV, HV and EHV power systems, IEC, 2008, 58 p.

[21] W. Hofmann, W. Just, Reactive Power Compensation : A Practical Guide, Wiley, Hoboken, 2012, 288 p.

[22] S. Corsi, Voltage Control and Protection in Electrical Power Systems, Springer Verlag, 2015, 557 p.

[23] J. Dixon, L. Moran, J. Rodriguez, R. Domke, Reactive Power Compensation Technologies: State-of-the-Art Review, Proceedings of the IEEE, Vol. 93, Iss. 12, 2005, pp. 2144-2164.

[24] R. Smeets, L. van der Sluis, M. Kapetanovic, Switching in Electrical Transmission and Distribution Systems, John Wiley & Sons, New York, 2014, 425 p.

[25] CIGRE Working Group 14.30, Guide to the Specification and Design Evaluation of AC Filters for HVDC Systems, CIGRE, 1999, 251 p.

[26] R.S. Thallam, G. Joós, Reactive Power Compensation, in: L. Grigsby (ed.), Electric Power Generation, Transmission, and Distribution, CRC Press, 2012, pp. 789.

[27] D.P. Kothari, I.J. Nagrath, Modern Power System Analysis, Third ed. Tata McGraw-Hill Publishing Company Limited, New Delhi, 2003, 694 p.

[28] R.M. Mathur, R.K. Varma, Thyristor-Based FACTS Controllers for Electrical Transmission Systems, IEEE, Piscataway, NJ, 2002, 505 p.

[29] CIGRE Working Group 38-01 Task Force No. 2, Static Var Compensators, CIGRE, 1986, 128 p.

[30] E. Barrios-Martínez, C. Ángeles-Camacho, Technical comparison of FACTS controllers in parallel connection, Journal of Applied Research and Technology, Vol. 15, Iss. 1, 2017, pp. 36-44.

[31] B. Singh, R. Saha, A. Chandra, K. Al-Haddad, Static synchronous compensators (STATCOM): a review, IET Power Electronics, Vol. 2, Iss. 4, 2009, pp. 297-324.

[32] S. Khomfoi, L.M. Tolbert, Multilevel Power Converters, in: M.H. Rashid (ed.), Power Electronics Handbook, Elsevier Science, 2011, pp. 455-486.

[33] M. Hagiwara, H. Akagi, Control and Experiment of Pulsewidth-Modulated Modular Multilevel Converters, IEEE Transactions on Power Electronics, Vol. 24, Iss. 7, 2009, pp. 1737-1746.

[34] K. Sharifabadi, L. Harnefors, H. Nee, S. Norrga, R. Teodorescu, Design, Control, and Application of Modular Multilevel Converters for HVDC Transmission Systems, IEEE Press, United Kingdom, 2016, 386 p.

[35] R. Teodorescu, F. Blaabjerg, M. Liserre, P.C. Loh, Proportional-resonant controllers and filters for grid-connected voltage-source converters, IEE Proceedings - Electric Power Applications, Vol. 153, Iss. 5, 2006, pp. 750-762.

[36] E. Twining, D.G. Holmes, Grid current regulation of a three-phase voltage source inverter with an LCL input filter, IEEE Transactions on Power Electronics, Vol. 18, Iss. 3, 2003, pp. 888-895.

[37] X. Wang, X. Ruan, S. Liu, C.K. Tse, Full Feedforward of Grid Voltage for Grid-Connected Inverter With LCL Filter to Suppress Current Distortion Due to Grid Voltage Harmonics, IEEE Transactions on Power Electronics, Vol. 25, Iss. 12, 2010, pp. 3119-3127.

[38] Q. Yan, X. Wu, X. Yuan, Y. Geng, An Improved Grid-Voltage Feedforward Strategy for High-Power Three-Phase Grid-Connected Inverters Based on the Simplified Repetitive Predictor, IEEE Transactions on Power Electronics, Vol. 31, Iss. 5, 2016, pp. 3880-3897.

[39] A. Tarkiainen, R. Pollanen, M. Niemela, J. Pyrhonen, Identification of grid impedance for purposes of voltage feedback active filtering, IEEE Power Electronics Letters, Vol. 2, Iss. 1, 2004, pp. 6-10.

[40] C. Korlinchak, M. Comanescu, Discrete time integration of observers with continuous feedback based on Tustin's method with variable prewarping, Proceedings of the 6th IET International Conference on Power Electronics, Machines and Drives, Bristol,

United Kingdom, March 27-29, 2012, The Institution of Engineering & Technology, pp. 1-6.

[41] W.Y. Yang, Continuous-Time Systems and Discrete-Time Systems, in: W.Y. Yang (ed.), Signals and Systems with MATLAB, Springer, Berlin, 2009, pp. 277-306.

[42] Current Transducer ITL 4000-S Datasheet, LEM, 2017, 8 p. Available: http://www.lem.com/docs/products/itl_4000-s.pdf.

[43] P. Rodriguez, J. Pou, J. Bergas, J.I. Candela, R.P. Burgos, D. Boroyevich, Decoupled Double Synchronous Reference Frame PLL for Power Converters Control, IEEE Transactions on Power Electronics, Vol. 22, Iss. 2, 2007, pp. 584-592.

APPENDIX A: CONTROL BLOCK DIAGRAM

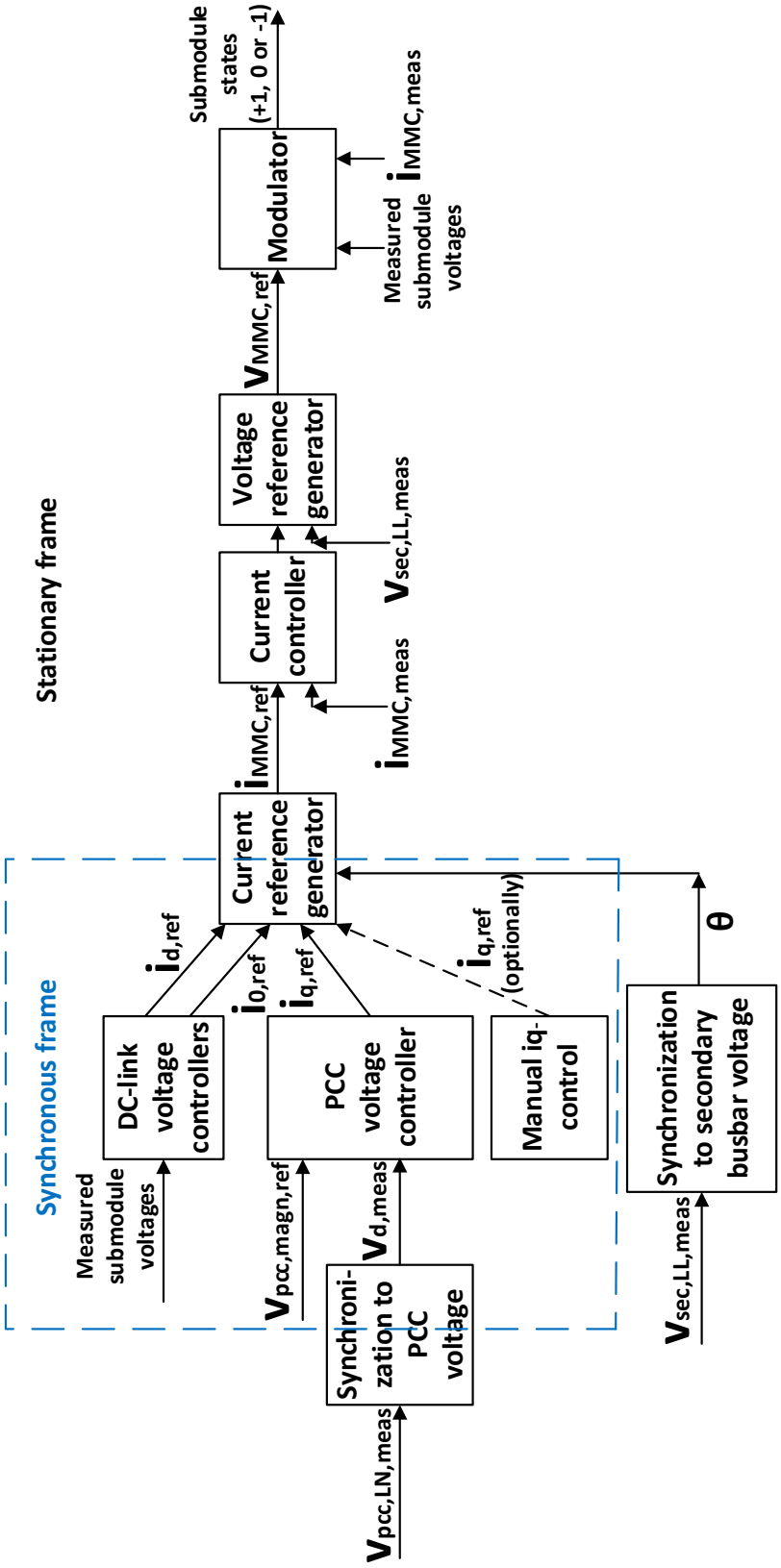

Appendix A, Figure 1. *Control block diagram of STATCOM.*

Explanations for the abbreviations in the control block diagram:

$i_{MMC,meas}$	Measured currents in MMC delta branches
$i_{MMC,ref}$	References for currents in MMC delta branches
$i_{d,ref}$	Reference for current d-component
$i_{q,ref}$	Reference for current q-component
$i_{0,ref}$	Reference for current zero-sequence component
$v_{d,meas}$	d-component of measured PCC voltage
$v_{MMC,ref}$	References for MMC delta branch voltages
$v_{pcc,LN,meas}$	Measured line-to-neutral voltages at PCC
$v_{pcc,magn,ref}$	Reference for PCC voltage magnitude
$v_{sec,LL,meas}$	Measured secondary busbar line-to-line voltages
θ	Synchronization angle for dq-to-abc transformation

APPENDIX B: SIMULATION PARAMETERS

Appendix B, Table 1. *Parameters of the first simulations.*

Parameter	Value	Unit
Grid		
System frequency	50	Hz
System positive sequence voltage, line-to-line	138	kV (RMS)
System negative sequence voltage, line-to-line	0	kV (RMS)
Resistance of the transmission line	0.9292	Ω
Inductive reactance of the transmission line (at fundamental frequency)	9.477	Ω
Transformer		
Rated power	100	MVA
Connection	YNd11	-
Secondary nominal voltage, line-to-line	34.5	kV (RMS)
Leakage reactance	0.115	p.u
STATCOM		
Rated power	100	MVAr
Number of submodules per MMC branch	40	-
Submodule capacitance	7000	µF
MMC branch inductance	11	mH
Resistance of the inductor	20	mΩ